SYSTEMIC RISK MEASURES BASED ON VALUE-AT-RISK

A THESIS SUBMITTED TO
THE GRADUATE SCHOOL OF ENGINEERING AND SCIENCE
OF BILKENT UNIVERSITY
IN PARTIAL FULFILLMENT OF THE REQUIREMENTS FOR
THE DEGREE OF
MASTER OF SCIENCE
IN
INDUSTRIAL ENGINEERING

By
Wissam Al-Ali
July 2023

Systemic Risk Measures Based On Value-at-Risk
By Wissam Al-Ali
July 2023

We certify that we have read this thesis and that in our opinion it is fully adequate, in scope and in quality, as a thesis for the degree of Master of Science.

Çağın Ararat(Advisor)

Firdevs Ulus

Nils-Christian Detering

Approved for the Graduate School of Engineering and Science:

Orhan Arıkan
Director of the Graduate School

ABSTRACT

SYSTEMIC RISK MEASURES BASED ON VALUE-AT-RISK

Wissam Al-Ali
M.S. in Industrial Engineering
Advisor: Çağın Ararat
July 2023

This thesis addresses the problem of computing systemic set-valued risk measures. The proposed method incorporates the clearing mechanism of the Eisenberg-Noe model, used as an aggregation function, with the value-at-risk, used as the underlying risk measure. The sample-average approximation (SAA) of the corresponding set-valued systemic risk measure can be calculated by solving a vector optimization problem. For this purpose, we propose a variation of the so-called grid algorithm in which grid points are evaluated by solving certain scalar mixed-integer programming problems, namely, the Pascoletti Serafini and norm-minimizing scalarizations. At the initialization step, we solve weighted sum scalarizations to establish a compact region for the algorithm to work on. We prove the convergence of the SAA optimal values of the scalarization problems to their respective true values. Moreover, we prove the convergence of the approximated set-valued risk measure to the true set-valued risk measure in both the Wijsman and Hausdorff senses. In order to demonstrate the applicability of our findings, we construct a financial network based on the Bollobás preferential attachment model. In addition, we model the economic disruptions using identically distributed random variables with a Pareto distribution. We conduct a comprehensive sensitivity analysis to investigate the effect of the number of scenarios, correlation coefficient, and Bollobás network parameters on the systemic risk measure. The results highlight the minimal influence of the number of scenarios and correlation coefficient on the risk measure, demonstrating its stability and robustness, while shedding light on the profound significance of Bollobás network parameters in determining the network dynamics and the overall level of systemic risk.

Keywords: Systemic risk measure, aggregation function, value-at-risk, sensitive set-valued systemic risk measures, non-convex vector optimization, two-stage stochastic programming, chance constraint, weighted sum scalarizations, Pascoletti Serafini scalirizations, norm-minimizing scalarization, Wijsman topology, Hausdorff convergence.

ÖZET

RİSKE MARUZ DEĞER TEMELLİ SİSTEMİK RİSK ÖLÇÜLERİ

Wissam Al-Ali
Endüstri Mühendisliği, Yüksek Lisans
Tez Danışmanı: Çağın Ararat
Temmuz 2023

Bu tezde sistemik risk ölçülerinin hesaplanması problemi incelenmiştir. Önerilen yöntem, birleştirici fonksiyon olarak Eisenberg-Noe modelinin takas mekanizmasını, temel risk ölçüsü olarak da riske maruz değeri kullanmaktadır. Buna karşılık gelen sistemik risk ölçüsünün örneklem ortalaması yaklaşıklaması, bir vektör eniyileme problemi çözerek hesaplanabilmektedir. Bu amaçla, bilimsel yazında yer alan ızgara algoritmasının bir varyasyonu önerilmiştir; buna göre, ızgara noktaları değerlendirilirken Pascoletti Serafini ve norm enküçükleme skalerizasyonları olarak iki tür karışık tamsayılı eniyileme problemi çözülmektedir. Algoritmanın başlangıç aşamasındaysa, ağırlıklı toplam skalerizasyonu çözülerek algoritmanın üzerinde çalışacağı bir tıkız küme elde edilmektedir. Tezde skalerizasyon problemlerinin örnekleme ortalaması yaklaşıklamalarının bu problemlerin gerçek değerlerine yakınsadığı gösterilmiştir. Ayrıca, yaklaşıklama ile hesaplanan küme değerli risk ölçüsünün gerçek küme değerli risk ölçüsüne yakınsadığı Wijsman ve Hausdorff topolojilerine göre gösterilmiştir. Bulguların uygulanabilirliğini göstermek için Bollobás tercihli iliştirme modeline göre bir finansal ağ inşa edilmiş; ayrıca, ekonomik bozulmalar aynı dağılıma sahip Pareto rassal değişkenleri olarak modellenmiştir. Hesaplanan sistemik risk ölçülerine senaryo sayısı, korelasyon katsayısı ve Bollobás ağ parametrelerinin etkisini incelemek için kapsamlı bir duyarlılık analizi yapılmıştır. Elde edilen sonuçlar, senaryo sayısı ve korelasyon katsayılarının sistemik risk ölçüsüne en az düzeyde etkisi olduğunu düşündürürken Bollobás ağ parametlerinin ağ dinamiklerini ve sistemik risk düzeyini belirlemede büyük öneme sahip olduğunu ortaya koymaktadır.

Anahtar sözcükler: Sistemik risk ölçüleri, birleştirici fonksiyon, riske maruz değer, hassas küme değerli sistemik risk ölçüleri, dışbükey olmayan vektör optimizasyonu, iki aşamalı stokastik programlama, olasılık kısıtı, toplam skalerizasyonu, Pascoletti Serafini skalerizasyonu, norm enküçükleme skalerizasyonu, Wijsman topolojisi, Hausdorff yakınsaması.

Acknowledgement

First and foremost, my sincere gratitude goes to my advisor, Çağın Ararat, whose support and guidance have been instrumental in shaping the outcome of this research. His expertise and dedication have been a constant source of inspiration throughout this journey. I extend my thanks to my thesis committee, Firdevs Ulus and Nils-Christian Detering, for their valuable insights and constructive feedback. Their contributions have played a crucial role in enhancing the quality of this thesis. I also wish to acknowledge the esteemed professors at Bilkent University. Their knowledge and expertise shared during the courses have enriched my learning experience.

To my beloved family, I owe a debt of gratitude for their unwavering love and continuous support. I especially want to thank my dear mother, Lina, and my late father, Ibrahim, whose memory remains a source of strength. My siblings, Rima, Batoul, Kamel, Hassan, and Yousef, have been pillars of encouragement throughout my academic journey. I am also indebted to my relatives in Houston, including uncles, aunts, and their families, for their constant motivation and encouragement.

To my girlfriend, Dima Ahmed, I express my heartfelt thanks for her love, understanding, and support during both the triumphs and challenges of this thesis. I am truly grateful to my close friends, Fahaar Pirani, Yunus Emre Yurdagül and Hilal Khan, for their friendship, support, and positive influence. Your companionship has made this journey memorable and enjoyable.

I cannot overlook the profound influence of my homeland, Palestine. It has been the wellspring of my inspiration and the driving force behind my determination.

In Loving Memory

This thesis is dedicated to my beloved father, Ibrahim, who was not only a source of endless inspiration but also the pillar of strength in my life. Though he is no longer with us, his love and support continue to guide me. May his soul rest in peace.

Contents

List of Figures

List of Tables

Chapter 1

Introduction

The concepts of systemic risk and financial contagion hold significant importance within the domain of global economics. Systemic risk is a term used to describe the possibility of a disturbance occurring within the financial system, which has the potential to propagate throughout various institutions, markets, and economies, resulting in substantial adverse outcomes. When systemic risk emerges, it frequently initiates a cascading sequence of events, leading to the spreading of financial contagion. Hence, it is important to acknowledge that the potential ramifications of systemic risk and financial contagion emphasize the necessity for proactive measures and risk management strategies.

The field of risk management has garnered significant attention over an extended period, with heightened interest following the rapid onset of the 2008 financial crisis. This crisis was characterized by the swift devaluation of mortgage-related securities that had permeated both the United States and global financial systems, resulting in the erosion of numerous prominent financial institutions in the United States and other countries [1]. Moreover, this financial crisis served as a clear demonstration of the significant interconnectedness of global financial systems, highlighting how even minor shocks have the potential to generate substantial disruptions within the economy [2].

In recent research, there have been various new ideas about systemic risk measures and allocation methods. Systemic risk measures that can be broken down into an aggregation function and a linear measure of risk have gotten considerable focus, see [3], [4] and the references therein. In this framework, the aggregation function captures the societal impact

of the system, while capital allocations are added after aggregation to represent prospective bailout costs. Recently, a framework has emerged in which capital allocations are assigned to institutions prior to aggregation. As discussed in [5], [6] and [7], this interpretation proves particularly useful for regulatory purposes and the prevention of financial crises. In each of these models, the set of all feasible capital allocations results in a multivariate risk measure.

The association between systemic risk and complex interconnections among organizations—rather than with individual entities themselves—is what sparks interest in this concept. Traditional risk measures like value-at-risk, conditional value-at-risk, and negative expectation would often be sufficient if the risk was purely based on the performance of a single firm, regardless of how interconnected it may be. Systemic risk requires a broader perspective, necessitating an analysis of the distribution of total profits and losses across all firms in the economy, as demonstrated in [8], [9], and [10].

Recent research has examined the measurement of systemic risk within the context of traditional monetary risk measures [11]. The literature defines systemic risk measures as a three-step structure (see [12] and [13]).

In this study, we concentrate on financial networks, whose members are linked by contractual obligations and whose interbank payments are decided by a clearing process based on their uncertain operating cash flows. The model put forth by Eisenberg and Noe portrays a financial system as a static directed network of banks with interbank liabilities specified along the edges [14]. Their paper presents two methods for calculating a clearing vector, which represents the payments necessary to satisfy interbank obligations, assuming positive operating cash flows for each bank. The first approach is a simple algorithm known as the fictitious default algorithm, which computes the clearing vector iteratively using a finite number of updates. The second strategy formulates a concise mathematical programming problem with linear constraints based on liabilities, operating cash flows, and an arbitrary objective function that is strictly increasing. By selecting a linear objective function, the optimal solution to a linear programming problem gives a clearing vector [14].

The fictitious default algorithm is favored by the vast majority of researchers working with network models of systemic risk. In [15], Suzuki presents an analogous method for evaluating clearing vectors, expanding on the work of Eisenberg and Noe [14]. Additionally, Suzuki considers cross-shareholdings among members of a financial system. In [16], Cifuentes

et al., examine systemic risk in terms of institution liquidity and asset price instability. In [17], Elsinger extends the Eisenberg-Noe (EN) model in by integrating a cross-holdings structure similar to Suzuki [15]. Elsinger relaxes the assumption of positive operating cash flows and examines the model under certain assumptions regarding seniority. In [18], Rogers and Veraart introduce default costs to the Eisenberg-Noe model and investigate the necessity of bailing out delinquent institutions. They demonstrate that solvent institutions may find it advantageous to acquire insolvent institutions under rigorous positive default costs. In their work, Weber and Weske [19] develop a comprehensive network model that integrates multiple factors that contribute to systemic risk. The model consists of cross-holdings (refer to [15] and [17]), fire sales (refer to [16]), and bankruptcy costs (refer to [17] and [18]). They also extend the Eisenberg-Noe model by incorporating all of these factors simultaneously, resulting in a more realistic and intricate framework. For a comprehensive overview of network models of systemic risk, we refer readers to the survey by Kabanov et al. [20], which investigates the existence and uniqueness of clearing vectors in the aforementioned models and their calculation using various variants of the fictitious default algorithm introduced by Eisenberg and Noe [14]. However, none of those works have utilized the second approach of mathematical programming proposed by Eisenberg and Noe [14].

The operating cash flows of a network's members are typically subject to uncertainty due to correlated risk factors. These cash flows can therefore be represented as a realization of a random vector with possibly correlated components. The resultant clearing vector is a deterministic function of the random operating cash flow vector, with the precise form of the function being determined by the clearing mechanism. Building on this idea, a recent line of research initiated by Chen et al. in [3] centers on defining systemic risk measures that capture the necessary capital allocations for network members to control certain (non-linear) averages across various scenarios. Using the clearing mechanism, a random aggregate quantity associated with the clearing vector, such as the total debt paid in the system or the total equity generated by all participants during clearing, is defined. This sum functions as a deterministic and scalar function, referred to as the aggregation function, of the operating cash flow vector. In [3], a systemic risk measure is defined as a scalar functional of the operating cash flow vector that quantifies the risk of the random aggregate quantity using convex risk measures such as negative expected value, average value-at-risk, or entropic risk measures.

The systemic risk measure in [3], represents the total capital requirement for the system

in order to maintain an acceptable level of risk for the aggregate quantity. Due to the fact that the total capital is only utilized after the shock has been aggregated, the allocation of this capital back to the members of the system remains an unresolved question that will require a separate procedure. To tackle this, Feinstein et al. and Biagini et al. in [5] and [6], respectively, propose set-valued and scalar systemic risk measures that are "sensitive" to capital levels to address this issue. The objective of these measures is to identify deterministic capital allocation vectors that can directly supplement the random operating cash flow vector. Therefore, the augmented cash flow vector is aggregated, and the risk of the resulting random aggregate quantity is controlled using a convex risk measure, similar to [3]. The set-valued systemic risk measure in [5] represents the set of all feasible capital allocation vectors, considering the measurement and allocation of systemic risk as a joint problem.

When the underlying aggregation function is suitably simple, the sensitive systemic risk measures studied in [5] and [6] exhibit advantageous theoretical properties. Ararat and Rudloff demonstrate in [21] that, assuming a monotone and concave aggregation function and a convex base risk measure, the set-valued sensitive systemic risk measure becomes a convex set-valued risk measure according to the definition of Hamel et al. in [22], and dual representations can be obtained in terms of the conjugate function of the aggregation function.

In this thesis, similar to the study conducted by Ararat and Meimanjan in [23], our primary objective is to calculate a systemic risk measure by establishing its connection to a vector (multiobjective) optimization problem. The vector optimization problem involves a risk constraint that is expressed in terms of the aggregation function and the underlying univariate risk measure. The primary obstacle in addressing this issue lies in the requirement to assess the aggregation function for each scenario within the underlying probability space, as well as for every potential selection of the capital allocation vector, which serves as the decision variable in the optimization problem.

In contrast, our selection of the aggregation function and the underlying risk measure serves as a complement to the research conducted in [23]. Specifically, while their aggregation function encompasses models that extend beyond the standard Eisenberg-Noe framework, incorporating a singular characteristic expressed through binary variables, our aggregation function focuses on the standard Eisenberg-Noe model, which can be expressed in terms of a linear programming problem parameterized by the scenario and the capital allocation

vector. On the other hand, in [23], Ararat and Meimanjan examine the negative expectation (and also polyhedral convex risk measures) as the underlying risk measure. In contrast, our research focuses on value-at-risk (V@R) as the underlying risk measure. Therefore, the overarching vector optimization problem can still be conceptualized as a nested optimization problem. In order to compute the set-valued systemic risk measure, we employ mixed-binary linear programming scalarizations for non-convex vector optimization problems, given the inherent nature of the underlying risk measure V@R. As a result, the sensitive systemic risk measures in both our and their models lack the desirable theoretical properties, such as convexity and dual representations, that have been examined in previous studies on systemic risk measures. In fact, the convexity property is not satisfied by the values of these systemic risk measures, in general. Hence, a key finding of their study is that binary variables and the associated absence of concavity/convexity arise when employing more advanced aggregation mechanisms beyond the standard Eisenberg-Noe framework. However, our own fundamental observation is that binary variables and the accompanying lack of concavity/convexity manifest naturally when utilizing a more sophisticated underlying risk measure.

In [23], the authors utilize the Benson-type algorithm, as introduced in [24], to compute the set-valued sensitive risk measure. Given that the *non-trivial* boundary of our systemic risk measure is contained within a compact region, we propose a variation of the so-called grid algorithm introduced in [5], where grid points are evaluated by solving certain scalar mixed-integer programming problems, namely, the Pascoletti-Serafini and norm-minimizing scalarizations.

In order to implement the grid algorithm, we first solve the weighted-sum scalarization problem in order to construct the grid compact region. Using the upper set property of sensitive risk measures, we determine that if a grid point is acceptable, all grid points within the point's positive orthant are also acceptable and should be included in the set-valued risk measure, and vice versa. Using the Pascoletti-Serafini and norm-minimizing scalarization problems, the grid algorithm evaluates the acceptability of grid points.

As the grid algorithm requires solving finite-dimensional optimization problems (or feasibility checks in general), it relies on the assumption that the underlying probability space is finite. This potentially brings an obstacle for the applicability of our methods in cases where the random shock has a continuous distribution. For this reason, we also study the

sample-average approximations (SAA) of set-valued systemic risk measures hosted by a general probability space. We employ the SAA framework proposed in [25], [26], and [27]. This approximation entails sampling independent random variables with identical distributions from the underlying probability space. By employing the previously mentioned scalarization techniques, we show that the sample-average approximated set-valued risk measure converges to its true set-valued risk measure, taking into account the Wijsman and Hausdorff topologies discussed in [28] and [29].

In the final phase of our research, we conduct a comprehensive computational study to validate the methodologies we have proposed. After reviewing the literature on preferential attachment models in [30, Chapter 8], we generate data for a network using the preferential attachment model described in [31]. To represent the inherent unpredictability of financial systems, we generate scenarios characterized by independent random vectors with identical distributions. In accordance with empirical findings in [32], we model the distributions of these vectors using the Pareto distribution, which depicts heavy-tailed behavior effectively. In addition, sensitivity analyses are performed to assess the impact of scenarios, correlation coefficients, and Bollobás network parameters on systemic risk measures.

The subsequent chapters of this thesis are structured as follows. In Chapter 2, we discuss the preliminary concepts and notations that are utilized throughout the remainder of the thesis. In Chapter 3, we thoroughly examine the Eisenberg-Noe network model and its mathematical programming characterizations of the set of all clearing vectors. In Chapter 4, we examine the sensitive systemic risk measures and the corresponding mixed-integer scalarizations. In Chapter 5, we study the sample-average approximation and show the convergence of the set-valued sample-average approximated risk measure to its true counterpart in the Wijsman and Hausdorff senses. The computational results are presented in Chapter 6.

Chapter 2

Preliminaries

In this chapter, we will introduce some fundamental concepts and notations that will be utilized throughout the remainder of the discussion. To that end, given $a, b \in \mathbb{R}$, we define $a \wedge b$ as the minimum of a and b, and $a \vee b$ as the maximum of a and b. We also denote $a^+ = 0 \vee a$ and $a^- = 0 \vee (-a)$.

Similarly, let $n \in \mathbb{N}$, we denote by $\mathbb{R}^n$, the n-dimensional Euclidean space. For vectors $\boldsymbol{a} = (a_1, \ldots, a_n)^\top$, $\boldsymbol{b} = (b_1, \ldots, b_n)^\top \in \mathbb{R}^n$, we define the element-wise minimum and maximum as follows:

$$\boldsymbol{a} \wedge \boldsymbol{b} = (a_1 \wedge b_1, \ldots, a_n \wedge b_n)^\top, \quad \boldsymbol{a} \vee \boldsymbol{b} = (a_1 \vee b_1, \ldots, a_n \vee b_n)^\top.$$

Moreover, we denote $\mathbf{1} = (1, \ldots, 1)^\top \in \mathbb{R}^n$, $\mathbf{0} = (0, \ldots, 0)^\top \in \mathbb{R}^n$, where the dimension n of the vector is understood from the context. Additionally, we define $\boldsymbol{a}^+ = \mathbf{0} \vee \boldsymbol{a}$ and $\boldsymbol{a}^- = \mathbf{0} \vee (-\boldsymbol{a})$.

The notations $\boldsymbol{a} \leq \boldsymbol{b}$ and $\boldsymbol{a} < \boldsymbol{b}$ indicate that $a_i \leq b_i$ and $a_i < b_i$ respectively, for each $i \in \{1, \ldots, n\}$. We also introduce $\mathbb{R}^n_+ = \{\boldsymbol{x} \in \mathbb{R}^n \mid \mathbf{0} \leq \boldsymbol{x}\}$, where the elements are referred to as non-negative. Similarly, we define $\mathbb{R}^n_{++} = \{\boldsymbol{x} \in \mathbb{R}^n \mid \mathbf{0} < \boldsymbol{x}\}$, where the elements are referred to as positive.

We say that a function $f : \mathbb{R}^n \to \mathbb{R}$ is strictly increasing if $\boldsymbol{a} \leq \boldsymbol{b}$ and $\boldsymbol{a} \neq \boldsymbol{b}$ imply $f(\boldsymbol{a}) < f(\boldsymbol{b})$ for every $\boldsymbol{a}, \boldsymbol{b} \in \mathbb{R}^n$.

The ℓ^∞ norm of a vector $\boldsymbol{a}$, denoted as $\|\boldsymbol{a}\|_\infty$, is defined as the maximum absolute value of its elements. In other words,

$$\|\boldsymbol{a}\|_\infty = \max_{i\in\{1,\dots,n\}} |a_i|.$$

Consider a matrix $\boldsymbol{A} \in \mathbb{R}^{m\times n}$, where m, $n \in \mathbb{N}$. We define $\|\boldsymbol{A}\|_\infty$ as the maximum of the ℓ^∞ norms of each row of $\boldsymbol{A}$. Mathematically,

$$\|\boldsymbol{A}\|_\infty = \max_{1\le i\le m} \|\boldsymbol{A}_i\|_\infty,$$

where, $\boldsymbol{A}_i$ denotes the i-th row of matrix $\boldsymbol{A}$.

For every $\boldsymbol{y} \in \mathbb{R}^n$, the distance from a point $\boldsymbol{y}$ to a set $A \subseteq \mathbb{R}^n$ is defined as $d(\boldsymbol{y}, A) := \inf_{\boldsymbol{x}\in A} \|\boldsymbol{y} - \boldsymbol{x}\|_2$, with the convention $\inf\{\emptyset\} = +\infty$. Let $B \subseteq \mathbb{R}^n$. The Hausdorff distance between A and B, denoted as $\mathbb{H}(A, B)$, is given by [33, Theorem 7.3.1]

$$\mathbb{H}(A, B) = \max\{\mathbb{D}(A, B), \mathbb{D}(B, A)\},$$

where $\mathbb{D}(A, B) = \sup_{\boldsymbol{x}\in A} d(\boldsymbol{x}, B)$.

The indicator function of set A, denoted as $1_A(\cdot) : \mathbb{R} \to \mathbb{R}$, is defined as

$$1_A(x) = \begin{cases} 1, & \text{if } x \in A \\ 0, & \text{otherwise,} \end{cases}$$

where $x \in A$ denotes that x belongs to the set A.

Chapter 3

The Eisenberg-Noe Model

In the realm of financial networks, the concept of systemic risk pertains to the possibility of a shock or disruption spreading across interlinked financial institutions, specifically banks, resulting in the collapse or distress of numerous institutions and potentially triggering extensive financial instability [3]. Furthermore, in the context of financial networks, aggregation functions assume a critical role in establishing measures of systemic risk. The function Λ is defined as a mapping from the vector space $\mathbb{R}^n$ to the scalar field $\mathbb{R}$ [5, 3].

The field of financial networks has experienced notable progress, primarily due to the pioneering contributions made by the Eisenberg-Noe network model. The model proposed in [14] has provided a foundational framework for conducting a comprehensive analysis of interbank payment systems. This model has yielded valuable insights into the complex interconnections between financial institutions, shedding light on the transmission of shocks and the possibility of contagion [14]. This chapter extensively examines the profound implications of the Eisenberg-Noe model.

To begin, we establish the conceptual framework of an Eisenberg-Noe network, which serves as a representation of a financial system comprising interconnected institutions:

Definition 3.0.1. *[14, Section 2.2] A quadruple* $(\mathcal{N}, \boldsymbol{\pi}, \bar{\boldsymbol{p}}, \boldsymbol{x})$ *is called an Eisenberg-Noe network if it satisfies the following conditions:*

- $\mathcal{N} = \{1, \ldots, n\}$ *is the index set of nodes in a network representing a financial system*

of n institutions.

- *For every $i \in \mathcal{N}$, $\bar{p}_i > 0$ denotes the total amount of liabilities of node i. We refer to $\bar{\boldsymbol{p}}$ as the* total obligation vector*.*
- $\boldsymbol{\pi} = (\pi_{ij})_{i,j\in\mathcal{N}} \in \mathbb{R}_+^{n\times n}$ *is the relative liability matrix with $\pi_{ii} = 0$ and $\sum_{j=1}^n \pi_{ij} < n$ for each $i \in \mathcal{N}$.*
- $\boldsymbol{x} = (x_1, \ldots, x_n)^\top \in \mathbb{R}_+^n$ *denotes the operating cash flow vector.*

The matrix $\boldsymbol{\pi}$ represents the relative liability distribution among nodes, indicating the proportion of liabilities that a node owes to other nodes. The adoption of the assumption of zero diagonal entries serves to prevent nodes from having liabilities towards themselves. The inequality $\sum_{j=1}^n \pi_{ij} < n$ ensures that no node in the network possesses all the claims. By utilizing the total obligation vector $\bar{\boldsymbol{p}}$ and the relative liability matrix $\boldsymbol{\pi}$, it is possible to calculate the nominal liability l_{ij} of node i to node j as $l_{ij} = \pi_{ij}\bar{p}_i$.

Next, we proceed to introduce the notion of a clearing payment vector, which adheres to the principles of limited liability and absolute priority within an EN network.

Definition 3.0.2. *[14, Definition 1] A vector $\boldsymbol{p} \in [\boldsymbol{0}, \bar{\boldsymbol{p}}]$ is called a clearing payment vector for the Eisenberg-Noe network if it satisfies the following two properties:*

- Limited liability*: For each $i \in \mathcal{N}$, $p_i \leq \sum_{j=1}^n \pi_{ji}p_j + x_i$, indicating that each node cannot pay more than it possesses.*
- Absolute priority*: For each $i \in \mathcal{N}$, $p_i = \bar{p}_i$ or $p_i = \sum_{j=1}^n \pi_{ji}p_j + x_i$, implying that each node meets its obligations in full or defaults by paying as much as it has.*

In the context of the EN network, consider the function $\psi : [\boldsymbol{0}, \bar{\boldsymbol{p}}] \to [\boldsymbol{0}, \bar{\boldsymbol{p}}]$ defined as follows:

$$\psi(\boldsymbol{p}) = (\boldsymbol{\pi}^\top \boldsymbol{p} + \boldsymbol{x}) \wedge \bar{\boldsymbol{p}}.$$

Eisenberg and Noe in [14] show that a clearing vector $\boldsymbol{p}$ in an EN network is a fixed point of the function ψ, meaning that $\psi(\boldsymbol{p}) = \boldsymbol{p}$.

We now state the main results of Eisenberg-Noe model.

Theorem 3.0.3. *[14, Theorem 1] For every EN network $(\boldsymbol{\pi}, \bar{\boldsymbol{p}}, \boldsymbol{x})$, the following statements hold:*

a. There exist a greatest clearing payment vector $\boldsymbol{p}^+$ and a least clearing payment vector $\boldsymbol{p}^-$.

b. Given two arbitrary clearing payment vectors $\boldsymbol{p'}$ and $\boldsymbol{p''}$, the net equities after clearing are the same, i.e.,

$$\left(\boldsymbol{\pi}^\top \boldsymbol{p'} + \boldsymbol{x} - \bar{\boldsymbol{p}}\right)^+ = \left(\boldsymbol{\pi}^\top \boldsymbol{p''} + \boldsymbol{x} - \bar{\boldsymbol{p}}\right)^+.$$

In addition to the theoretical analysis of clearing payment vectors in the Eisenberg-Noe model, a mathematical programming characterization exists that offers a computational methodology for identifying these vectors. The formulation takes into account the constraints of limited liability and absolute priority in order to ascertain the clearing payment vector.

We denote a payment vector as $\boldsymbol{p} = (p_1, \ldots, p_n)^\top$. The model for finding a clearing payment vector can be defined in the following lemma.

Lemma 3.0.4. *[14, Lemma 6] For EN network, let $f : \mathbb{R}^n \to \mathbb{R}$ be a strictly increasing function. Consider the following mathematical programming problem:*

$$\begin{aligned} \max \quad & f(\boldsymbol{p}) \\ s.t. \quad & \boldsymbol{p} \leq \boldsymbol{\pi}^\top \boldsymbol{p} + \boldsymbol{x} \\ & \boldsymbol{p} \in [\boldsymbol{0}, \bar{\boldsymbol{p}}]. \end{aligned} \tag{3.0.1}$$

If $\boldsymbol{p}^\star \in \mathbb{R}^n_+$ is an optimal solution to (3.0.1)*, then it is a clearing payment vector for the network.*

Lemma 3.0.4 establishes the correlation between the optimization problem denoted as (3.0.1) and the process of determining clearing payment vectors. The statement asserts that any optimal solution of the given equation, denoted as (3.0.1), is a valid clearing payment vector that adheres to both the limited liability and absolute priority conditions.

Based on the formulation in (3.0.1), an aggregation function $\Lambda^{\mathrm{EN}} : \mathbb{R}^n \to \mathbb{R} \cup \{-\infty\}$ for the Eisenberg-Noe model can be defined as:

$$\Lambda^{\mathrm{EN}}(\boldsymbol{x}) := \begin{cases} \sup\{\boldsymbol{1}^\top \boldsymbol{p} \mid \boldsymbol{p} \leq \boldsymbol{\pi}^\top \boldsymbol{p} + \boldsymbol{x}, \boldsymbol{p} \in [\boldsymbol{0}, \bar{\boldsymbol{p}}]\}, & \text{if } \boldsymbol{x} \in \mathbb{R}^n_+ \\ -\infty, & \text{if } \boldsymbol{x} \notin \mathbb{R}^n_+, \end{cases} \tag{3.0.2}$$

that is, $\Lambda^{\mathrm{EN}}(\boldsymbol{x})$ represents the optimal value of the mathematical programming problem (3.0.1) when $f(\boldsymbol{p}) = \mathbf{1}^\top \boldsymbol{p}$.

Furthermore, an important property of the aggregation function Λ^{EN} can be observed in the following lemma

Lemma 3.0.5. *Λ^{EN} is a continuous, concave and increasing function on $\mathbb{R}^n_+$.*

Proof. We will prove the continuity and concavity parts of $\Lambda^{\mathrm{EN}}(\boldsymbol{x})$ by taking its dual formulation as follows:

$$\begin{aligned} \min \quad & \boldsymbol{\lambda}^\top \bar{\boldsymbol{p}} + \boldsymbol{\mu}^\top \boldsymbol{x} \\ \text{s.t.} \quad & \boldsymbol{\lambda} + (\boldsymbol{I} - \boldsymbol{\pi})^\top \boldsymbol{\mu} \geq \mathbf{1} \\ & \boldsymbol{\lambda} \geq \mathbf{0} \\ & \boldsymbol{\mu} \geq \mathbf{0}, \end{aligned} \tag{3.0.3}$$

where $\boldsymbol{I}$ is the $n \times n$ identity matrix.

Based on the fact that the objective function in (3.0.3) is composed of pointwise affine functions, it can be inferred that (3.0.3) exhibits concavity in relation to $\boldsymbol{x} \in \mathbb{R}^n_+$. Furthermore, it can be observed that the objective function in (3.0.3) is bounded from below. As a result, the optimal value of the dual problem demonstrates continuity in relation to the variable $\boldsymbol{x}$. Given that the formulation presented in equation (3.0.2) represents a feasible linear programming (LP) formulation, it can be concluded that the principle of strong duality is applicable. As a result, the function Λ^{EN} exhibits continuity and concavity with respect to the variable $\boldsymbol{x}$.

To show that Λ^{EN} is increasing in $\boldsymbol{x}$, we fix $\bar{\boldsymbol{p}}$ and $\boldsymbol{\pi}$ as the liability vector and relative liability matrix, respectively. Furthermore, let $\boldsymbol{p}(\boldsymbol{x})$ be a feasible solution to $\Lambda^{\mathrm{EN}}(\boldsymbol{x})$, and assume that $\boldsymbol{z} \geq \boldsymbol{x}$. Then, $\boldsymbol{p}(\boldsymbol{x}) \leq \boldsymbol{\pi}^\top \boldsymbol{p}(\boldsymbol{x}) + \boldsymbol{x} \leq \boldsymbol{\pi}^\top \boldsymbol{p}(\boldsymbol{x}) + \boldsymbol{z}$, which implies that $\boldsymbol{p}(\boldsymbol{x})$ is a feasible solution to $\Lambda^{\mathrm{EN}}(\boldsymbol{z})$. Therefore, $\Lambda^{\mathrm{EN}}(\boldsymbol{z}) \geq \Lambda^{\mathrm{EN}}(\boldsymbol{x})$. Thus, Λ^{EN} is increasing in $\boldsymbol{x}$. □

Expanding upon the aforementioned outcome, we hereby present a lemma that offers a comprehensive depiction of the set of the collection of *all* clearing payment vectors.

Lemma 3.0.6. *Given an operating cash flow vector $\boldsymbol{x}$, a relative liability matrix $\boldsymbol{\pi}$, and a liability vector $\bar{\boldsymbol{p}}$, the set of all clearing payment vectors of the EN network can be represented*

as follows:

$$C(\boldsymbol{x}) := \Big\{\boldsymbol{p} \in [\boldsymbol{0}, \bar{\boldsymbol{p}}] \mid \boldsymbol{p} \leq \boldsymbol{\pi}^\top \boldsymbol{p} + \boldsymbol{x}, \exists \boldsymbol{y} \in \{0,1\}^n : \boldsymbol{p} \geq \bar{\boldsymbol{p}}\boldsymbol{y}, \boldsymbol{p} \geq \boldsymbol{\pi}^\top \boldsymbol{p} + \boldsymbol{x} - \boldsymbol{y}Q\Big\}, \quad (3.0.4)$$

where $Q \geq \max\limits_{1 \leq i \leq n} \left(\sum_{j=1}^n \pi_{ji}\bar{p}_i + x_i\right)$ *is a constant.*

Remark 3.0.7. *Note that for each node* i *and* $\boldsymbol{p} \in [\boldsymbol{0}, \bar{\boldsymbol{p}}]$*, it holds that* $\sum_{j=1}^n \pi_{ji} p_j \leq \max\limits_{1 \leq i \leq n} \sum_{j=1}^n \pi_{ji}\bar{p}_i$*. Thus,* $Q \geq \max\limits_{1 \leq i \leq n} (\sum_{j=1}^n \pi_{ji}\bar{p}_i + x_i)$ *ensures that when* $y_i = 1$*, the constraint* $\boldsymbol{p} \geq \boldsymbol{\pi}^\top \boldsymbol{p} + \boldsymbol{x} - \boldsymbol{y}Q$ *is trivial.*

Proof.

Claim 1: If $\boldsymbol{p}$ is a clearing payment vector, then $\boldsymbol{p} \in C$.

Proof of Claim 1: Since $\boldsymbol{p}$ is a clearing payment vector, it satisfies the limited liability axiom, which is represented by the constraint $\boldsymbol{p} \leq \boldsymbol{\pi}^\top \boldsymbol{p} + \boldsymbol{x}$. To show that the other constraints in (3.0.4) also hold, let us set $\boldsymbol{y}$ as follows:

$$y_i = \begin{cases} 0, & \text{if } p_i < \bar{p}_i \\ 1, & \text{if } p_i = \bar{p}_i, \end{cases} \quad (3.0.5)$$

and consider the following two cases:

- Case 1: For a particular node i, assume that $p_i = \bar{p}_i$. Then, by (3.0.5), $y_i = 1$. Thus, the constraint $p_i \geq \bar{p}_i y_i$ is satisfied and the constraint $p_i \geq \sum_{j=1}^n \pi_{ji} p_j + x_i - yQ$ is trivially satisfied by Remark 3.0.7. Hence, (p_i, y_i) satisfies all the constraints in (3.0.4).
- Case 2: For a particular node i, assume that $p_i = \sum_{j=1}^n \pi_{ji} p_j + x_i < \bar{p}_i$. Then, by (3.0.5), $y_i = 0$. Thus, the constraint $p_i \geq \bar{p}_i y_i$ is trivially satisfied and the constraint $p_i \geq \sum_{j=1}^n \pi_{ji} p_j + x_i - yQ$ yields that $p_i = \sum_{j=1}^n \pi_{ji} p_j + x_i$. Hence, (p_i, y_i) satisfies all the constraints in (3.0.4).

Hence, Claim 1 holds.

Claim 2: If $\boldsymbol{p} \in C$, then $\boldsymbol{p}$ is a clearing payment vector.

Proof of Claim 2: Assume that $\boldsymbol{p} \in C$. Then, there exists $\boldsymbol{y}$ such that $(\boldsymbol{p}, \boldsymbol{y})$ satisfies all the constraints in (3.0.4). In order to show that $\boldsymbol{p}$ is a clearing payment vector, we need to

demonstrate that $\boldsymbol{p}$ satisfies two conditions: limited liability and absolute priority. The fact that $\boldsymbol{p} \in C$ enforces $\boldsymbol{p}$ to satisfy the limited liability condition by the constraint $\boldsymbol{p} \leq \boldsymbol{\pi}^\top \boldsymbol{p} + \boldsymbol{x}$. To show that $\boldsymbol{p}$ must also satisfy the absolute priority condition, we consider the following two cases:

- Case 1: For a particular node i, if $y_i = 1$, then $p_i = \bar{p}_i \leq \sum_{j=1}^n \pi_{ij} p_j + x_i$ by the constraints $p_i \leq \bar{p}_i$, $p_i \geq \bar{p}_i y_i$ and $p_i \leq \sum_{j=1}^n \pi_{ji} p_j + x_i$. Therefore, $p_i = \bar{p}_i \wedge (\sum_{j=1}^n \pi_{ij} p_j + x_i)$, and thus the absolute priority condition holds.
- Case 2: For a particular node i, if $y_i = 0$, then $p_i = \sum_{j=1}^n \pi_{ji} p_j + x_i \leq \bar{p}_i$ by the constraints $p_i \geq \sum_{j=1}^n \pi_{ji} p_j + x_i - yQ$, $p_i \leq \sum_{j=1}^n \pi_{ji} p_j + x_i$ and $p_i \leq \bar{p}_i$. Therefore, $p_i = \bar{p}_i \wedge (\sum_{j=1}^n \pi_{ij} p_j + x_i)$, and thus the absolute priority condition holds.

Hence, Claim 2 holds. □

Chapter 4

Sensitive Set-Valued Systemic Risk Measures

In the framework of systemic risk analysis, we take into account a set-valued systemic risk measure, R, which represents the set of disturbances to the cash flows of individual firms that preserve the measure's acceptance criteria. This metric depicts the joint behavior and related risks of a group of firms' operating cash flow. It is built by combining the EN aggregation function structure with the value-at-risk base risk measure. Allowable amounts of aggregate risk are specified by the acceptance set of V@R.

We look at the concept of bank grouping in order to apply the sensitive set-valued systemic risk measure to a network of banks. This helps us keep the dimensions of the risk measure under control. Then, to regulate the total clearing payments in the network, we create a set-valued grouped sensitive systemic risk measure. The metric accounts for equal capital injections among bank groupings. The risk measure sensitively combines the Eisenberg-Noe aggregation function with V@R, with capital requirements applied before aggregation.

To that aim, consider Ω to be a set of scenarios. A random vector $\boldsymbol{X} : \Omega \to \mathbb{R}^n$ describes an operating cash flow, where $\boldsymbol{X}(\omega^s)$ represents the operating cash flow across the firms if the scenario ω^s is realized, where $s \in \mathbb{N}$. We have $\boldsymbol{X} \in \boldsymbol{\mathcal{X}} \subseteq L^0(\mathbb{R}^n)$ containing all constants, e.g., $\boldsymbol{\mathcal{X}} = L^\infty(\mathbb{R}^n)$ the linear space of all bounded measurable random vectors on $(\Omega, \mathcal{F})$.

To begin, we provide a definition of V@R, a widely used monetary risk measure. It

calculates the least capital amount z necessary to maintain the probability of a negative outcome below a certain threshold λ [34, Section 4.4]. V@R can be defined using the notion of acceptance set as follows:

Definition 4.0.1. *[34, Section 4.4] The function V@R is a mapping from the space of univariate measurable functions including all constants, denoted as L_1^0, to $\mathbb{R}$, defined as:*

$$V@R_\lambda(Y) = \inf\{z \in \mathbb{R} \mid Y + z \in \mathcal{A}_\lambda^{V@R}\}, \tag{4.0.1}$$

where $Y \in L_1^0$ and the acceptance set *of V@R is defined as:*

$$\mathcal{A}_\lambda^{V@R} = \{Y \in L_1^0 \mid V@R_\lambda(Y) \leq 0\} = \{Y \in L_1^0 \mid \mathbb{P}(Y < 0) \leq \lambda\}. \tag{4.0.2}$$

The V@R function meets the properties in the following proposition:

Proposition 4.0.2. *[34, Section 4.4] $V@R : L_1^0 \to \mathbb{R}$ is a univariate function satisfying the following properties:*

1. ***Monotonicity**: For any $X, Y \in L_1^0$, if $X \geq Y$, then $V@R(Y) \geq V@R(X)$.*
2. ***Translativity**: For any $X \in L_1^0$ and $k \in \mathbb{R}$, $V@R(X + k) = V@R(X) - k$.*
3. ***Positive Homogeneity**: For any $X \in L_1^0$ and $\gamma > 0$, $V@R(\gamma X) = \gamma\, V@R(X)$.*

Let $\Lambda : \mathbb{R}^n \to \mathbb{R}$ be an aggregation function, and take into account the following assumption before continuing with the discussion of the systemic set-valued risk measure.

Assumption 4.0.3. *The aggregation function Λ satisfies the monotonicity property. That is, for any $\boldsymbol{x}, \boldsymbol{y} \in \mathbb{R}^n$ such that $\boldsymbol{x} \geq \boldsymbol{y}$, it holds that $\Lambda(\boldsymbol{x}) \geq \Lambda(\boldsymbol{y})$.*

When applied to the base risk measure V@R, the set-valued systemic risk measure introduced in [5] is defined as follows:

Definition 4.0.4. *The set-valued sensitive systemic risk measure is a function mapping from L_n^0 to $2^{\mathbb{R}^n}$, the power set of $\mathbb{R}^n$ including the empty set, defined by the following:*

$$\begin{aligned} R(\boldsymbol{X}) &= \{\boldsymbol{z} \in \mathbb{R}^n \mid \Lambda(\boldsymbol{X} + \boldsymbol{z}) \in \mathcal{A}_\lambda^{V@R}\} \\ &= \{\boldsymbol{z} \in \mathbb{R}^n \mid \mathbb{P}[(\Lambda(\boldsymbol{X} + \boldsymbol{z})) < \alpha] \leq \lambda\} \\ &= \{\boldsymbol{z} \in \mathbb{R}^n \mid V@R_\lambda(\Lambda(\boldsymbol{X} + \boldsymbol{z})) \leq \alpha\}, \end{aligned} \tag{4.0.3}$$

where $\alpha \geq 0$, $\lambda \in (0, 1)$, $\boldsymbol{X} \in L_n^0$ and $\mathcal{A}_\lambda^{V@R} = \{Y \in L_1^0 \mid V@R_\lambda(Y) \leq \alpha\}$.

The operating cash flow of a group of n banks is denoted here by the expression $\boldsymbol{X} \in L_n^0$. Potential systemic hazards posed by the coordinated actions of these firms are quantified by R, a set-valued sensitive systemic risk measure. Set-valued systemic risk measures are characterized by the capital injections $\boldsymbol{z} \in \mathbb{R}^n$ to the cash flows $\boldsymbol{X}$ of individual firms that satisfy the measure's acceptance criteria.

Incorporating the single-firm risk measure V@R into the framework for systemic risk yields the sensitive systemic risk measure. The Λ function maps the cash flow profiles of the n firms $\boldsymbol{X}$ to a singular aggregate risk measure. The acceptance set $\mathcal{A}_\lambda^{\mathrm{V@R}}$ defines the acceptable aggregate risk levels at a predefined threshold λ.

Now, we present a demonstration of certain properties pertaining to set-valued systemic risk measures, as outlined in the work of [5]. We commence our analysis by considering the subsequent lemma:

Lemma 4.0.5. *The set-valued sensitive risk measure $R : L_n^0 \to 2^{\mathbb{R}^n}$ in Definition 4.0.4 satisfies the following properties:*

i. ***Monotonicity**: For any $\boldsymbol{X}, \boldsymbol{Y} \in L_n^0$, if $\boldsymbol{X} \geq \boldsymbol{Y}$, then $R(\boldsymbol{X}) \supseteq R(\boldsymbol{Y})$.*

ii. ***Translativity**: For any $\boldsymbol{X} \in L_n^0$ and $\boldsymbol{k} \in \mathbb{R}^n$, $R(\boldsymbol{X} + \boldsymbol{k}) = R(\boldsymbol{X}) - \boldsymbol{k}$.*

Proof.

i. For any $\boldsymbol{X}, \boldsymbol{Y} \in L_n^0$, let $\boldsymbol{z}$ be an element of $R(\boldsymbol{Y})$ so that $\mathrm{V@R}_\lambda(\Lambda(\boldsymbol{Y} + \boldsymbol{z})) \leq \alpha$. By assuming $\boldsymbol{X} \geq \boldsymbol{Y}$, we have $\boldsymbol{X} + \boldsymbol{z} \geq \boldsymbol{Y} + \boldsymbol{z}$. Utilizing the monotonicity properties of Λ and V@R, we find $\Lambda(\boldsymbol{X} + \boldsymbol{z}) \geq \Lambda(\boldsymbol{Y} + \boldsymbol{z})$ and $\mathrm{V@R}_\lambda(\Lambda(\boldsymbol{X} + \boldsymbol{z})) \leq \mathrm{V@R}_\lambda(\Lambda(\boldsymbol{Y} + \boldsymbol{z}))$. As $\mathrm{V@R}_\lambda(\Lambda(\boldsymbol{Y} + \boldsymbol{z})) \leq \alpha$, it follows that $\mathrm{V@R}_\lambda(\Lambda(\boldsymbol{X} + \boldsymbol{z})) \leq \alpha$. Therefore, $\boldsymbol{z} \in R(\boldsymbol{X})$, establishing $R(\boldsymbol{X}) \supseteq R(\boldsymbol{Y})$.

ii. Let $\boldsymbol{X} \in L_n^0$, $\boldsymbol{k} \in \mathbb{R}^n$ and $\boldsymbol{z} \in R(\boldsymbol{X})$. This means that $\mathrm{V@R}_\lambda(\Lambda(\boldsymbol{X} + \boldsymbol{z})) \leq \alpha$. Now, we need to show that $\mathrm{V@R}_\lambda(\Lambda((\boldsymbol{X} + \boldsymbol{k}) + (\boldsymbol{z} - \boldsymbol{k}))) \leq \alpha$. Therefore, we have $\mathrm{V@R}_\lambda(\Lambda(\boldsymbol{X} + \boldsymbol{z})) \leq \alpha$. Hence, we have shown that $\boldsymbol{z} - \boldsymbol{k} \in R(\boldsymbol{X} + \boldsymbol{k})$. Now, let $\boldsymbol{z'} \in R(\boldsymbol{X} + \boldsymbol{k})$. This means that $\mathrm{V@R}_\lambda(\Lambda((\boldsymbol{X} + \boldsymbol{k}) + \boldsymbol{z'})) \leq \alpha$. Therefore, $\mathrm{V@R}_\lambda(\Lambda(\boldsymbol{X} + (\boldsymbol{z'} + \boldsymbol{k}))) \leq \alpha$. Hence, we have shown that $\boldsymbol{z'} + \boldsymbol{k} \in R(\boldsymbol{X})$. Therefore, we can conclude that $R(\boldsymbol{X} + \boldsymbol{k}) = R(\boldsymbol{X}) - \boldsymbol{k}$.

□

In the subsequent analysis, we will examine the concept of bank grouping, which involves the partitioning of banks into distinct groups denoted by $\mathcal{J} = \{1, \ldots, i\}$, where $i \in \mathbb{N}$. Let n_j denote the cardinality of the set of banks in group j, where j belongs to the set $\mathcal{J}$. The banks within each group will possess an identical designated capital level. The categorization of banks into these distinct groups enables us to effectively manage the dimension of the risk measure [5].

For example, let us consider a network comprising a total of n banks. Let us consider a case where i is equal to 2, indicating the presence of two distinct bank groups: core banks and peripheral banks. The partition of $\mathcal{N}$ is denoted as $\mathcal{C}$ and $\mathcal{P}$, where $\mathcal{C}$ corresponds to the set of core banks and $\mathcal{P}$ corresponds to the set of peripheral banks in the given network. Let $\boldsymbol{B}_{\mathcal{C}} \in \mathbb{R}^{i \times |\mathcal{C}|}$ be a matrix with a row of 1's in the first row and a row of 0's in the second row. Similarly, let $\boldsymbol{B}_{\mathcal{P}} \in \mathbb{R}^{i \times |\mathcal{P}|}$ be a matrix with a row of 1's in the second row and a row of 0's in the first row. The grouping matrix $\boldsymbol{B} \in \mathbb{R}^{i \times n}$ is defined as

$$\boldsymbol{B} := [\boldsymbol{B}_{\mathcal{C}} \quad \boldsymbol{B}_{\mathcal{P}}].$$

Example 4.0.6. *Assume that there is a network of 5 banks. Therefore,* $|\mathcal{N}| = 5$*, namely, banks 1 to 5. Let* $\mathcal{C} = \{1, 2\}$ *and* $\mathcal{P} = \{3, 4, 5\}$*. Then:*

$$\boldsymbol{B}_{\mathcal{C}} = \begin{bmatrix} 1 & 1 \\ 0 & 0 \end{bmatrix}, \quad \boldsymbol{B}_{\mathcal{P}} = \begin{bmatrix} 0 & 0 & 0 \\ 1 & 1 & 1 \end{bmatrix},$$

therefore,

$$\boldsymbol{B} = \begin{bmatrix} 1 & 1 & 0 & 0 & 0 \\ 0 & 0 & 1 & 1 & 1 \end{bmatrix}.$$

Next, our objective is to alter the predefined variable R in Definition 4.0.4 so that it becomes a set-valued grouped sensitive systemic risk measure that is constructed using an aggregation function of the underlying network model and the V@R base risk measure. In this modification, the capital injections are distributed equally among each bank group, and

the resulting measure is defined as follows:

$$\begin{aligned} R(\boldsymbol{X}) &= \{\boldsymbol{z} \in \mathbb{R}^i \,|\, \Lambda(\boldsymbol{X} + \boldsymbol{B}^\top \boldsymbol{z}) \in \mathcal{A}_\lambda^{\mathrm{V@R}}\} \\ &= \{\boldsymbol{z} \in \mathbb{R}^i \,|\, \mathbb{P}(\Lambda(\boldsymbol{X} + \boldsymbol{B}^\top \boldsymbol{z}) < \alpha) \leq \lambda\} \\ &= \{\boldsymbol{z} \in \mathbb{R}^i \,|\, \mathrm{V@R}_\lambda(\Lambda(\boldsymbol{X} + \boldsymbol{B}^\top \boldsymbol{z})) \leq \alpha\}, \end{aligned} \tag{4.0.4}$$

where $\alpha \geq 0$, $\lambda \in (0,1)$, $\boldsymbol{X} \in L_n^0$ and $\mathcal{A}_\lambda^{\mathrm{V@R}} = \{Y \in L_1^0 \mid \mathrm{V@R}_\lambda(Y) \leq \alpha\}$.

Remark 4.0.7. *The set-valued insensitive systemic risk measure can be described as follows:*

$$\begin{aligned} \boldsymbol{R}^{insensitive}(\boldsymbol{X}) &= \{\boldsymbol{z} \in \mathbb{R}^i \,|\, \Lambda(\boldsymbol{X}) + \boldsymbol{z}^\top \boldsymbol{B}\mathbf{1} \in \mathcal{A}_\lambda^{V@R}\} \\ &= \{\boldsymbol{z} \in \mathbb{R}^i \,|\, \mathbb{P}(\Lambda(\boldsymbol{X}) + \boldsymbol{z}^\top \boldsymbol{B}\mathbf{1} < \alpha) \leq \lambda\} \\ &= \{\boldsymbol{z} \in \mathbb{R}^i \,|\, V@R_\lambda(\Lambda(\boldsymbol{X})) \leq \boldsymbol{z}^\top \boldsymbol{B}\mathbf{1} + \alpha\}. \end{aligned} \tag{4.0.5}$$

$R^{insensitive}$ is a monotonic set-valued function such that if $\boldsymbol{X}, \boldsymbol{Y} \in \boldsymbol{L}_n^0$ and $\boldsymbol{X} \geq \boldsymbol{Y}$, then $R^{insensitive}(\boldsymbol{X}) \supseteq R^{insensitive}(\boldsymbol{Y})$. Moreover, $R^{insensitive}(\boldsymbol{X})$ is a halfspace.

Lemma 4.0.8. *For $\boldsymbol{X} \in \boldsymbol{L}_n^0$, R satisfies the upper set property such that:*

$$R(\boldsymbol{X}) = R(\boldsymbol{X}) + \mathbb{R}_+^i.$$

Proof. $R(\boldsymbol{X}) \subseteq R(\boldsymbol{X}) + \mathbb{R}_+^i$ is obvious. To prove the other subset, assume that $\boldsymbol{z} \in R(\boldsymbol{X})$, i.e., $\mathrm{V@R}_\lambda(\Lambda(\boldsymbol{X}+\boldsymbol{B}^\top \boldsymbol{z})) \leq \alpha$, and assume that $\boldsymbol{k} \in \mathbb{R}_+^i$. We need to show that $\boldsymbol{z}+\boldsymbol{k} \in R(\boldsymbol{X})$, that is, $\mathrm{V@R}_\lambda(\Lambda(\boldsymbol{X} + \boldsymbol{B}^\top(\boldsymbol{z} + \boldsymbol{k}))) \leq \alpha$. Since Λ is a monotonic aggregation function,

$$\Lambda(\boldsymbol{X} + \boldsymbol{B}^\top(\boldsymbol{z} + \boldsymbol{k})) \geq \Lambda(\boldsymbol{X} + \boldsymbol{B}^\top \boldsymbol{z}).$$

Since V@R is a monotonic risk measure,

$$\mathrm{V@R}_\lambda(\Lambda(\boldsymbol{X} + \boldsymbol{B}^\top(\boldsymbol{z} + \boldsymbol{k}))) \leq \mathrm{V@R}_\lambda(\Lambda(\boldsymbol{X} + \boldsymbol{B}^\top \boldsymbol{z})) \leq \alpha.$$

Therefore, $\boldsymbol{z} + \boldsymbol{k} \in R(\boldsymbol{X})$. Hence, $R(\boldsymbol{X}) \supseteq R(\boldsymbol{X}) + \mathbb{R}_+^i$. □

Remark 4.0.9. *Since Λ^{EN} possesses the monotonicity property as shown in Lemma 3.0.5, when Λ is specifically Λ^{EN}, R satisfies the monotonicity, translativity and upper set properties.*

Remark 4.0.10. *When $\Lambda = \Lambda^{EN}$ in the definition of $R(\boldsymbol{X})$,* (3.0.2) *implies the implicit condition $\boldsymbol{X} + \boldsymbol{B}^\top \boldsymbol{z} \geq 0$.*

Proposition 4.0.11. *When $\Lambda = \Lambda^{EN}$, as defined in* (3.0.2)*, we have $R(\boldsymbol{X}) \neq \emptyset$ if and only if $\alpha \leq 1^\top \bar{\boldsymbol{p}}$.*

Proof. Assume that $\alpha \leq \mathbf{1}^\top \bar{\boldsymbol{p}}$. Let $\boldsymbol{z} = \|\bar{\boldsymbol{p}}\|_2 \mathbf{1} \in \mathbb{R}^i$. We claim that $\boldsymbol{z} \in R(\boldsymbol{X})$. To prove the claim, it is enough to show that $\mathbb{P}\left(\Lambda^{\mathrm{EN}}(\boldsymbol{X} + \boldsymbol{B}^\top(\|\bar{\boldsymbol{p}}\|_2 \mathbf{1})) < \mathbf{1}^\top \bar{\boldsymbol{p}}\right) \leq \lambda$. To that end, for any scenario $\omega^s \in \Omega$, $s \in \mathbb{N}$,

$$\Lambda^{\mathrm{EN}}(\boldsymbol{x_s} + \boldsymbol{B}^\top(\|\bar{\boldsymbol{p}}\|_2 \mathbf{1})) = \sup\{\mathbf{1}^\top \boldsymbol{p} \mid \boldsymbol{p} \leq \boldsymbol{\pi}^\top \boldsymbol{p} + \boldsymbol{x_s} + \boldsymbol{B}^\top(\|\bar{\boldsymbol{p}}\|_2 \mathbf{1}), \boldsymbol{p} \in [\mathbf{0}, \bar{\boldsymbol{p}}]\}. \tag{4.0.6}$$

It is clear that $\boldsymbol{p} = \bar{\boldsymbol{p}}$ is a feasible solution to (4.0.6) as $\boldsymbol{x_s} \geq \mathbf{0}$ and $\boldsymbol{B}^\top(\|\bar{\boldsymbol{p}}\|_2 \mathbf{1}) \geq \bar{\boldsymbol{p}}$. Indeed, the optimal solution to (4.0.6) is $\boldsymbol{p}^\star = \bar{\boldsymbol{p}}$ as $\boldsymbol{p} \in [\mathbf{0}, \bar{\boldsymbol{p}}]$. Therefore, $\Lambda^{\mathrm{EN}}(\boldsymbol{x_s} + \boldsymbol{B}^\top(\|\bar{\boldsymbol{p}}\|_2 \mathbf{1})) = \mathbf{1}^\top \bar{\boldsymbol{p}}$ and $\mathbb{P}\{\omega^s\} 1_{(-\infty, 1^\top \bar{\boldsymbol{p}})}(\Lambda^{\mathrm{EN}}(\boldsymbol{x_s} + \boldsymbol{B}^\top(\|\bar{\boldsymbol{p}}\|_2 \mathbf{1}))) = 0$ for each $\omega^s \in \Omega$, $s \in \mathbb{N}$. Thus, $\mathbb{P}\left(\Lambda^{\mathrm{EN}}(\boldsymbol{X} + \boldsymbol{B}^\top(\|\bar{\boldsymbol{p}}\|_2 \mathbf{1})) < \mathbf{1}^\top \bar{\boldsymbol{p}}\right) = 0 \leq \lambda$ as $\lambda \in (0, 1)$. Hence, $\boldsymbol{z} \in R(\boldsymbol{X})$.

Conversely, if $\alpha > \mathbf{1}^\top \bar{\boldsymbol{p}}$, since $\boldsymbol{p} \in [\mathbf{0}, \bar{\boldsymbol{p}}]$, $\Lambda^{\mathrm{EN}}(\boldsymbol{x_s} + \boldsymbol{B}^\top \boldsymbol{z}) \leq \mathbf{1}^\top \bar{\boldsymbol{p}}$, for each $\omega^s \in \Omega$, $s \in \mathbb{N}$ and $z \in \mathbb{R}^i$. Therefore, $\mathbb{P}(\Lambda^{\mathrm{EN}}(\boldsymbol{X} + \boldsymbol{B}^\top \boldsymbol{z}) < \alpha) = 1 > \lambda$ as $\lambda \in (0, 1)$. Hence, $R(\boldsymbol{X}) = \emptyset$. □

4.1 Weighted-Sum Scalarizations

In this section, our objective is to address the weighted-sum scalarization problem of $R(\boldsymbol{X})$ as discussed in [35]. Solving the weighted-sum scalarization of $R(\boldsymbol{X})$ will serve as the initial step in order to compute $R(\boldsymbol{X})$. To achieve this, we assume Ω to be a finite fixed set of scenarios, with each $\omega^s \in \Omega = \{\omega^1, \ldots, \omega^S\}$ such that $S \in \mathbb{N}$, $\mathbb{P}\{\omega^s\} = 1/S$, $s \in \mathcal{S} = \{1, \ldots, S\}$. Note that when the sample space Ω is finite then the L^0 and L^∞ spaces are equivalent. Subsequently, we propose the utilization of a mixed-integer linear programming (MILP) formulation. We control the total amount of clearing payments to ensure that it does not fall below a specified threshold, denoted as α. Specifically, we focus on the evaluation of clearing payments using the aggregation function denoted as Λ^{EN}. In order to achieve this objective, let $(\mathcal{N}, \boldsymbol{\pi}, \bar{\boldsymbol{p}}, \boldsymbol{X})$ be an Eisenberg-Noe network.

Lemma 4.1.1. *Consider the following optimization problems:*

$$\mathcal{P}^{WS}(\boldsymbol{w}) = \inf\left\{\boldsymbol{w}^\top \boldsymbol{z} \,|\, \mathbb{P}\left(\Lambda^{EN}(\boldsymbol{X} + \boldsymbol{B}^\top \boldsymbol{z}) < \alpha\right) \leq \lambda,\, \boldsymbol{z} \in \mathbb{R}^i\right\}, \tag{4.1.1}$$

$$\begin{aligned}\mathcal{Z}^{WS}(\boldsymbol{w}) = \inf\Big\{\boldsymbol{w}^\top \boldsymbol{z} \,\Big|\, &\sum_{s=1}^{S} \mathbb{P}\{\omega^s\} y_s \geq 1 - \lambda,\, \boldsymbol{p}_s \leq \boldsymbol{\pi}^\top \boldsymbol{p}_s + \boldsymbol{x}_s + \boldsymbol{B}^\top \boldsymbol{z},\, \mathbf{0} \leq \boldsymbol{p}_s \leq \bar{\boldsymbol{p}},\\ &\mathbf{1}^\top \boldsymbol{p}_s \geq \alpha y_s,\, y_s \in \{0,1\},\, \boldsymbol{z} \in \mathbb{R}^i,\, \forall s \in \mathcal{S}\Big\},\end{aligned} \tag{4.1.2}$$

where $\alpha \geq 0$, $\lambda \in (0,1)$, $\boldsymbol{w} \in \mathbb{R}^i_+ \setminus \{\mathbf{0}\}$ *is a fixed direction, and* $\Lambda^{EN}(\boldsymbol{t})$ *as defined in* (3.0.2). *Then,* $\mathcal{P}^{WS}(\boldsymbol{w}) = \mathcal{Z}^{WS}(\boldsymbol{w})$. *If either problem has a finite optimal value, then the other problem also has a finite optimal value, and the optimal values are the same.*

The aforementioned lemma considers a two-stage stochastic programming problem with a chance constraint, denoted by (4.1.1). In order to solve this problem, a linearization approach is employed by incorporating binary variables. This transformation converts the problem into a mixed-integer optimization problem, denoted as (4.1.2).

Proof. Let $\left(\boldsymbol{z}, (\boldsymbol{p}_s, \boldsymbol{y}_s)_{s\in\mathcal{S}}\right)$ be a feasible solution for (4.1.2). Then, for each $s \in \mathcal{S}$, $\boldsymbol{p}_s$ is a feasible solution to $\Lambda^{\mathrm{EN}}(\boldsymbol{x_s} + \boldsymbol{B}^\top \boldsymbol{z})$. Hence, for each $s \in \mathcal{S}$:

$$\Lambda^{\mathrm{EN}}(\boldsymbol{x}_s + \boldsymbol{B}^\top \boldsymbol{z}) \geq \mathbf{1}^\top \boldsymbol{p}_s.$$

Thus, for each $s \in \mathcal{S}$,

$$\mathbb{P}\{\omega^s\} 1_{[\alpha,\infty)}(\Lambda^{\mathrm{EN}}(\boldsymbol{x}_s + \boldsymbol{B}^\top \boldsymbol{z})) \geq \mathbb{P}\{\omega^s\} 1_{[\alpha,\infty)}(\mathbf{1}^\top \boldsymbol{p}_s).$$

Then,

$$\sum_{s=1}^{S} \mathbb{P}\{\omega^s\} 1_{[\alpha,\infty)}(\Lambda^{\mathrm{EN}}(\boldsymbol{x}_s + \boldsymbol{B}^\top \boldsymbol{z})) \geq \sum_{s=1}^{S} \mathbb{P}\{\omega^s\} 1_{[\alpha,\infty)}(\mathbf{1}^\top \boldsymbol{p}_s) \geq \sum_{s=1}^{S} \mathbb{P}\{\omega^s\} y_s \geq 1 - \lambda.$$

Hence, $\boldsymbol{z}$ is a feasible solution to (4.1.1).

Now, let $\boldsymbol{z}$ be a feasible solution to (4.1.1). For each $s \in \mathcal{S}$, there exists an optimal

solution $\boldsymbol{p}_s$ to $\Lambda^{\mathrm{EN}}(\boldsymbol{x_s} + \boldsymbol{B}^\top \boldsymbol{z})$ such that:

$$\begin{aligned}
\mathbb{P}\big(\Lambda^{\mathrm{EN}}(\boldsymbol{X} + \boldsymbol{B}^\top \boldsymbol{z}) \geq \alpha\big) &= \sum_{s=1}^{S} \mathbb{P}\{\omega^s\} 1_{[\alpha,\infty)}(\Lambda^{\mathrm{EN}}(\boldsymbol{x}_s + \boldsymbol{B}^\top \boldsymbol{z})) \\
&= \sum_{s=1}^{S} \mathbb{P}\{\omega^s\} 1_{[\alpha,\infty)}(\mathbf{1}^\top \boldsymbol{p}_s) \\
&= \sum_{s=1}^{S} \mathbb{P}\{\omega^s\} y_s \\
&\geq 1 - \lambda,
\end{aligned}$$

where the third equality is reached by setting y_s as follows:

$$y_s = \begin{cases} 1, & \text{if } \mathbf{1}^\top \boldsymbol{p}_s \geq \alpha \\ 0, & \text{if } \mathbf{1}^\top \boldsymbol{p}_s < \alpha. \end{cases}$$

Hence, $\big(\boldsymbol{k}, (\boldsymbol{p}_s, y_s)_{s\in\mathcal{S}}\big)$ is a feasible solution to (4.1.2). □

Remark 4.1.2. *Let $j \in \mathcal{J}$, and let $\boldsymbol{e}^j$ be the corresponding standard unit vector in $\mathbb{R}^i$. It is worth noting that the weighted sum scalarization problem $\mathcal{P}^{WS}(\boldsymbol{e}^j)$ reduces to a single-objective optimization problem. According to Lemma 4.1.1, we have $\mathcal{P}^{WS}(\boldsymbol{e}^j) = \mathcal{Z}^{WS}(\boldsymbol{e}^j)$.*

Remark 4.1.3. *The ideal point of the vector optimization problem in* (4.1.1)*, denoted by $\boldsymbol{z}^{ideal} \in \mathbb{R}^i$, is defined as:*

$$\boldsymbol{z}^{ideal} = (\mathcal{P}^{WS}(\boldsymbol{e}^1), \ldots, \mathcal{P}^{WS}(\boldsymbol{e}^i))^\top.$$

Proposition 4.1.4. *Let $j \in \mathcal{J}$. When $\boldsymbol{w} = \boldsymbol{e^j}$, if the problem in* (4.1.2) *has an optimal solution, then we have:*

$$\mathcal{P}^{WS}(\boldsymbol{e}^j) = \mathcal{Z}^{WS}(\boldsymbol{e}^j) \leq \|\bar{\boldsymbol{p}}\|_\infty.$$

Proof. Let $\big(\boldsymbol{z}, (\boldsymbol{p}_s, \boldsymbol{y}_s)_{s\in\mathcal{S}}\big)$ be an optimal solution for the problem in (4.1.2) when $\boldsymbol{w} = \boldsymbol{e^j}$. To get a contradiction, suppose that $z_j > \|\bar{\boldsymbol{p}}\|_\infty$. Let $\boldsymbol{z'} \in \mathbb{R}^i$ be the vector such that $z'_j = \|\bar{\boldsymbol{p}}\|_\infty$ and $z'_{\hat{j}} = z_{\hat{j}}$ for each $\hat{j} \in \mathcal{J} \setminus \{j\}$. We claim that $\big(\boldsymbol{z'}, (\boldsymbol{p}_s, \boldsymbol{y}_s)_{s\in\mathcal{S}}\big)$ is a feasible solution of the problem in (4.1.2). To prove the claim, for each bank r in group j, $s \in \mathcal{S}$ such that $(\boldsymbol{B}^\top \boldsymbol{z'})^r = \|\bar{\boldsymbol{p}}\|_\infty$, consider the following constraints:

$$0 \leq p_s^r \leq \sum_{t=1}^{n} \boldsymbol{\pi}_{tr} p_s^t + x_s^r + \|\bar{\boldsymbol{p}}\|_\infty \leq \bar{p}^r.$$

Since $\sum_{t=1}^{n} \pi_{tr} p_s^t + x_s^r \geq 0$ and $\|\bar{\boldsymbol{p}}\|_\infty \geq \bar{p}^r$, the constraints reduced to $0 \leq p_s^r \leq \bar{p}^r$. Moreover, the rest of the constraints hold as they are independent of $\boldsymbol{z}$.

Now for each bank $\hat{r}$ in group $\hat{j} \in \mathcal{J} \setminus \{j\}$, $s \in \mathcal{S}$ such that $(\boldsymbol{B}^\top \boldsymbol{z'})^{\hat{r}} = z_{\hat{j}}$, all the constraints hold by the feasibility of $\big(\boldsymbol{z}, (\boldsymbol{p}_s, \boldsymbol{y}_s)_{s\in\mathcal{S}}\big)$. Hence, the claim follows, which yields

$$z_j = \mathcal{Z}^{\mathrm{WS}}(\boldsymbol{e^j}) \leq z'_j = \|\bar{\boldsymbol{p}}\|_\infty .$$

As this is a contradiction, the result follows. □

Proposition 4.1.5. *Let $j \in \mathcal{J}$. When $\boldsymbol{w} = \boldsymbol{e^j}$, if the problem in* (4.1.2) *has a feasible solution, then it has a finite optimal value, i.e., $\mathcal{Z}^{WS}(\boldsymbol{e}^j) \in \mathbb{R}$.*

Proof. To get a contradiction, when $\boldsymbol{w} = \boldsymbol{e^j}$, suppose that the problem in (4.1.2) has a feasible solution but $\mathcal{Z}^{\mathrm{WS}}(\boldsymbol{e^j}) = -\infty$. Since $\mathcal{Z}^{\mathrm{WS}}(\boldsymbol{e^j}) = -\infty$, there exists $\epsilon > 0$ and $\big(\boldsymbol{z}, (\boldsymbol{p}_s, \boldsymbol{y}_s)_{s\in\mathcal{S}}\big)$ such that $\boldsymbol{z}^\top \boldsymbol{e^j} = -(n\|\bar{\boldsymbol{p}}\|_\infty + \|\bar{\boldsymbol{X}}\|_\infty)$ and $\big(\boldsymbol{z} - \epsilon \boldsymbol{e^j}, (\boldsymbol{p}_s, \boldsymbol{y}_s)_{s\in\mathcal{S}}\big)$ is a feasible solution to the problem in (4.1.2). For each bank r in group j, $s \in \mathcal{S}$ such that $(\boldsymbol{B}^\top \boldsymbol{z})^r = -(n\|\bar{\boldsymbol{p}}\|_\infty + \|\bar{\boldsymbol{X}}\|_\infty)$, consider the following constraint:

$$p_s^r \leq \sum_{t=1}^{n} \boldsymbol{\pi}_{tr} p_s^t + x_s^r + (\boldsymbol{B}^\top \boldsymbol{z})^r,$$

which reduces to

$$p_s^r \leq \sum_{t=1}^{n} \boldsymbol{\pi}_{tr} p_s^t + x_s^r - n\|\bar{\boldsymbol{p}}\|_\infty - \|\bar{\boldsymbol{X}}\|_\infty - \epsilon.$$

As $\sum_{t=1}^{n} \boldsymbol{\pi}_{tr} p_s^t < n\|\bar{\boldsymbol{p}}\|_\infty$, $x_s^r \leq \|\bar{\boldsymbol{X}}\|_\infty$ and $-\epsilon < 0$, we reach the following:

$$p_s^r < 0,$$

which contradicts with the constraint $0 \leq p_s^r \leq \bar{p}^r$. Therefore, $\big(\boldsymbol{z} - \epsilon \boldsymbol{e^j}, (\boldsymbol{p}_s, \boldsymbol{y}_s)_{s\in\mathcal{S}}\big)$ is infeasible, which is a contradiction to the assumption. Thus, $\mathcal{Z}^{ws}(\boldsymbol{e^j}) > -\infty$. The existence of a feasible solution implies that $\mathcal{Z}^{\mathrm{WS}}(\boldsymbol{e^j}) < +\infty$ and $\mathcal{Z}^{\mathrm{WS}}(\boldsymbol{e^j}) \in \mathbb{R}$. □

4.2 Pascoletti-Serafini Scalarizations

In this section, our objective is to address the Pascoletti-Serafini scalarizations of $R(\boldsymbol{X})$ as presented in [36]. The Pascoletti-Serafini scalarization of $R(\boldsymbol{X})$ will serve as a crucial

tool in order to compute $R(\boldsymbol{X})$. To achieve this, we assume Ω to be a finite fixed set of scenarios, with each $\omega^s \in \Omega = \{\omega^1, \ldots, \omega^S\}$ such that $S \in \mathbb{N}$, $\mathbb{P}\{\omega^s\} = 1/S$, $s \in \mathcal{S} = \{1, \ldots, S\}$. Subsequently we propose a formulation based on MILP. We control the amount of clearing payments to ensure that it does not fall below a specified threshold, denoted as α. Specifically, we consider the aggregation function, Λ^{EN}, to evaluate the clearing payments. The Pascoletti-Serafini scalarizations problem aims to determine the minimum distance z required to reach a given set from a point $\boldsymbol{k} \in \mathbb{R}^i$. In order to achieve this objective, let $(\mathcal{N}, \boldsymbol{\pi}, \bar{\boldsymbol{p}}, \boldsymbol{X})$ be an Eisenberg-Noe network.

Lemma 4.2.1. *Consider the following optimization problems:*

$$\mathcal{P}^{PS}(\boldsymbol{k}) = \inf\{z \in \mathbb{R} \,|\, \mathbb{P}(\Lambda^{EN}(\boldsymbol{X} + \boldsymbol{B}^\top(\boldsymbol{k} + z\mathbf{1})) < \alpha) \leq \lambda\}, \tag{4.2.1}$$

$$\mathcal{Z}^{PS}(\boldsymbol{k}) = \inf\Big\{z \in \mathbb{R} \,|\, \sum_{s=1}^{S} \mathbb{P}\{\omega^s\} y_s \geq 1 - \lambda,\, \boldsymbol{p}_s \leq \boldsymbol{\pi}^\top \boldsymbol{p}_s + \boldsymbol{x}_s + \boldsymbol{B}^\top(\boldsymbol{k} + z\mathbf{1}),\, \mathbf{0} \leq \boldsymbol{p}_s \leq \bar{\boldsymbol{p}},$$
$$\mathbf{1}^\top \boldsymbol{p}_s \geq \alpha y_s,\, y_s \in \{0,1\},\, \forall s \in \mathcal{S}\Big\}, \tag{4.2.2}$$

where $\alpha \geq 0$, $\lambda \in (0,1)$, $\boldsymbol{k} \in \mathbb{R}^i$ is a fixed point, and Λ^{EN} is defined by (3.0.2)*. Then, $\mathcal{P}^{PS}(\boldsymbol{k}) = \mathcal{Z}^{PS}(\boldsymbol{k})$. If either problem has a finite optimal value, then the other problem also has a finite optimal value and the optimal values are the same.*

Note that, (4.2.1) is a two-stage stochastic programming with a chance constraint. In order to solve this problem, we were able to linearize it by introducing binary variables, which transformed the problem into a mixed-integer optimization programming, namely, (4.2.2).

Proof. Let $\big(\mu, (\boldsymbol{p}_s, \boldsymbol{y}_s)_{s\in\mathcal{S}}\big)$ be a feasible solution for (4.2.2). Then, for each $s \in \{1, \ldots, S\}$, $\boldsymbol{p}_s$ is a feasible solution to $\Lambda^{\mathrm{EN}}(\boldsymbol{x_s} + \boldsymbol{B}^\top(\boldsymbol{k} + z\mathbf{1}))$. Hence, for each $s \in \mathcal{S}$,

$$\Lambda^{\mathrm{EN}}(\boldsymbol{x}_s + \boldsymbol{B}^\top(\boldsymbol{k} + z\mathbf{1})) \geq \mathbf{1}^\top \boldsymbol{p}_s.$$

Thus, for each $s \in \mathcal{S}$,

$$\mathbb{P}\{\omega^s\} 1_{[\alpha,\infty)}(\Lambda^{\mathrm{EN}}(\boldsymbol{x}_s + \boldsymbol{B}^\top(\boldsymbol{k} + z\mathbf{1}))) \geq \mathbb{P}\{\omega^s\} 1_{[\alpha,\infty)}(\mathbf{1}^\top \boldsymbol{p}_s).$$

Then,

$$\sum_{s=1}^{S} \mathbb{P}\{\omega^s\} 1_{[\alpha,\infty)}(\Lambda^{\mathrm{EN}}(\boldsymbol{x}_s + \boldsymbol{B}^\top(\boldsymbol{k} + z\mathbf{1}))) \geq 1_{[\alpha,\infty)}(\mathbf{1}^\top \boldsymbol{p}_s).$$

$$\mathbb{P}\big(\Lambda^{\mathrm{EN}}(\boldsymbol{X}+\boldsymbol{B}^\top(\boldsymbol{k}+z\mathbf{1}))\geq\alpha\big)\geq\sum_{s=1}^{S}\mathbb{P}\{\omega^s\}1_{[\alpha,\infty)}(\mathbf{1}^\top\boldsymbol{p}_s)\geq\sum_{s=1}^{S}\mathbb{P}\{\omega^s\}y_s\geq 1-\lambda.$$

Hence, z is a feasible solution to (4.2.1).

Now, let z be a feasible solution to (4.2.1). For each $s\in\mathcal{S}$, there exists an optimal solution $\boldsymbol{p_s}$ to $\Lambda^{\mathrm{EN}}(\boldsymbol{x_s}+\boldsymbol{B}^\top(\boldsymbol{k}+z\mathbf{1}))$ such that:

$$\begin{aligned}\Big(\mathbb{P}(\Lambda^{\mathrm{EN}}(\boldsymbol{X}+\boldsymbol{B}^\top(\boldsymbol{k}+z\mathbf{1})))\geq\alpha\Big)&=\sum_{s=1}^{S}\mathbb{P}\{\omega^s\}1_{[\alpha,\infty)}(\Lambda^{\mathrm{EN}}(\boldsymbol{x_s}+\boldsymbol{B}^\top(\boldsymbol{k}+z\mathbf{1})))\\&=\sum_{s=1}^{S}\mathbb{P}\{\omega^s\}1_{[\alpha,\infty)}(\mathbf{1}^\top\boldsymbol{p}_s)\\&=\sum_{s=1}^{S}\mathbb{P}\{\omega^s\}y_s\\&\geq 1-\lambda,\end{aligned}$$

where the third equality is reached by setting y_s as follows:

$$y_s=\begin{cases}1, & \text{if } \mathbf{1}^\top\boldsymbol{p}_s\geq\alpha\\ 0, & \text{if } \mathbf{1}^\top\boldsymbol{p}_s<\alpha.\end{cases}$$

Hence, $\big(z,(\boldsymbol{p}_s,y_s)_{s\in\mathcal{S}}\big)$ is a feasible solution to (4.2.2). □

Proposition 4.2.2. *Let $\boldsymbol{k}\in\mathbb{R}^i$. If the problem in* (4.2.2) *has an optimal solution, then we have:*

$$\mathcal{P}^{PS}(\boldsymbol{k})=\mathcal{Z}^{PS}(\boldsymbol{k})\leq\|\bar{\boldsymbol{p}}\|_\infty+\|\boldsymbol{k}\|_\infty.$$

Proof. Let $\big(z,(\boldsymbol{p}_s,\boldsymbol{y}_s)_{s\in\mathcal{S}}\big)$ be an optimal solution for the problem in (4.2.2). To get a contradiction, suppose that $z>\|\bar{\boldsymbol{p}}\|_\infty+\|\boldsymbol{k}\|_\infty$. Let $\boldsymbol{z'}=\|\bar{\boldsymbol{p}}\|_\infty+\|\boldsymbol{k}\|_\infty$. We claim that $\big(z',(\boldsymbol{p}_s,\boldsymbol{y}_s)_{s\in\mathcal{S}}\big)$ is a feasible solution of the problem in (4.2.2). To prove the claim, for each bank $r\in\mathcal{N}$, $s\in\mathcal{S}$ such that $(\boldsymbol{B}^\top(\boldsymbol{k}+z'\mathbf{1}))^r\geq\|\bar{\boldsymbol{p}}\|_\infty$, consider the following constraints:

$$0\leq p_s^r\leq\sum_{t=1}^{n}\boldsymbol{\pi}_{tr}p_s^t+x_s^r+\|\bar{\boldsymbol{p}}\|_\infty\leq\bar{p}^r.$$

Since $\sum_{t=1}^{n}\pi_{tr}p_s^t+x_s^r\geq 0$ and $\|\bar{\boldsymbol{p}}\|_\infty\geq\bar{p}^r$, the constraints reduced to $0\leq p_s^r\leq\bar{p}^r$. Moreover, the rest of the constraints hold as they are independent of z. Hence, the claim follows, which yields

$$z=\mathcal{Z}^{ps}(\boldsymbol{k})\leq z'=\|\bar{\boldsymbol{p}}\|_\infty+\|\boldsymbol{k}\|_\infty.$$

As this is a contradiction, the result follows. □

Proposition 4.2.3. *Let $\boldsymbol{k} \in \mathbb{R}^i$. If the problem in* (4.2.2) *has a feasible solution, then it has a finite optimal value, i.e., $\mathcal{Z}^{ps}(\boldsymbol{k}) \in \mathbb{R}$.*

Proof. To get a contradiction, suppose that the problem in (4.2.2) has a feasible solution but $\mathcal{Z}^{\mathrm{PS}}(\boldsymbol{k}) = -\infty$. Since $\mathcal{Z}^{\mathrm{PS}}(\boldsymbol{k}) = -\infty$, there exists $\epsilon > 0$ and $\big(z, (\boldsymbol{p}_s, \boldsymbol{y}_s)_{s\in\mathcal{S}}\big)$ such that $z = -(n\left\|\bar{\boldsymbol{p}}\right\|_\infty + \left\|\bar{\boldsymbol{X}}\right\|_\infty + \left\|\bar{\boldsymbol{k}}\right\|_\infty)$ and $\big(z-\epsilon, (\boldsymbol{p}_s, \boldsymbol{y}_s)_{s\in\mathcal{S}}\big)$ is a feasible solution to the problem in (4.2.2). For each bank $r \in \mathcal{N}$, $s \in \mathcal{S}$ such that $(\boldsymbol{B}^\top(\boldsymbol{k} + z\boldsymbol{1}))^r \leq -(n\left\|\bar{\boldsymbol{p}}\right\|_\infty + \left\|\bar{\boldsymbol{X}}\right\|_\infty)$, consider the following constraint:

$$p_s^r \leq \sum_{t=1}^{n} \boldsymbol{\pi}_{tr} p_s^t + x_s^r + (\boldsymbol{B}^\top(\boldsymbol{k} + z\boldsymbol{1}))^r,$$

which reduces to

$$p_s^r \leq \sum_{t=1}^{n} \boldsymbol{\pi}_{tr} p_s^t + x_s^r - n\left\|\bar{\boldsymbol{p}}\right\|_\infty - \left\|\bar{\boldsymbol{X}}\right\|_\infty - \epsilon.$$

As $\sum_{t=1}^{n} \boldsymbol{\pi}_{tr} p_s^t < n\left\|\bar{\boldsymbol{p}}\right\|_\infty$, $x_s^r \leq \left\|\bar{\boldsymbol{X}}\right\|_\infty$ and $-\epsilon < 0$, we reach the following:

$$p_s^r < 0,$$

which contradicts with the constraint $0 \leq p_s^r \leq \bar{p}^r$. Therefore, $\big(z-\epsilon, (\boldsymbol{p}_s, \boldsymbol{y}_s)_{s\in\mathcal{S}}\big)$ is infeasible, which is a contradiction to the assumption. Thus, $\mathcal{Z}^{\mathrm{PS}}(\boldsymbol{k}) > -\infty$. The existence of a feasible solution implies that $\mathcal{Z}^{\mathrm{PS}}(k) < +\infty$ and $\mathcal{Z}^{\mathrm{PS}}(\boldsymbol{k}) \in \mathbb{R}$. □

4.3 Norm-Minimizing Scalarizations

The purpose of this section is to address the problem of norm-minimizing scalarizations of $R(\boldsymbol{X})$, as discussed in [37]. The norm-minimizing scalarization of $R(\boldsymbol{X})$ will serve as a crucial tool in order to compute $R(\boldsymbol{X})$. To achieve this, we assume Ω to be a finite fixed set of scenarios, with each $\omega^s \in \Omega = \{\omega^1, \ldots, \omega^S\}$ such that $S \in \mathbb{N}$, $\mathbb{P}\{\omega^s\} = 1/S$, $s \in \mathcal{S} = \{1, \ldots, S\}$. Subsequently, we propose a formulation based on MILP. We control the amount of clearing payments and the number of defaulting nodes to ensure that they do not fall below a specified threshold, denoted as α. Specifically, we consider the aggregation function, Λ^{EN}, to evaluate the clearing payments. In order to accomplish this objective, the problem of norm-minimizing scalarizations, from a given point $\boldsymbol{k} \in \mathbb{R}^i$, seeks to find the minimum Euclidean distance $\|\boldsymbol{k} - \boldsymbol{z}\|_2$ to a predefined set and identify the corresponding point $\boldsymbol{z} \in \mathbb{R}^i$

where the minimum distance is attained. In order to achieve this objective, let $(\mathcal{N}, \boldsymbol{\pi}, \bar{\boldsymbol{p}}, \boldsymbol{X})$ be an Eisenberg-Noe network.

Lemma 4.3.1. *Consider the following optimization problems:*

$$\mathcal{P}^{NM}(\boldsymbol{k}) = \inf\{\|\boldsymbol{k} - \boldsymbol{z}\|_2 \mid \mathbb{P}(\Lambda^{EN}(\boldsymbol{X} + \boldsymbol{B}^\top \boldsymbol{z}) < \alpha) \leq \lambda,\, \boldsymbol{z} \in \mathbb{R}^i\}, \tag{4.3.1}$$

$$\begin{aligned}\mathcal{Z}^{NM}(\boldsymbol{k}) = \inf \Big\{ \|\boldsymbol{k} - \boldsymbol{z}\|_2 \mid \sum_{s=1}^{S} \mathbb{P}\{\omega^s\} y_s \geq 1 - \lambda, \boldsymbol{p}_s \leq \boldsymbol{\pi}^\top \boldsymbol{p}_s + \boldsymbol{x}_s + \boldsymbol{B}^\top \boldsymbol{z}, \\ \mathbf{0} \leq \boldsymbol{p}_s \leq \bar{\boldsymbol{p}}, \mathbf{1}^\top \boldsymbol{p}_s \geq \alpha y_s, y_s \in \{0,1\},\, \boldsymbol{z} \in \mathbb{R}^i,\, \forall s \in \mathcal{S} \Big\},\end{aligned} \tag{4.3.2}$$

where $\alpha \geq 0$, $\lambda \in (0,1)$, $\boldsymbol{k} \in \mathbb{R}^i$ *is a fixed point, and* Λ^{EN} *is defined by* (3.0.2)*. Then,* $\mathcal{P}^{NM}(\boldsymbol{k}) = \mathcal{Z}^{NM}(\boldsymbol{k})$*. If either problem has a finite optimal value, then the other problem also has a finite optimal value and the optimal values are the same.*

It should be noted that the equation (4.3.1) corresponds to a two-stage stochastic programming problem with a chance constraint. In order to address this issue, we successfully linearize it by introducing binary variables. This transformation effectively converted the problem into a mixed-integer optimization programming model, denoted as (4.3.2).

Proof. Fix $\boldsymbol{k} \in \mathbb{R}^i$ and let $\big(\boldsymbol{z}, (\boldsymbol{p}_s, \boldsymbol{y}_s)_{s\in\mathcal{S}}\big)$ be a feasible solution for (4.3.2). Then, for each $s \in \mathcal{S}$, $\boldsymbol{p}_s$ is a feasible solution to $\Lambda^{\mathrm{EN}}(\boldsymbol{x_s} + \boldsymbol{B}^\top \boldsymbol{z})$. Hence, for each $s \in \{1, \ldots, S\}$:

$$\Lambda^{\mathrm{EN}}(\boldsymbol{x}_s + \boldsymbol{B}^\top \boldsymbol{z}) \geq \mathbf{1}^\top \boldsymbol{p}_s.$$

Thus, for each $s \in \mathcal{S}$,

$$\mathbb{P}\{\omega^s\} 1_{[\alpha,\infty)}(\Lambda^{\mathrm{EN}}(\boldsymbol{x}_s + \boldsymbol{B}^\top \boldsymbol{z})) \geq \mathbb{P}\{\omega^s\} 1_{[\alpha,\infty)}(\mathbf{1}^\top \boldsymbol{p}_s).$$

Then,

$$\sum_{s=1}^{S} \mathbb{P}\{\omega^s\} 1_{[\alpha,\infty)}(\Lambda^{\mathrm{EN}}(\boldsymbol{x}_s + \boldsymbol{B}^\top \boldsymbol{z})) \geq \sum_{s=1}^{S} \mathbb{P}\{\omega^s\} 1_{[\alpha,\infty)}(\mathbf{1}^\top \boldsymbol{p}_s).$$

$$\mathbb{P}\big(\Lambda^{\mathrm{EN}}(\boldsymbol{X} + \boldsymbol{B}^\top \boldsymbol{z}) \geq \alpha\big) \geq \sum_{s=1}^{S} \mathbb{P}\{\omega^s\} 1_{[\alpha,\infty)}(\mathbf{1}^\top \boldsymbol{p}_s) \geq \sum_{s=1}^{S} \mathbb{P}\{\omega^s\} y_s \geq 1 - \lambda.$$

Hence, $\boldsymbol{z}$ is a feasible solution to (4.3.1).

Now, let $\boldsymbol{z}$ be a feasible solution to (4.3.1). For each $s \in \mathcal{S}$, there exists an optimal solution $\boldsymbol{p_s}$ to $\Lambda^{\mathrm{EN}}(\boldsymbol{x_s} + \boldsymbol{B}^\top \boldsymbol{z})$ such that:

$$\begin{aligned}
\mathbb{P}\big(\Lambda^{\mathrm{EN}}(\boldsymbol{X} + \boldsymbol{B}^\top \boldsymbol{z}) \geq \alpha\big) &= \sum_{s=1}^{S} \mathbb{P}\{\omega^s\} 1_{[\alpha,\infty)}(\Lambda^{\mathrm{EN}}(\boldsymbol{x}_s + \boldsymbol{B}^\top \boldsymbol{z})) \\
&= \sum_{s=1}^{S} \mathbb{P}\{\omega^s\} 1_{[\alpha,\infty)}(\mathbf{1}^\top \boldsymbol{p}_s) \\
&= \sum_{s=1}^{S} \mathbb{P}\{\omega^s\} y_s \\
&\geq 1 - \lambda,
\end{aligned}$$

where the third equality is reached by setting y_s as follows:

$$y_s = \begin{cases} 1, & \text{if } \mathbf{1}^\top \boldsymbol{p}_s \geq \alpha \\ 0, & \text{if } \mathbf{1}^\top \boldsymbol{p}_s < \alpha. \end{cases}$$

Hence, $\big(\boldsymbol{z}, (\boldsymbol{p}_s, y_s)_{s\in\mathcal{S}}\big)$ is a feasible solution to (4.3.2). □

Proposition 4.3.2. *Let $\boldsymbol{k} \in \mathbb{R}^i$. If the problem in* (4.2.2) *has an optimal solution, then we have:*

$$\mathcal{P}^{NM}(\boldsymbol{k}) = \mathcal{Z}^{NM}(\boldsymbol{k}) \leq \|\boldsymbol{k} - \|\bar{\boldsymbol{p}}\|_\infty \mathbf{1}\|_2.$$

Proof. Let $\big(\boldsymbol{z}, (\boldsymbol{p}_s, \boldsymbol{y}_s)_{s\in\mathcal{S}}\big)$ be an optimal solution for the problem in (4.3.2). To get a contradiction, suppose that $\mathcal{Z}^{\mathrm{NM}}(\boldsymbol{k}) > \|\boldsymbol{k} - \|\bar{\boldsymbol{p}}\|_\infty \mathbf{1}\|_2$. Let $\boldsymbol{z'} = \|\bar{\boldsymbol{p}}\|_\infty \mathbf{1}$. We claim that $\big(\boldsymbol{z'}, (\boldsymbol{p}_s, \boldsymbol{y}_s)_{s\in\mathcal{S}}\big)$ is a feasible solution of the problem in (4.3.2). To prove the claim, for each bank $r \in \mathcal{N}$, $s \in \mathcal{S}$ such that $(\boldsymbol{B}^\top \boldsymbol{z'})^r = \|\bar{\boldsymbol{p}}\|_\infty$, consider the following constraints:

$$0 \leq p_s^r \leq \sum_{t=1}^{n} \boldsymbol{\pi}_{tr} p_s^t + x_s^r + \|\bar{\boldsymbol{p}}\|_\infty \leq \bar{p}^r.$$

Since $\sum_{t=1}^{n} \pi_{tr} p_s^t + x_s^r \geq 0$ and $\|\bar{\boldsymbol{p}}\|_\infty \geq \bar{p}^r$, the constraints reduced to $0 \leq p_s^r \leq \bar{p}^r$. Moreover, the rest of the constraints hold as they are independent of $\boldsymbol{z}$. Hence, the claim follows, which yields

$$\|\boldsymbol{k} - \boldsymbol{z}\|_2 = \mathcal{Z}^{\mathrm{NM}}(\boldsymbol{k}) \leq \|\boldsymbol{k} - \boldsymbol{z'}\|_2 = \|\boldsymbol{k} - \|\bar{\boldsymbol{p}}\|_\infty \mathbf{1}\|_2.$$

As this is a contradiction, the result follows. □

Proposition 4.3.3. *Let $\boldsymbol{k} \in \mathbb{R}^i$. If the problem in* (4.3.2) *has a feasible solution, then it has a finite optimal value, i.e., $\mathcal{Z}^{NM}(\boldsymbol{k}) \in \mathbb{R}$.*

Proof. To get a contradiction, suppose that the problem in (4.3.2) has a feasible solution but $\mathcal{Z}^{nm}(\boldsymbol{k}) = -\infty$. Since $\mathcal{Z}^{nm}(\boldsymbol{k}) = -\infty$, there exists $\epsilon > 0$ and $\left(\boldsymbol{z}, (\boldsymbol{p}_s, \boldsymbol{y}_s)_{s\in\mathcal{S}}\right)$ such that $\boldsymbol{z}^\top \boldsymbol{e^j} = -(n \left\|\bar{\boldsymbol{p}}\right\|_\infty + \left\|\bar{\boldsymbol{X}}\right\|_\infty)$ and $\left(\boldsymbol{z} - \epsilon \boldsymbol{e^j}, (\boldsymbol{p}_s, \boldsymbol{y}_s)_{s\in\mathcal{S}}\right)$ is a feasible solution to the problem in (4.1.2), where $j \in \mathcal{J}$. For each bank r in group j, $s \in \mathcal{S}$ such that $(\boldsymbol{B}^\top \boldsymbol{z})^r = -(n \left\|\bar{\boldsymbol{p}}\right\|_\infty + \left\|\bar{\boldsymbol{X}}\right\|_\infty)$, consider the following constraint:

$$p_s^r \leq \sum_{t=1}^{n} \boldsymbol{\pi}_{tr} p_s^t + x_s^r + (\boldsymbol{B}^\top \boldsymbol{z})^r,$$

which reduces to

$$p_s^r \leq \sum_{t=1}^{n} \boldsymbol{\pi}_{tr} p_s^t + x_s^r - n \left\|\bar{\boldsymbol{p}}\right\|_\infty - \left\|\bar{\boldsymbol{X}}\right\|_\infty - \epsilon.$$

As $\sum_{t=1}^{n} \boldsymbol{\pi}_{tr} p_s^t < n \left\|\bar{\boldsymbol{p}}\right\|_\infty$, $x_s^r \leq \left\|\bar{\boldsymbol{X}}\right\|_\infty$ and $-\epsilon < 0$, we reach the following:

$$p_s^r < 0,$$

which contradicts with the constraint $0 \leq p_s^r \leq \bar{p}^r$. Therefore, $\left(\boldsymbol{z} - \epsilon \boldsymbol{e^j}, (\boldsymbol{p}_s, \boldsymbol{y}_s)_{s\in\mathcal{S}}\right)$ is infeasible, which is a contradiction to the assumption. Thus, $\mathcal{Z}^{nm}(\boldsymbol{k}) > -\infty$. The existence of a feasible solution implies that $\mathcal{Z}^{nm}(\boldsymbol{k}) < +\infty$ and $\mathcal{Z}^{nm}(\boldsymbol{k}) \in \mathbb{R}$. □

4.4 Algorithms for Calculating Systemic Risk Measures

In this section, we will examine techniques for approximating the set-valued sensitive systemic risk measure $R(\boldsymbol{X})$, with the aggregation function chosen as $\Lambda = \Lambda^{\mathrm{EN}}$. To achieve this, we assume Ω to be a finite fixed set of scenarios, with each $\omega^s \in \Omega = \{\omega^1, \ldots, \omega^S\}$ such that $S \in \mathbb{N}$, $\mathbb{P}\{\omega^s\} = 1/S$, $s \in \mathcal{S} = \{1, \ldots, S\}$. Subsequently, the set $R(\boldsymbol{X})$ will be approximated through the utilization of a variation of the so-called grid algorithm introduced in [5], where grid points are evaluated by solving certain scalar mixed-integer programming problems, namely, the Pascoletti Serafini and norm-minimizing scalarizations. It should be noted that value-at-risk is non-convex in nature. Consequently, the sensetive systemic risk measures generally do not possess the convexity property.

In order to implement the grid algorithm, it is necessary to divide a grid across a compact region of interest. The level of accuracy achieved by the algorithm is determined by the

distance between grid points, denoted as ϵ [5]. By approximating the boundary of the set $R(\boldsymbol{X})$ within a specified compact region, we are able to approximate the entirety of $R(\boldsymbol{X})$. This can be achieved by representing $R(\boldsymbol{X})$ as the union of sets formed by each acceptable grid point within the compact region of interest, in addition to the positive orthant $\mathbb{R}^i_+$.

To illustrate, given i groups of banks, each grid point corresponds to $\boldsymbol{k} \in \mathbb{R}^i$, representing the capital injections to i groups of banks. The compact region of interest is determined by solving the weighted sum scalarization problem for i different $\boldsymbol{w} \in \mathbb{R}^i$ vectors, where $\boldsymbol{k_1^\star}, \ldots, \boldsymbol{k_i^\star}$ are the optimal solutions to the weighted sum scalarization problems, given $\boldsymbol{e^1}$, $\ldots$, $\boldsymbol{e^i}$, respectively. In other words, we are solving a single-objective optimization problem for each bank group $j \in \mathcal{J}$. Then, we construct the compact set formed by the combinations of i $\boldsymbol{k^\star}$'s. For instance, if $i = 2$, i.e., there exist core and peripheral groups of banks, we solve the weighted sum scalarization problem for $\boldsymbol{e^1}$ and $\boldsymbol{e^2}$. Let $\boldsymbol{k_1^{\star\top}} = (k_{11}^\star, k_{12}^\star)$, $\boldsymbol{k_2^{\star\top}} = (k_{21}^\star, k_{22}^\star)$ be optimal solutions to the weighted sum scalarization problem when $\boldsymbol{w} = \boldsymbol{e^1}$ and $\boldsymbol{w} = \boldsymbol{e^2}$, respectively. The grid region of interest is formed by four points, namely, $(k_{11}^\star, k_{12}^\star)^\top$, $(k_{21}^\star, k_{22}^\star)^\top$, $(k_{11}^\star, k_{22}^\star)^\top$, and $(k_{21}^\star, k_{12}^\star)^\top$. The point $(k_{11}^\star, k_{22}^\star)^\top$ is called the *ideal point*, which serves as the starting point to check its acceptability. To illustrate, refer to Figure 4.1. The green region, labeled as "Acceptable" belongs to $R(\boldsymbol{X})$ due to the upper set property that $R(\boldsymbol{X})$ possesses, as the points $(k_{11}^\star, k_{12}^\star)^\top$ and $(k_{21}^\star, k_{22}^\star)^\top$ are acceptable. However, the red region, labeled as "Not Acceptable," does not belong to $R(\boldsymbol{X})$ because it would contradict the optimality of $(k_{11}^\star, k_{12}^\star)^\top$ and $(k_{21}^\star, k_{22}^\star)^\top$ in their respective weighted sum scalarizations. Therefore, the *interested* part of $R(\boldsymbol{X})$ lies within the box labeled as "The Grid Region." Thus, approximating the boundary of $R(\boldsymbol{X})$ within the grid region of interest allows us to approximate the whole set $R(\boldsymbol{X})$.

Once the weighted sum scalarization problem is addressed to define the grid region, the next step involves establishing a grid within this specified region. The arrangement of the grid is such that the distance between neighboring grid points is either equal to or less than a user-specified approximation error denoted by ϵ. Figure 4.2 illustrates a graphical depiction of a grid points construction in a grid region when epsilon is 100 and $i = 2$, which indicates the presence of two groups of banks, which we will refer to as the "core" and "peripheral" groups. Following this, grid points evaluation is undertaken to assess their acceptability, as illustrated in Figure 4.3, Figure 4.4, and Figure 4.5 when Algorithm 1, Algorithm 2, and Algorithm 3 are applied, respectively. At each iteration, certain points are classified as acceptable, indicated by green markers, while others are classified as not acceptable,

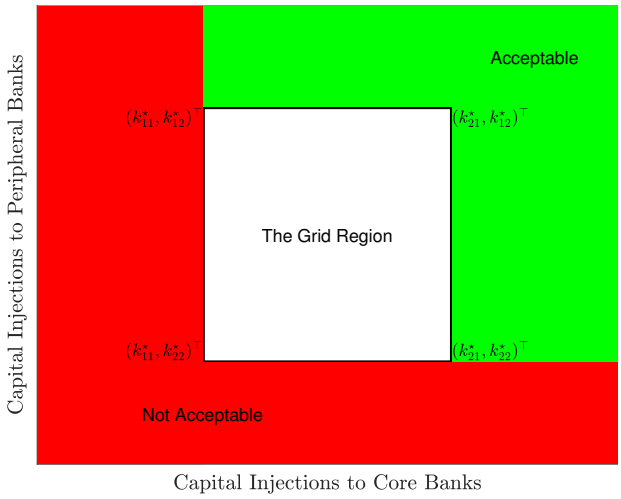

Figure 4.1: Illustration of the Grid Region.

indicated by red markers. The process of evaluating acceptability persists until all grid points have been classified as either acceptable or not acceptable, as depicted in Figure 4.6. The final step involves the approximation of $R(\boldsymbol{X})$. This process requires taking the union of the sets formed by each acceptable grid point, plus the positive orthant, as depicted in Figure 4.7.

Remark 4.4.1. *If there are 3 or more groups, i.e., $i \geq 3$, several distinct arrangements of grid points can be considered. One notable approach involves arranging the grid points according to their respective Euclidean distances from the ideal point. Specifically, prioritizing grid points with shorter Euclidean distances to the ideal point, thereby establishing an ordered set of grid points.*

To finalize the discussion of this section, it is crucial to clarify the methodology utilized for evaluating the acceptability of the grid points. This task is achieved by employing three algorithms, which are utilized to assess the acceptability of the aforementioned grid points.

1. Acceptability check without any scalarization, which will be used as a benchmark for comparison. Let G denote the set of grid points within the grid region, subject to a specified approximation error ϵ. The first step involves assessing the acceptability of the ideal point $\boldsymbol{k}^{\text{ideal}}$ by verifying whether $\mathbb{P}(\Lambda(\boldsymbol{X} + \boldsymbol{B}^\top \boldsymbol{k}^{\text{ideal}}) < \alpha) \leq \lambda$ is satisfied by checking a "computable" condition. If it is satisfied, then the set $\boldsymbol{k}^{\text{ideal}} + \mathbb{R}_+^i$ is

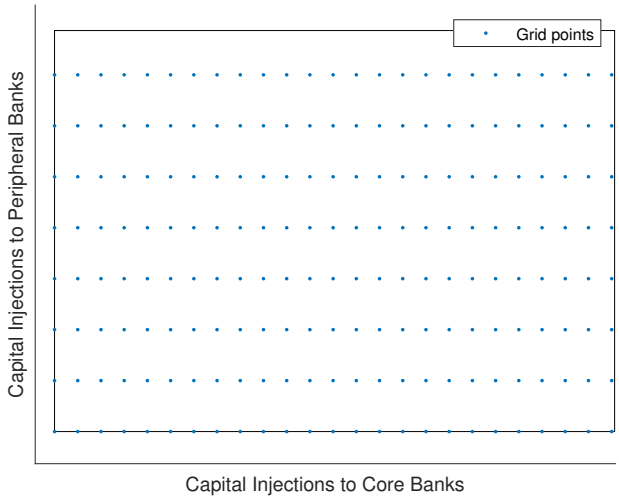

Figure 4.2: Illustration of the Initial Step in the Grid Algorithm: Construction of the Grid with $\epsilon = 100$.

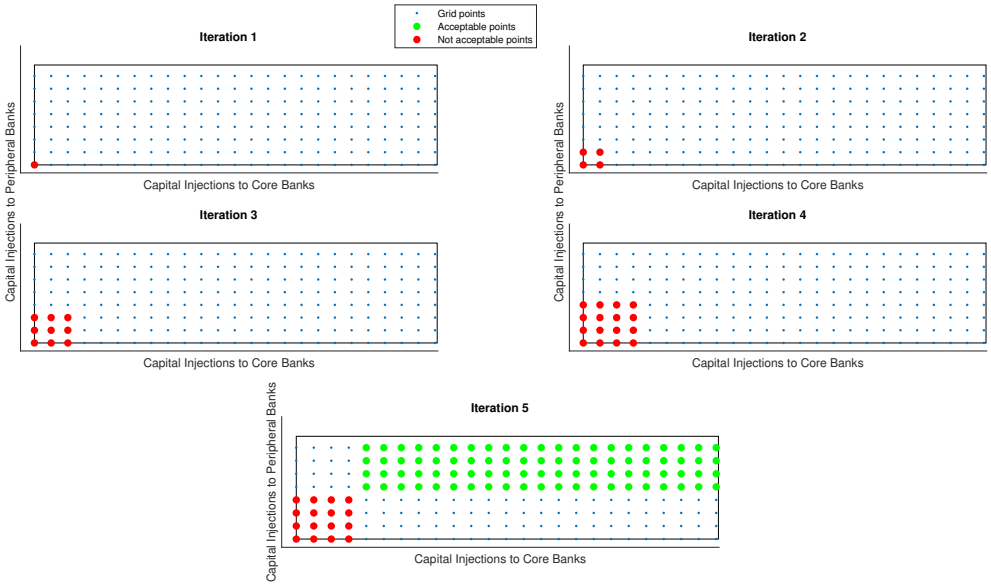

Figure 4.3: Illustration of the First 5 Iterations of the Grid Algorithm with $\epsilon = 100$ When Algorithm 1 is Applied.

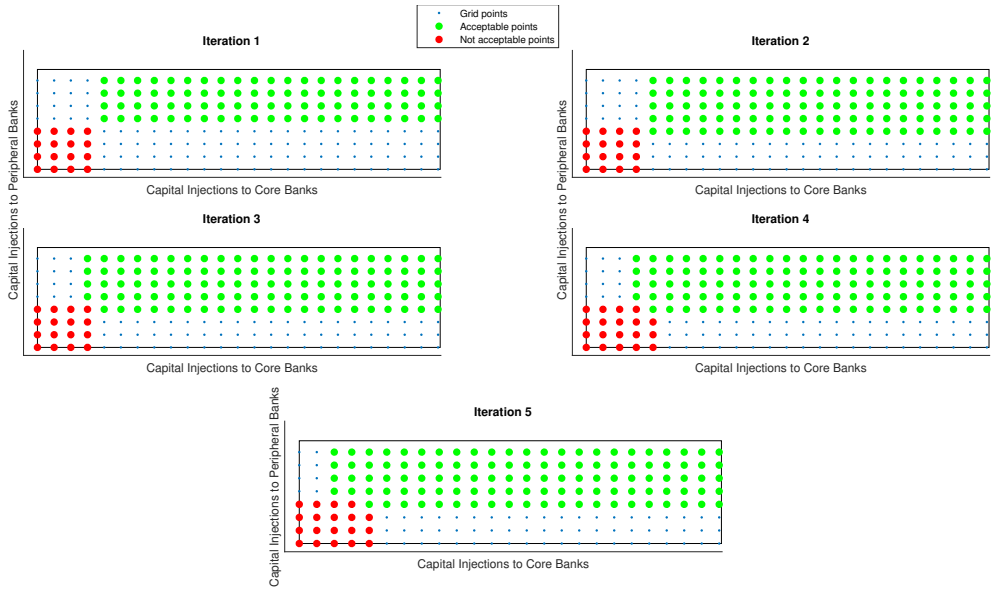

Figure 4.4: Illustration of the First 5 Iterations of the Grid Algorithm with $\epsilon = 100$ When Algorithm 2 is Applied.

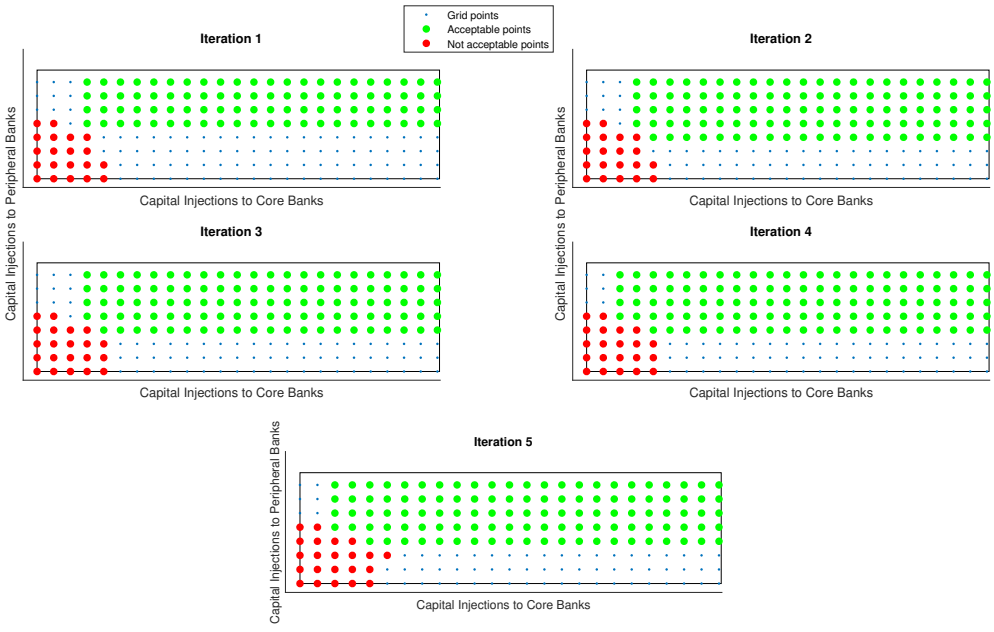

Figure 4.5: Illustration of the First 5 Iterations of the Grid Algorithm with $\epsilon = 100$ When Algorithm 3 is Applied.

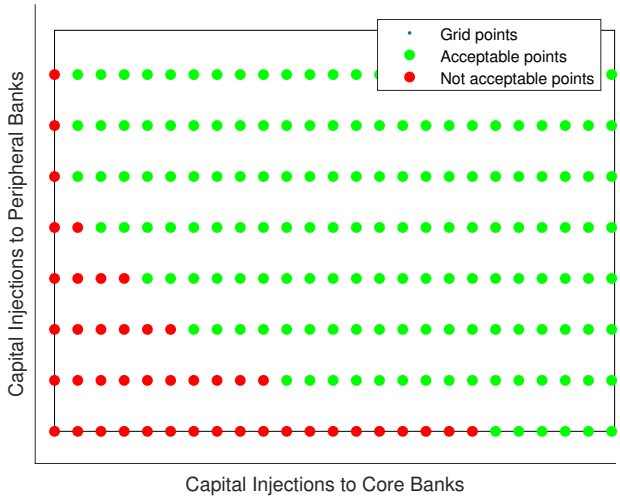

Figure 4.6: Illustration of Grid Points Check Completion in the Grid Algorithm with $\epsilon = 100$.

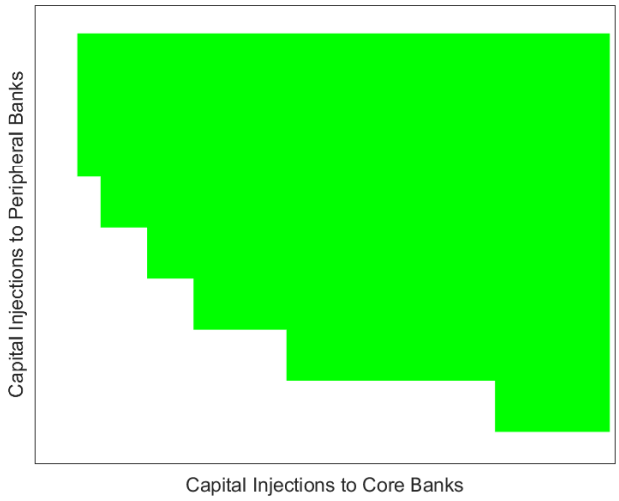

Figure 4.7: Illustration of the Final Step in the Grid Algorithm: Approximating $R(\boldsymbol{X})$ with $\epsilon = 100$.

deemed acceptable. Conversely, if it is not satisfied, then the the set $\boldsymbol{k}^{\text{ideal}} + \mathbb{R}^i_-$ is deemed unacceptable. Subsequently, we proceed to the subsequent grid point along the diagonal trajectory. The termination of the algorithm occurs when all grid points have been classified as either acceptable or not acceptable. Ultimately, the algorithm provides an approximation of the set $R(\boldsymbol{X})$. Please consult the pseudocode provided in Algorithm 1.

Algorithm 1 Acceptability Check Without Any Scalarization

Require: $\boldsymbol{X}, \boldsymbol{\pi}, \bar{\boldsymbol{p}}, \boldsymbol{B}, G, S, \lambda, \alpha$.
Ensure: AS {The set of acceptable grid points}.
Initialize counter $\leftarrow 0$.
Initialize AS $\leftarrow \{\}$.
Initialize NA $\leftarrow \{\}$ {The set of not acceptable grid points}.
while $|G| > 0$ **do**
  $\boldsymbol{k} \leftarrow G(1)$;
  for $s \leftarrow 1$ to S **do**
    Solve $\Lambda^{\text{EN}}(\boldsymbol{x}_s + \boldsymbol{B}^T\boldsymbol{k})$;
    if $\Lambda^{\text{EN}}(\boldsymbol{x}_s + \boldsymbol{B}^T\boldsymbol{k}) < \alpha$ **then**
      counter $\leftarrow$ counter $+ \frac{1}{S}$;
    end if
  end for
  if counter $\leq \lambda$ **then**
    Add the grid points in $\boldsymbol{k} + \mathbb{R}^i_+$ to AS;
    Remove the grid points in $\boldsymbol{k} + \mathbb{R}^i_+$ from G;
  else
    Add the grid points in $\boldsymbol{k} + \mathbb{R}^i_-$ to NA;
    Remove the grid points in $\boldsymbol{k} + \mathbb{R}^i_-$ from G;
  end if
  counter $\leftarrow 0$;
end while
return $\bar{R}(\boldsymbol{X}) := \text{AS} + \mathbb{R}^i_+$.

2. Acceptability check using the Pascoletti Serafini scalarization method. Let G denote the set of grid points within the grid region, subject to a specified approximation error ϵ. The acceptability of the grid points is assessed by solving the Pascoletti Serafini scalarizations problem as described in Section 4.2. In order to accomplish this, we initially examine the minimum distance $z^\star \in \mathbb{R}$ between the ideal point $\boldsymbol{k}^{\text{ideal}}$ and the set $R(\boldsymbol{X})$. Upon evaluating the minimum distance $z^\star$ from the ideal point, we designate $\boldsymbol{m} = z^\star\mathbf{1}$ as the point at which it intersects the acceptance set. Consequently, we classify the grid points within $\boldsymbol{m} + \mathbb{R}^i_+$ as acceptable, while the grid points within

$\boldsymbol{m} + \mathbb{R}^i_-$ are deemed unacceptable. Next, we proceed to the subsequent grid point in a diagonal direction. The termination of the algorithm occurs when all grid points have been classified as either acceptable or not acceptable. In essence, the algorithm offers an approximation of the set $R(\boldsymbol{X})$. Please consult the pseudocode provided in Algorithm 2.

Algorithm 2 Acceptability Check Using the Pascoletti Serafini Scalarization

Require: $\boldsymbol{X}, \boldsymbol{\pi}, \bar{\boldsymbol{p}}, \boldsymbol{B}, G, S, \lambda, \alpha$.
Ensure: AS {The set of acceptable grid points}.
Initialize AS $\leftarrow \{\}$.
Initialize NA $\leftarrow \{\}$ {The set of not acceptable grid points}.
while $|G| > 0$ **do**
  $\boldsymbol{k} \leftarrow G(1)$;
  Get $z^\star$ by solving the Pascoletti Serafini scalarization;
  $\boldsymbol{m} = z^\star \mathbf{1}$;
  Add the grid points in $\boldsymbol{m} + \mathbb{R}^i_+$ to AS;
  Remove the grid points in $\boldsymbol{m} + \mathbb{R}^i_+$ from G;
  Add the grid points in $\boldsymbol{m} + \mathbb{R}^i_-$ to NA;
  Remove the grid points in $\boldsymbol{m} + \mathbb{R}^i_-$ from G;
end while
return $\bar{R}(\boldsymbol{X}) := \mathtt{AS} + \mathbb{R}^i_+$.

3. Acceptability check using the norm-minimizing scalarization method. Let G denote the set of grid points within the grid region, where the grid region is determined by a specified approximation error ϵ. The acceptability of the grid points is assessed by solving the problem of norm-minimizing scalarizations, as described in Section 4.3. In order to assess the acceptability of the grid points, the first step involves computing the minimum Euclidean distance between the ideal point $\boldsymbol{k}^{\text{ideal}}$ and the set $R(\boldsymbol{X})$. Let m represent the Euclidean norm of the difference between the ideal vector $\boldsymbol{k}^{\text{ideal}}$ and the vector $\boldsymbol{z}^\star$ in $\mathbb{R}^i$, which is the optimal solution to the norm-minimizing scalarization problem. Determine the point $\boldsymbol{z}^\star$ in $\mathbb{R}^i$ that lies within the acceptance set and achieves the minimum distance $m := \|\boldsymbol{k} - \boldsymbol{z}^\star\|_2$. Consequently, we classify the grid points within $\boldsymbol{z}^\star + \mathbb{R}^i_+$ as acceptable, while grid points are considered not acceptable if their distance from $\boldsymbol{k}^{\text{ideal}}$ is less than m. The algorithm follows a systematic approach by sequentially advancing to the subsequent grid point in a diagonal direction until all points have been categorized as either acceptable or not acceptable. Please consult the pseudocode provided in Algorithm 3.

Theorem 4.4.2. *Let an approximation error $\bar{\epsilon} > 0$ be given. If any of Algorithms 1, 2 or*

Algorithm 3 Acceptability Check Using the Norm-Minimizing Scalarization

Require: $\boldsymbol{X}, \boldsymbol{\pi}, \bar{\boldsymbol{p}}, \boldsymbol{B}, G, S, \lambda, \alpha$.
Ensure: AS {The set of acceptable grid points}.
1: Initialize AS $\leftarrow \{\}$.
2: Initialize NA $\leftarrow \{\}$ {The set of not acceptable grid points}.
3: **while** $|G| > 0$ **do**
4: $\quad \boldsymbol{k} \leftarrow G(1)$;
5: $\quad$ Get $\boldsymbol{z}^\star$ by solving the norm-minimizing scalarization;
6: $\quad m = \|\boldsymbol{k} - \boldsymbol{z}^\star\|_2$;
7: $\quad$ Add the grid points in $\boldsymbol{z}^\star + \mathbb{R}^i_+$ to AS;
8: $\quad$ Remove the grid points in $\boldsymbol{z}^\star + \mathbb{R}^i_+$ from G;
9: $\quad$ Add the grid points, whose Euclidean distance from $\boldsymbol{k}$ less than m to NA;
10: $\quad$ Remove the grid points, whose Euclidean distance from $\boldsymbol{k}$ less than m from G;
11: **end while**
12: **return** $\bar{R}(\boldsymbol{X}) := \mathtt{AS} + \mathbb{R}^i_+$.

3 is run, then $\bar{R}(\boldsymbol{X}) \subseteq R(\boldsymbol{X})$ *and* $\mathbb{H}(R(\boldsymbol{X}), \bar{R}(\boldsymbol{X})) \leq \bar{\epsilon}$*, where* $\bar{R}(\boldsymbol{X})$ *and* $R(\boldsymbol{X})$ *are the set-valued systemic risk measures when* $\epsilon = \bar{\epsilon}$ *and* $\epsilon = 0$*, respectively.*

Proof. Let $\bar{\boldsymbol{k}} \in \bar{R}(\boldsymbol{X})$. Then, $\mathrm{V@R}_\lambda(\Lambda^{\mathrm{EN}}(\boldsymbol{X} + \boldsymbol{B}^\top \bar{\boldsymbol{k}})) \leq \alpha$. By the definition of $R(\boldsymbol{X})$ in Chapter 4, we have $\bar{\boldsymbol{k}} \in R(\boldsymbol{X})$.

Now to show that $\mathbb{H}(R(\boldsymbol{X}), \bar{R}(\boldsymbol{X})) \leq \bar{\epsilon}$, we first show that for any point $\boldsymbol{k} \in R(\boldsymbol{X})$,

$$\inf_{\bar{\boldsymbol{k}} \in \bar{R}(\boldsymbol{X})} \|\boldsymbol{k} - \bar{\boldsymbol{k}}\|_2 \leq \bar{\epsilon}$$

by considering the following two cases:

- If $\boldsymbol{k}$ is not in the grid region, as $\bar{R}(\boldsymbol{X})$ and $R(\boldsymbol{X})$ coincide outside the grid region, then,
$$\inf_{\bar{\boldsymbol{k}} \in \bar{R}(\boldsymbol{X})} \|\boldsymbol{k} - \bar{\boldsymbol{k}}\|_2 = 0.$$
- If $\boldsymbol{k}$ is in the grid region, then, by the construction of the grid region, the distance between neighbor grid points is less than or equal to $\bar{\epsilon}$. Then, there exists a grid point $\dot{\boldsymbol{k}}$ such that $\boldsymbol{k} \leq \dot{\boldsymbol{k}} \leq \boldsymbol{k} + \bar{\epsilon}\mathbf{1}$. We claim that $\dot{\boldsymbol{k}}$ is an acceptable grid point. To show our claim, we know that since $\boldsymbol{k} \in R(\boldsymbol{X})$,
$$\mathbb{P}(\Lambda^{\mathrm{EN}}(\boldsymbol{X} + \boldsymbol{B}^\top \boldsymbol{k}) < \alpha) \leq \lambda.$$

In other words,

$$\sum_{s=1}^{S} \mathbb{P}\{\omega^s\} 1_{(-\infty,\alpha)}(\Lambda^{\mathrm{EN}}(\boldsymbol{x}_s + \boldsymbol{B}^\top \boldsymbol{k})) \leq \lambda.$$

Since $\boldsymbol{k} \leq \dot{\boldsymbol{k}}$, by the monotonicity property of Λ^{EN}, for any $\omega^s \in \Omega$,

$$\Lambda^{\mathrm{EN}}(\boldsymbol{x}_s + \boldsymbol{B}^\top \dot{\boldsymbol{k}}) \geq \Lambda^{\mathrm{EN}}(\boldsymbol{x}_s + \boldsymbol{B}^\top \boldsymbol{k}).$$

Therefore,

$$\mathbb{P}\{\omega^s\} 1_{(-\infty,\alpha)}(\Lambda^{\mathrm{EN}}(\boldsymbol{x}_s + \boldsymbol{B}^\top \dot{\boldsymbol{k}})) \leq \mathbb{P}\{\omega^s\} 1_{(-\infty,\alpha)}(\Lambda^{\mathrm{EN}}(\boldsymbol{x}_s + \boldsymbol{B}^\top \boldsymbol{k})).$$

Then,

$$\sum_{s=1}^{S} \mathbb{P}\{\omega^s\} 1_{(-\infty,\alpha)}(\Lambda^{\mathrm{EN}}(\boldsymbol{x}_s + \boldsymbol{B}^\top \dot{\boldsymbol{k}})) \leq \sum_{s=1}^{S} \mathbb{P}\{\omega^s\} 1_{(-\infty,\alpha)}(\Lambda^{\mathrm{EN}}(\boldsymbol{x}_s + \boldsymbol{B}^\top \boldsymbol{k})) \leq \lambda.$$

Therefore, $\dot{\boldsymbol{k}}$ is an acceptable grid point by Algorithm 1. Thus, $\dot{\boldsymbol{k}} \in \bar{R}(\boldsymbol{X})$. Hence,

$$\inf_{\bar{\boldsymbol{k}} \in \bar{R}(\boldsymbol{X})} \|\boldsymbol{k} - \bar{\boldsymbol{k}}\|_2 \leq \|\boldsymbol{k} - \dot{\boldsymbol{k}}\|_2 \leq \bar{\epsilon}.$$

Moreover, since $\bar{R}(\boldsymbol{X}) \subseteq R(\boldsymbol{X})$, for any point $\bar{\boldsymbol{k}} \in \bar{R}(\boldsymbol{X})$,

$$\inf_{\boldsymbol{k} \in R(\boldsymbol{X})} \|\boldsymbol{k} - \bar{\boldsymbol{k}}\|_2 = 0.$$

Then, $\sup_{\bar{\boldsymbol{k}} \in \bar{R}(\boldsymbol{X})} \inf_{\boldsymbol{k} \in R(\boldsymbol{X})} \|\boldsymbol{k} - \bar{\boldsymbol{k}}\|_2 = 0$. Thus, $\mathbb{H}(R(\boldsymbol{X}), \bar{R}(\boldsymbol{X})) \leq \max(\bar{\epsilon}, 0) = \bar{\epsilon}$. □

Chapter 5

Sample-Average Approximation (SAA)

In this chapter, our objective is to provide a justification for the assumption regarding the finiteness of the sample space made in Chapter 4. This will be achieved by introducing the concept of sample-average approximation as discussed in [25] for chance-constrained problems. In particular, under specific assumptions, we establish that the SAA solutions of the scalarizations of set-valued systemic risk measures converge to the solutions of their respective true problems as the sample size N goes to infinity.

The true scalarization problems we aimed to address, namely the weighted sum scalarization, Pascoletti-Serafini scalarization, and norm-minimizing scalarization problems, where we do not assume the finiteness of the sample space, are presented in the following format:

$$\begin{aligned} \mathcal{P} = &\min_{\boldsymbol{z}\in\mathcal{Z}} \varphi(\boldsymbol{z}) \\ &\text{s.t.} \quad P(\boldsymbol{z}) \coloneqq \mathbb{P}(u(\boldsymbol{z}, \boldsymbol{X}) < \alpha) \leq \lambda, \end{aligned} \tag{5.0.1}$$

where $\mathcal{Z} \subseteq \mathbb{R}^m$, $\boldsymbol{X} \in L_n^\infty$, which is a random vector measurable with respect to $(\Omega, \mathcal{F})$ supported with $\mathbb{P}$ on the set $\mathcal{E} \subseteq \mathbb{R}^n$, $\alpha \in \mathbb{R}$, $\lambda \in (0, 1)$, $\varphi : \mathbb{R}^m \to \mathbb{R}$ is a real-valued function, and $u : \mathbb{R}^m \times \mathbb{R}^n_+ \to \mathbb{R}$ is a bivariate real-valued function.

We assume that $\mathcal{Z}$ is a nonempty closed set and u is a Carathéodory function, that is, $u(\boldsymbol{z}, \cdot)$ is measurable for each $\boldsymbol{z} \in \mathbb{R}^m$ and $u(\cdot, \boldsymbol{x})$ is continuous for almost every $\boldsymbol{x} \in \mathcal{E}$. Note that we do not have any convexity assumptions on $\mathcal{Z}$ and $\mathcal{E}$.

Now, we fix $N \in \mathbb{N}$ and let $\boldsymbol{X}^1, \ldots, \boldsymbol{X}^N$ be independent copies of $\boldsymbol{X}$, i.e., $\boldsymbol{X}^1, \ldots, \boldsymbol{X}^N$ are independent random vectors with the same distribution as $\boldsymbol{X}$. For each $\boldsymbol{z} \in \mathcal{Z}$, define

$$\hat{P}_N(\boldsymbol{z}) \coloneqq \frac{1}{N} \sum_{j=1}^{N} 1_{(-\infty,\alpha)}(u(\boldsymbol{z}, \boldsymbol{X}^j));$$

note that $\hat{P}_N(\boldsymbol{z})$ is a random variable. Then, the problem associated with the generated sample $\boldsymbol{X}^1, \ldots, \boldsymbol{X}^N$ is given by

$$\begin{aligned} \hat{\mathcal{P}}_N = & \min_{\boldsymbol{z} \in \mathcal{Z}} \varphi(\boldsymbol{z}) \\ & \text{s.t.} \quad \hat{P}_N(\boldsymbol{z}) \leq \lambda. \end{aligned} \tag{5.0.2}$$

Note that $\hat{\mathcal{P}}_N$ is also a random variable, its measurability is shown in [25, Proposition 2.1] using [38, Proposition 14.45].

Next, we will examine the convergence of a solution of the SAA problem in (5.0.2) to the solution of the true problem in (5.0.1) with respect to the sample size N.

Definition 5.0.1. *[25, Section 2] A sequence $(\varphi_N)_{N \in \mathbb{N}}$ of extended real-valued functions on $\mathcal{Z}$ is said to* epiconverge *to a function $\varphi \colon \mathcal{Z} \to \bar{\mathbb{R}}$, written as $\varphi_N \xrightarrow{e} \varphi$, if for every $\boldsymbol{z} \in \mathcal{Z}$, the following conditions hold:*

i. For every sequence $(\boldsymbol{z_N})_{N \in \mathbb{N}}$ in $\mathcal{Z}$ converging to $\boldsymbol{z}$, one has

$$\liminf_{N \to \infty} \varphi_N(\boldsymbol{z_N}) \geq \varphi(\boldsymbol{z}).$$

ii. There exists a sequence $(\boldsymbol{z_N})_{N \in \mathbb{N}}$ in $\mathcal{Z}$ converging to $\boldsymbol{z}$ such that

$$\limsup_{N \to \infty} \varphi_N(\boldsymbol{z_N}) \leq \varphi(\boldsymbol{z}).$$

Lemma 5.0.2. *For each $\boldsymbol{z} \in \mathcal{Z}$, $(\hat{P}_N(\boldsymbol{z}))_{N \in \mathbb{N}}$ converges to $P(\boldsymbol{z})$ almost surely.*

Proof. This is a direct application of the strong law of large numbers. □

Proposition 5.0.3. *[25, Proposition 2.1] Let u be a Carathéodory function. Then, the functions $P, \hat{P}_1, \hat{P}_2, \ldots$ are lower semicontinuous and $(\hat{P}_N)_{N \in \mathbb{N}}$ epiconverges to P almost surely.*

Remark 5.0.4. *Let $\mathcal{V}$ denote the set of optimal solutions for the problem stated in* (5.0.1)*, and let $\hat{\mathcal{V}}_N$ denote the set of optimal solutions for its sample-average approximation as stated in* (5.0.2)*. The lower semicontinuity property demonstrated by P and $\hat{P}_N$ implies that the feasible sets corresponding to* (5.0.1) *and* (5.0.2) *are closed sets. Therefore, if the set $\mathcal{Z}$ is compact, it can be inferred that both $\mathcal{V}$ and $\hat{\mathcal{V}}_N$ are nonempty, provided that these problems have nonempty feasible sets.*

Proposition 5.0.3 demonstrates that, given mild regularity assumptions, the estimators $\hat{\mathcal{V}}_N$ and $\hat{\mathcal{P}}_N$ converge to the true values $\mathcal{V}$ and $\mathcal{P}$, respectively, as $N \to \infty$.

Assumption 5.0.5. *[25, Condition (A)] There exists an optimal solution $\bar{\boldsymbol{z}}$ of the true problem* (5.0.1) *such that for each $\epsilon > 0$, there exists $\boldsymbol{z} \in \mathcal{Z}$ satisfying $\|\boldsymbol{z} - \bar{\boldsymbol{z}}\|_2 < \epsilon$ and $P(\boldsymbol{z}) < \lambda$.*

This assumption guarantees the existence of a sequence $(\boldsymbol{z_n})_{n\in\mathbb{N}}$ in $\mathcal{Z}$ that converges to an optimal solution $\bar{\boldsymbol{z}} \in \mathcal{V}$ while satisfying the strict feasibility condition $P(\boldsymbol{z_n}) < \lambda$ for each $n \in \mathbb{N}$. In particular, Assumption 5.0.5 guarantees that the set $\mathcal{V}$ is nonempty and there is $\boldsymbol{z} \in \mathcal{Z}$ such that $P(\boldsymbol{z}) < \lambda$.

Proposition 5.0.6. *[25, Proposition 2.2] Suppose that $\mathcal{Z}$ is compact, φ is continuous, u is a Carathéodory function, and Assumption 5.0.5 holds. Then, as $N \to \infty$,*

$$\mathbb{D}(\hat{\mathcal{V}}_N, \mathcal{V}) \to 0,$$
$$\hat{\mathcal{P}}_N \to \mathcal{P}.$$

almost surely.

5.1 Sample-Average Approximation for Weighted Sum Scalarization

Within this section, we shall delve into the topic of the sample-average approximation of the weighted sum scalarization problem. We begin by introducing the true problem formulation, followed by the presentation of the SAA formulation. To that end, let $(\mathcal{N}, \boldsymbol{\pi}, \bar{\boldsymbol{p}}, \boldsymbol{X})$ be an Eisenberg-Noe network.

Let $\mathcal{Z} \subseteq \mathbb{R}^i$ be a nonempty closed set and fix a weight vector $\boldsymbol{w} \in \mathbb{R}^i_+ \setminus \{0\}$. The true weighted sum scalarization problem can be written as

$$\begin{aligned} \mathcal{P}^{\mathrm{WS}}(\boldsymbol{w}) = & \min_{\boldsymbol{z} \in \mathcal{Z}} \boldsymbol{w}^\top \boldsymbol{z} \\ & \text{s.t.} \quad \mathbb{P}(\Lambda^{\mathrm{EN}}(\boldsymbol{X} + \boldsymbol{B}^\top \boldsymbol{z}) < \alpha) \leq \lambda, \end{aligned} \tag{5.1.1}$$

where Λ^{EN} is defined by (3.0.2). Then, the corresponding SAA formulation for each sample size $N \in \mathbb{N}$ can be written as

$$\begin{aligned} \hat{\mathcal{P}}^{\mathrm{WS}}_N(\boldsymbol{w}) = & \min_{\boldsymbol{z} \in \mathcal{Z}} \boldsymbol{w}^\top \boldsymbol{z} \\ & \text{s.t.} \quad \frac{1}{N} \sum_{j=1}^{N} 1_{(-\infty,\alpha)}(\Lambda^{\mathrm{EN}}(\boldsymbol{X}^j + \boldsymbol{B}^\top \boldsymbol{z})) \leq \lambda. \end{aligned} \tag{5.1.2}$$

Note that according to the formulations in (5.0.1) and (5.0.2), in this section, we take $\varphi(\boldsymbol{z}) = \boldsymbol{w}^\top \boldsymbol{z}$, $u(\boldsymbol{z}, \boldsymbol{x}) = u^{\mathrm{EN}}(\boldsymbol{z}, \boldsymbol{x}) \coloneqq \Lambda^{\mathrm{EN}}(\boldsymbol{x} + \boldsymbol{B}^\top \boldsymbol{z})$, $P(\boldsymbol{z}) = \mathbb{P}(\Lambda^{\mathrm{EN}}(\boldsymbol{X} + \boldsymbol{B}^\top \boldsymbol{z}) < \alpha)$ and $\hat{P}_N(\boldsymbol{z}) = \frac{1}{N} \sum_{j=1}^{N} 1_{(-\infty,\alpha)}(\Lambda^{\mathrm{EN}}(\boldsymbol{X}^j + \boldsymbol{B}^\top \boldsymbol{z}))$.

We now assume that $\boldsymbol{X} \in L^\infty_n$, and define the set $\mathcal{Z}$ as follows:

$$\mathcal{Z} := \left\{ \boldsymbol{z} \in \mathbb{R}^i \mid -\|\boldsymbol{X}\|_\infty \mathbf{1} \leq \boldsymbol{z} \leq \|\bar{\boldsymbol{p}}\|_\infty \mathbf{1} \right\}.$$

Note that $\mathcal{Z}$ is a compact set.

We now present a lemma related to the nature of the function u^{EN}:

Lemma 5.1.1. *u^{EN} is a Carathéodory function on $\mathbb{R}^i \times \mathbb{R}^n_+$.*

Proof. Since $u^{\mathrm{EN}}(\boldsymbol{z}, \boldsymbol{x}) = \Lambda^{\mathrm{EN}}(\boldsymbol{x} + \boldsymbol{B}^\top \boldsymbol{z})$ for each $(\boldsymbol{z}, \boldsymbol{x}) \in \mathbb{R}^i \times \mathbb{R}^n_+$ and Λ^{EN} is a continuous function by Lemma 3.0.5, u^{EN} is a continuous function, hence it is also a Carathéodory function. □

Proposition 5.1.2. *For each $N \in \mathbb{N}$, the functions P and $\hat{P}_N$ are lower semicontinuous. Moreover, the sequence $(\hat{P}_N)_{N \in \mathbb{N}}$ epiconverges to P a.s.*

Proof. Since u^{EN} is a Carathéodory function by Lemma 5.1.1, the result is a direct consequence of Proposition 5.0.3. □

Finally, we present a corollary that demonstrates the convergence of the sample-average approximation problem in (5.1.2), to its corresponding true problem in (5.1.1).

Corollary 5.1.3. *Suppose that $\alpha \leq \mathbf{1}^\top \bar{\boldsymbol{p}}$ and Assumption 5.0.5 holds for $u = u^{EN}$. Then, for a fixed $\boldsymbol{w} \in \mathbb{R}^i_+ \setminus \{\mathbf{0}\}$, we have*

$$\hat{\mathcal{P}}_N^{WS}(\boldsymbol{w}) \to \mathcal{P}^{WS}(\boldsymbol{w}) \text{ a.s.}$$

as $N \to \infty$.

Proof. This is a direct consequence of Proposition 5.0.6 as $\mathcal{Z}$ is compact, φ is continuous, and u^{EN} is a Carathéodory function by Lemma 5.1.1. □

5.2 Sample-Average Approximation for Pascoletti-Serafini Scalarization

In this section, we shall delve into the topic of the sample-average approximation of the Pascoletti Serafini scalarization Problem. We begin by introducing the true problem formulation, followed by the presentation of the SAA formulation. To that end, let $(\mathcal{N}, \boldsymbol{\pi}, \bar{\boldsymbol{p}}, \boldsymbol{X})$ be an Eisenberg-Noe network.

Let $\mathcal{Z} \subseteq \mathbb{R}$ be a nonempty closed set and fix $\boldsymbol{k} \in \mathbb{R}^i$. The true problem of Pascoletti Serafini scalarization can be written as

$$\begin{aligned} \mathcal{P}^{\mathrm{PS}}(\boldsymbol{k}) = &\min_{z \in \mathcal{Z}} z \\ &\text{s.t.} \quad \mathbb{P}(\Lambda^{\mathrm{EN}}(\boldsymbol{X} + \boldsymbol{B}^\top(\boldsymbol{k} + z\mathbf{1})) < \alpha) \leq \lambda. \end{aligned} \tag{5.2.1}$$

To approximate the true problem, we introduce the SAA formulation, which can be written as

$$\begin{aligned} \hat{\mathcal{P}}_N^{\mathrm{PS}}(\boldsymbol{k}) = &\min_{z \in \mathcal{Z}} z \\ &\text{s.t.} \quad \frac{1}{N} \sum_{j=1}^{N} 1_{(-\infty,\alpha)}(\Lambda^{\mathrm{EN}}(\boldsymbol{X}^j + \boldsymbol{B}^\top(\boldsymbol{k} + z\mathbf{1}))) \leq \lambda, \end{aligned} \tag{5.2.2}$$

where Λ^{EN} is defined by (3.0.2).

Note that according to the formulations in (5.0.1) and (5.0.2), in this section, we take $\varphi(z) = z$ and $u(z, \boldsymbol{x}) = u^{\mathrm{EN}}(z, \boldsymbol{x}) \coloneqq \Lambda^{\mathrm{EN}}(\boldsymbol{x}+\boldsymbol{B}^\top(\boldsymbol{k}+z\mathbf{1}))$, $P(z) = \mathbb{P}(\Lambda^{\mathrm{EN}}(\boldsymbol{X}+\boldsymbol{B}^\top(\boldsymbol{k}+z\mathbf{1})) < \alpha)$ and $\hat{P}_N(z) = \frac{1}{N}\sum_{j=1}^{N} 1_{(-\infty,\alpha)}(\Lambda^{\mathrm{EN}}(\boldsymbol{X}^j + \boldsymbol{B}^\top(\boldsymbol{k} + z\mathbf{1})))$.

We now assume that $\boldsymbol{X} \in L_n^\infty$ and define the compact set

$$\mathcal{Z} \coloneqq [-(\|\boldsymbol{X}\|_\infty + \|\boldsymbol{k}\|_\infty), \|\bar{\boldsymbol{p}}\|_\infty + \|\boldsymbol{k}\|_\infty].$$

Lemma 5.2.1. *u^{EN} is a Carathéodory function on $\mathbb{R} \times \mathbb{R}_+^n$.*

Proof. Since $u^{\mathrm{EN}}(z, \boldsymbol{x}) = \Lambda^{\mathrm{EN}}(\boldsymbol{x} + \boldsymbol{B}^\top(\boldsymbol{k} + z\mathbf{1}))$ for each $(z, \boldsymbol{x}) \in \mathbb{R} \times \mathbb{R}_+^n$ and Λ^{EN} is a continuous function by Lemma 3.0.5, u^{EN} is a continuous function, hence it is also a Carathéodory function. □

Proposition 5.2.2. *For each $N \in \mathbb{N}$, the functions P and $\hat{P}_N$ are lower semicontinuous. Moreover, the sequence $(\hat{P}_N)_{N\in\mathbb{N}}$ epiconverges to P a.s.*

Proof. Since u^{EN} is a Carathéodory function by Lemma 5.2.1, this is a direct implication of Proposition 5.0.3. □

Finally, we present a corollary that establishes the convergence of the SAA problem in (5.2.2) to its true problem in (5.2.1).

Corollary 5.2.3. *Suppose that $\alpha \leq \mathbf{1}^\top\bar{\boldsymbol{p}}$ and Assumption 5.0.5 holds. Then, for a fixed $\boldsymbol{k} \in \mathbb{R}^i$, we have*

$$\hat{\mathcal{P}}_N^{PS}(\boldsymbol{k}) \to \mathcal{P}^{PS}(\boldsymbol{k}) \text{ a.s.}$$

as $N \to \infty$.

Proof. This is a direct consequence of Proposition 5.0.6 as $\mathcal{Z}$ is compact, φ is continuous, and u^{EN} is a Carathéodory function by Lemma 5.2.1. □

5.3 Sample-Average Approximation for Norm-Minimizing Scalarization

In this section, we shall delve into the topic of the sample-average approximation of the norm-minimizing scalarization Problem. We begin by introducing the true problem formulation, followed by the presentation of the SAA formulation. To that end, let $(\mathcal{N}, \boldsymbol{\pi}, \bar{\boldsymbol{p}}, \boldsymbol{X})$ be an Eisenberg-Noe network.

Let $\mathcal{Z} \subseteq \mathbb{R}^i$ be a nonempty closed set, and fix $\boldsymbol{k} \in \mathbb{R}^i$. The true problem of the norm-minimizing scalarization can be written as

$$\begin{aligned} \mathcal{P}^{\mathrm{NM}}(\boldsymbol{k}) = & \min_{\boldsymbol{z} \in \mathcal{Z}} \|\boldsymbol{k} - \boldsymbol{z}\|_2 \\ & \text{s.t.} \quad \mathbb{P}(\Lambda^{\mathrm{EN}}(\boldsymbol{X} + \boldsymbol{B}^\top \boldsymbol{z}) < \alpha) \leq \lambda, \end{aligned} \tag{5.3.1}$$

where Λ^{EN} is defined by (3.0.2).

To approximate the true problem, we introduce the SAA formulation as

$$\begin{aligned} \hat{\mathcal{P}}_N^{\mathrm{NM}}(\boldsymbol{k}) = & \min_{\boldsymbol{z} \in \mathcal{Z}} \|\boldsymbol{k} - \boldsymbol{z}\|_2 \\ & \text{s.t.} \quad \frac{1}{N} \sum_{j=1}^{N} 1_{(-\infty, \alpha)}(\Lambda^{\mathrm{EN}}(\boldsymbol{X}^j + \boldsymbol{B}^\top \boldsymbol{z})) \leq \lambda. \end{aligned} \tag{5.3.2}$$

Note that according to the formulations in (5.0.1) and (5.0.2), in this section, we take $\varphi(\boldsymbol{z}) = \|\boldsymbol{k} - \boldsymbol{z}\|_2$, $u(\boldsymbol{z}, \boldsymbol{x}) = u^{\mathrm{EN}}(\boldsymbol{z}, \boldsymbol{x}) \coloneqq \Lambda^{\mathrm{EN}}(\boldsymbol{x} + \boldsymbol{B}^\top \boldsymbol{z})$, $P(\boldsymbol{z}) = \mathbb{P}(\Lambda^{EN}(\boldsymbol{X} + \boldsymbol{B}^\top \boldsymbol{z}) < \alpha)$ and $\hat{P}_N(\boldsymbol{z}) = \frac{1}{N} \sum_{j=1}^{N} 1_{(-\infty, \alpha)}(\Lambda^{\mathrm{EN}}(\boldsymbol{X}^j + \boldsymbol{B}^\top \boldsymbol{z}))$. By Lemma 5.1.1, u^{EN} is a Carathéodory function on $\mathbb{R}^i \times \mathbb{R}^n_+$.

We now assume that $\boldsymbol{X} \in L_n^\infty$, and define

$$\mathcal{Z} \coloneqq \left\{ \boldsymbol{z} \in \mathbb{R}^i \mid -\|\boldsymbol{X}\|_\infty \mathbf{1} \leq \boldsymbol{z} \leq \|\bar{\boldsymbol{p}}\|_\infty \mathbf{1} \right\}.$$

Note that $\mathcal{Z}$ is a compact set.

Proposition 5.3.1. *For each $N \in \mathbb{N}$, the functions P and $\hat{P}_N$ are lower semicontinuous. Moreover, the sequence $(\hat{P}_N)_{N \in \mathbb{N}}$ epiconverges to P a.s.*

Proof. Since u^{EN} is a Carathéodory function, this is a direct consequence of Proposition 5.0.3. □

Finally, we present a corollary that establishes the convergence of the SAA problem in (5.3.2) to its true problem in (5.3.1).

Corollary 5.3.2. *Suppose that $\alpha \leq \mathbf{1}^\top \bar{\boldsymbol{p}}$ and Assumption 5.0.5 holds. Then, for a fixed $\boldsymbol{k} \in \mathbb{R}^i$, we have*

$$\hat{\mathcal{P}}_N^{NM}(\boldsymbol{k}) \to \mathcal{P}^{NM}(\boldsymbol{k}) \text{ a.s.}$$

as $N \to \infty$.

Proof. This is a direct consequence of Proposition 5.0.6 as $\mathcal{Z}$ is compact, φ is continuous, and u^{EN} is a Carathéodory function. □

5.4 Convergence of Set-Valued Risk Measures

The purpose of this section is to show the convergence of the sample-average approximated set-valued risk measure to its true counterpart. In order to achieve this objective, we firstly, study two notions of convergence for sets, namely Hausdorff and Wijsman, and subsequently mention the correlation between these two concepts. To that end, let $(\mathcal{N}, \boldsymbol{\pi}, \bar{\boldsymbol{p}}, \boldsymbol{X})$ be an Eisenberg-Noe network.

Let $E \subseteq \mathbb{R}^n$ be a nonempty closed set and denote by $\mathcal{C}(E)$ the set of non-empty closed subsets of E. We proceed by providing formal definitions of the convergence notions:

Definition 5.4.1. *[28, Section 3.17] A sequence of sets $(\hat{R}_N)_{N\in\mathbb{N}}$ in $\mathcal{C}(E)$ is said to* Hausdorff converge *to a set $R \in \mathcal{C}(E)$ if the sequence $(d(\cdot, \hat{R}_N))_{N\in\mathbb{N}}$ of real functions converges uniformly to $d(\cdot, R)$. In this case, we write $\hat{R}_N \xrightarrow{H} R$ as $N \to \infty$.*

Definition 5.4.2. *[28, Section 3.17] A sequence of sets $(\hat{R}_N)_{N\in\mathbb{N}}$ in $\mathcal{C}(E)$ is said to* Wijsman converge *to a set $R \in \mathcal{C}(E)$ if $(d(\boldsymbol{x}, \hat{R}_N))_{N\in\mathbb{N}}$ converges to $d(\boldsymbol{x}, R)$ for each $\boldsymbol{x} \in E$. In this case, we write $\hat{R}_N \xrightarrow{W} R$ as $N \to \infty$.*

The aforementioned definitions encompass distinct concepts of convergence pertaining to sets situated within the metric space denoted as E. It is important to note that the

convergence in the Hausdorff metric typically implies the convergence in the Wijsman metric. Nevertheless, given the assumption of complete boundedness of the space, we examine a theorem that establishes a correlation between Hausdorff and Wijsman convergence in the converse direction.

Theorem 5.4.3. *[29, Theorem 2.5] The Hausdorff and Wijsman convergences coincide if and only if E is compact.*

Subsequently, we leverage the aforementioned convergence outcome to gain additional understanding regarding the dynamics exhibited by our set-valued risk measures. We first examine the Wijsman convergence of the sample-average approximated set-valued risk measure to its true set-valued risk measure. In order to achieve this objective, let us set

$$E \coloneqq \{\boldsymbol{z} \in \mathbb{R}^i \mid -(\|\boldsymbol{X}\|_\infty \mathbf{1} + \|\bar{\boldsymbol{p}}\|_\infty \mathbf{1}) \leq \boldsymbol{z} \leq \|\bar{p}\|_\infty \mathbf{1}\}.$$

Independent of the sample size N, the efficient frontier of our set-valued risk measure lies within set E thanks to the following lemma.

Lemma 5.4.4. *It holds $R(\boldsymbol{X}) = R(\boldsymbol{X}) \cap E + \mathbb{R}^i_+$.*

Proof. It is clear that $R(\boldsymbol{X}) \supseteq R(\boldsymbol{X}) \cap E + \mathbb{R}^i_+$ as $R(\boldsymbol{X}) = R(\boldsymbol{X}) + \mathbb{R}^i_+$ by Lemma 4.0.8. Now to show that $R(\boldsymbol{X}) \subseteq R(\boldsymbol{X}) \cap E + \mathbb{R}^i_+$, let $\boldsymbol{z} \in R(\boldsymbol{X})$. It is enough to show that there exists $\dot{\boldsymbol{z}} \in E \cap R(\boldsymbol{X})$ such that $\boldsymbol{z} \in \{\dot{\boldsymbol{z}}\} + \mathbb{R}^i_+$. To that end, let $\dot{\boldsymbol{z}}$ as follows:

$$\dot{z}_j = \begin{cases} \|\bar{\boldsymbol{p}}\|_\infty, & \text{if } z_j \geq \|\bar{\boldsymbol{p}}\|_\infty \\ z_j, & \text{otherwise.} \end{cases}$$

We claim that $\dot{\boldsymbol{z}} \in R(\boldsymbol{X})$. To prove the claim, it is enough to show that for each bank r in group j, scenario $\omega^s \in \Omega$, $s \in \mathbb{N}$ such that $(\boldsymbol{B}^\top \boldsymbol{z})^r_s \geq \|\bar{\boldsymbol{p}}\|_\infty$, $p^r_s(\boldsymbol{z}) = p^r_s(\dot{\boldsymbol{z}})$, where, $p^r_s(\boldsymbol{z})$ and $p^r_s(\dot{\boldsymbol{z}})$ represent the optimal clearing of bank r in scenario ω^s given the capital injection $\boldsymbol{z}$ and $\dot{\boldsymbol{z}}$, respectively. We know that $p^r_s(\boldsymbol{z}), p^r_s(\dot{\boldsymbol{z}}) \leq \bar{p}^r \leq \|\bar{\boldsymbol{p}}\|_\infty$. Since $z_j, \dot{z}_j \geq \|\bar{\boldsymbol{p}}\|_\infty$, then for bank r in scenario ω^s, $p^r_s(\boldsymbol{z}) = \bar{p}^r$ satisfies $0 \leq p^r_s(\boldsymbol{z}) \leq \sum_{t=1}^n \boldsymbol{\pi}_{tr} p^t_s + x^r_s + \|\bar{\boldsymbol{p}}\|_\infty \leq \bar{p}^r$, and $p^r_s(\dot{\boldsymbol{z}}) = \bar{p}^r$ satisfies $0 \leq p^r_s(\dot{\boldsymbol{z}}) \leq \sum_{t=1}^n \boldsymbol{\pi}_{tr} p^t_s + x^r_s + \|\bar{\boldsymbol{p}}\|_\infty \leq \bar{p}^r$, then $p^r_s(\boldsymbol{z}) = p^r_s(\dot{\boldsymbol{z}}) = \bar{p}^r$ and the result follows. Thus, $\dot{\boldsymbol{z}} \in R(\boldsymbol{X})$.

Note that as mentioned in Remark 4.0.10, $z_j \geq -(\|\boldsymbol{X}\|_\infty + \mathbf{1}^\top \bar{\boldsymbol{p}})$ for all $j \in \{1, \ldots, i\}$. Therefore, $\dot{\boldsymbol{z}} \in E$.

Hence and $\dot{\boldsymbol{z}} \in E \cap R(\boldsymbol{X})$ and $\boldsymbol{z} \in \{\dot{\boldsymbol{z}}\} + \mathbb{R}^i_+$. □

We now define the true and sample-average approximated set-valued risk measure restricted to the set E in the following sense:

$$R^{\text{restricted}}(\boldsymbol{X}) = \{\boldsymbol{z} \in E \mid \mathbb{P}(\Lambda^{\text{EN}}(\boldsymbol{X} + \boldsymbol{B}^\top \boldsymbol{z}) < \alpha) \leq \lambda\},$$

which represents the true set-valued risk measure restricted to E, and

$$\hat{R}_N^{\text{restricted}}(\boldsymbol{X}^{[N]}) = \{\boldsymbol{z}_N \in E \mid \frac{1}{N} \sum_{j=1}^{N} 1_{-\infty,\alpha}(\Lambda^{\text{EN}}(\boldsymbol{X}^j + \boldsymbol{B}^\top \boldsymbol{z})) \leq \lambda\},$$

which represents the sample-average approximated set-valued risk measure restricted to E. Here, $\boldsymbol{X}^{[N]} \coloneqq (\boldsymbol{X}^1, \ldots, \boldsymbol{X}^N)$.

Theorem 5.4.5. *Assume that $\alpha \leq \mathbf{1}^\top \bar{\boldsymbol{p}}$ and Assumption 5.0.5 holds. Then, the SAA set-valued restricted risk measure $\hat{R}_N^{restricted}(\boldsymbol{X}^{[N]})$ converges to its true set-valued risk measure $R^{restricted}(\boldsymbol{X})$ as $N \to \infty$ in the Wijsman sense a.s., i.e., $\hat{R}_N^{restricted}(\boldsymbol{X}^{[N]}) \xrightarrow{W} R^{restricted}(\boldsymbol{X})$ as $N \to \infty$ a.s.*

Proof. Let $\boldsymbol{k} \in \mathbb{R}^i$ be a point in E. Since $\alpha \leq \mathbf{1}^\top \bar{\boldsymbol{p}}$ and by Assumption 5.0.5, $\mathcal{P}^{nm}(\boldsymbol{k}) = \|\boldsymbol{k} - \boldsymbol{z}^\star\|_2$ is the optimal value of the true norm-minimizing scalarization problem, where $\boldsymbol{z}^\star \in R^{\text{restricted}}(\boldsymbol{X})$ exists. By Proposition 5.0.6, as $N \to \infty$, $\hat{\mathcal{P}}_N^{\text{NM}}(\boldsymbol{k}) = \|\boldsymbol{k} - \hat{\boldsymbol{z}}_N^\star\|_2$ converges to $\mathcal{P}^{\text{NM}}(\boldsymbol{k})$, where $\hat{\mathcal{P}}_N^{\text{NM}}(\boldsymbol{k})$ is the optimal value of the SAA norm-minimizing scalarization problem given $\boldsymbol{k}$, which exists since $\alpha \leq \mathbf{1}^\top \bar{\boldsymbol{p}}$ by Proposition 4.0.11, where $\hat{\boldsymbol{z}}_N^\star \in \hat{R}_N^{\text{restricted}}(\boldsymbol{X}^{[N]})$. Therefore, as $N \to \infty$,

$$d(\boldsymbol{k}, \hat{R}_N^{\text{restricted}}(\boldsymbol{X}^{[N]}) - d(\boldsymbol{k}, R^{\text{restricted}}(\boldsymbol{X})) = \hat{\mathcal{P}}_N^{\text{NM}}(\boldsymbol{k}) - \mathcal{P}^{\text{NM}}(\boldsymbol{k}) \to 0 \text{ a.s.}$$

Hence, for every point $\boldsymbol{k} \in E$, $(d(\boldsymbol{k}, \hat{R}_N^{\text{restricted}}(\boldsymbol{X}^{[N]})))_{N \in \mathbb{N}}$ converges to $d(\boldsymbol{k}, R^{\text{restricted}}(\boldsymbol{X}))$ a.s. Consequently, the sequence $(\hat{R}_N^{\text{restricted}}(\boldsymbol{X}^{[N]}))_{N \in \mathbb{N}}$ Wijsman converges to $R^{\text{restricted}}(\boldsymbol{X})$ a.s. □

In addition to examining the Wijsman convergence, we also explore the Hausdorff convergence of our restricted sample-average approximation set-valued risk measure to its true set-valued risk measure. The convergence property can be established in the following corollary, owing to the compactness of the set E.

Corollary 5.4.6. *Suppose that $\alpha \leq \mathbf{1}^\top \bar{\boldsymbol{p}}$ and Assumption 5.0.5 holds for the norm-minimizing scalarizations. Then, the SAA set-valued restricted risk measure $\hat{R}_N^{restricted}(\boldsymbol{X}^{[N]})$ converges to its true set-valued risk measure $R^{restricted}(\boldsymbol{X})$ in the Hausdorff sense as $N \to \infty$ a.s., i.e., $\hat{R}_N^{restricted}(\boldsymbol{X}^{[N]}) \xrightarrow{H} R^{restricted}(\boldsymbol{X})$ as $N \to \infty$ a.s.*

Proof. This is a direct result of Theorem 5.4.3 as the set E is a compact set. □

Next we will show that the sample-average approximated risk set-valued risk measure $\hat{R}_N(\boldsymbol{X}^{[N]}) = \{\boldsymbol{z} \in \mathbb{R}^i \mid \frac{1}{N}\sum_{j=1}^N 1_{(-\infty,\alpha)}(\Lambda^{\mathrm{EN}}(\boldsymbol{x}_j + \boldsymbol{B}^\top \boldsymbol{z})) \leq \lambda\}$ converges to its true set-valued risk measure $R(\boldsymbol{X}) = \{\boldsymbol{z} \in \mathbb{R}^i \mid \mathbb{P}(\Lambda^{\mathrm{EN}}(\boldsymbol{X} + \boldsymbol{B}^\top \boldsymbol{z}) < \alpha) \leq \lambda\}$ in the Wijsman and Hausorff senses as $N \to \infty$.

Proposition 5.4.7. *Suppose that $\alpha \leq \mathbf{1}^\top \bar{\boldsymbol{p}}$ and Assumption 5.0.5 holds for the norm-minimizing scalarizations. Then, the SAA set-valued risk measure $\hat{R}_N(\boldsymbol{X}^{[N]})$ converges to the true set-valued risk measure $R(\boldsymbol{X})$ in the Wijsman and Hausdorff senses a.s.*

Proof. For each $N \in \mathbb{N}$, we have

$$
\begin{aligned}
&\mathbb{D}(\hat{R}_N^{\mathrm{restricted}}(\boldsymbol{X}^{[N]}) + \mathbb{R}^i_+, R^{\mathrm{restricted}}(\boldsymbol{X}) + \mathbb{R}^i_+) \qquad (5.4.1)\\
&= \sup_{\boldsymbol{z} \in \hat{R}_N^{\mathrm{restricted}}(\boldsymbol{X}^{[N]}), \boldsymbol{y} \in \mathbb{R}^i_+} d(\boldsymbol{z} + \boldsymbol{y}, R(\boldsymbol{X}) + \mathbb{R}^i_+)\\
&= \sup_{\boldsymbol{z} \in \hat{R}(\boldsymbol{X}_N), \boldsymbol{y} \in \mathbb{R}^i_+} \inf_{\bar{\boldsymbol{z}} \in R^{\mathrm{restricted}}(\boldsymbol{X}), \bar{\boldsymbol{y}} \in \mathbb{R}^i_+} \|\boldsymbol{z} + \boldsymbol{y} - \bar{\boldsymbol{z}} - \bar{\boldsymbol{y}}\|_2\\
&\leq \sup_{\boldsymbol{z} \in \hat{R}_N^{\mathrm{restricted}}(\boldsymbol{X}^{[N]})} \inf_{\bar{\boldsymbol{z}} \in R^{\mathrm{restricted}}(\boldsymbol{X})} \|\boldsymbol{z} - \bar{\boldsymbol{z}}\|_2\\
&= \sup_{\boldsymbol{z} \in \hat{R}_N^{\mathrm{restricted}}(\boldsymbol{X}^{[N]})} d(\boldsymbol{z}, R^{\mathrm{restricted}}(\boldsymbol{X}))\\
&= \mathbb{D}(\hat{R}_N^{\mathrm{restricted}}(\boldsymbol{X}^{[N]}), R^{\mathrm{restricted}}(\boldsymbol{X}))\\
&\leq \mathbb{H}(\hat{R}_N^{\mathrm{restricted}}(\boldsymbol{X}^{[N]}), R^{\mathrm{restricted}}(\boldsymbol{X})).
\end{aligned}
$$

In the same way, we can also establish,

$$\mathbb{D}(R^{\mathrm{restricted}}(\boldsymbol{X}) + \mathbb{R}^i_+, \hat{R}_N^{\mathrm{restricted}}(\boldsymbol{X}^{[N]}) + \mathbb{R}^i_+) \leq \mathbb{H}(\hat{R}^{\mathrm{restricted}}(\boldsymbol{X}_N), R^{\mathrm{restricted}}(\boldsymbol{X})).$$

Thus, by Corollary 5.4.6,

$$\mathbb{H}(\hat{R}_N^{\mathrm{restricted}}(\boldsymbol{X}^{[N]}) + \mathbb{R}^i_+, R^{\mathrm{restricted}}(\boldsymbol{X}) + \mathbb{R}^i_+) \leq \mathbb{H}(\hat{R}_N^{\mathrm{restricted}}(\boldsymbol{X}^{[N]}), R^{\mathrm{restricted}}(\boldsymbol{X})) \to 0$$

as $N \to \infty$. Hence, $\hat{R}_N(\boldsymbol{X}^{[N]}) \xrightarrow{H} R(\boldsymbol{X})$ as $N \to \infty$ a.s. Since Hausdorff convergence implies Wijsman convergence, we also have $\hat{R}_N(\boldsymbol{X}^{[N]}) \xrightarrow{W} R(\boldsymbol{X})$ as $N \to \infty$ a.s. $\square$

Chapter 6

Computational Results

In this chapter, we present computational results regarding the sample average approximations of set-valued systemic risk measures based on value-at-risk. The objective of this chapter is twofold: First we assess the efficacy of the grid algorithm in estimating this risk measure through the utilization of the three algorithms discussed in Section 4.4 using three scalarization functions, namely weighted sum scalarization, Pascoleti Serafini scalarization, and norm-minimizing scalarization functions. Second, we do sensetivity analysis with respect to the network parameters, banks correlation factor and the number of scenarios.

In order to ascertain the reliability of our findings, we conduct a comparative analysis between the three algorithms mentioned in Section 4.4. The first algorithm, namely Algorithm 1, serves as a benchmark for assessing the acceptability of each grid point, taking into account the upper set property outlined in Lemma 4.0.8, which is an inherent characteristic of the set-valued risk measure of interest.

The computational implementation of our approach is conducted using the Matlab programming language, with the utilization of the CVX bundle and the incorporation of the Gurobi interface. The calculations are performed on a system that possesses the following specifications:

- Processor: Intel(R) Core(TM) i7-6500U CPU @2.50GHz 2.59GHz.
- Installed RAM: 8.00 GB.

The primary objective of our analysis is to calculate the systemic set-valued risk measure within a core-periphery framework.

In order to provide a framework for analysis, we will investigate a financial system comprising a set $\mathcal{N} = \{1, \ldots, n\}$ of n institutions, typically banks. These institutions can be divided into two separate groups: the core group, represented by $\mathcal{C}$, and the peripheral group, represented by $\mathcal{P}$. The total number of core banks is represented by the symbol $n_{\mathcal{C}}$, while the total number of peripheral banks is represented by $n_{\mathcal{P}}$. Furthermore, to account for a diverse range of potential scenarios, we integrate a finite set Ω of S scenarios that encompass the nature of the financial system.

6.1 Data Generation

In this section, we outline the procedure for generating data to construct an Eisenberg-Noe network $(\mathcal{N}, \boldsymbol{\pi}, \bar{\boldsymbol{p}}, \boldsymbol{X})$ within a core-periphery framework. The network comprises a total of 20 banks such that $\mathcal{N} = \mathcal{C} \cup \mathcal{P}$.

In order to establish the network, we utilize the directed preferential attachment model as suggested by Bollobás et al. in [31]. The presented model depicts a directed scale-free graph that demonstrates growth through the mechanism of preferential attachment, wherein the degree vertex progressively increases as time elapses [39, Chapter 8]. As a result, it is observed that the vertices with the longest existence tend to have the highest degrees, a phenomenon commonly known as the "rich-get-richer" effect [40, 41, 31, 42, 43]. In order to ensure comprehensiveness, we will present a concise explanation of the Bollobás model that has been incorporated into our framework.

Let θ, η, ζ, δ_{in}, and δ_{out} denote non-negative real numbers, subject to the constraint $\theta + \eta + \zeta = 1$. We begin with an initial directed graph $\mathcal{G}(0)$, which consists of two nodes and two edges directed reciprocally between the two nodes. At time t, the graph $\mathcal{G}(t)$ is characterized by $t + 2$ edges and a random variable $n(t)$ representing the number of nodes. Denote by $G(t) \subseteq \mathcal{N}$ as the set of nodes in graph $\mathcal{G}(t)$. For all values of t, the graph $\mathcal{G}(t+1)$ is derived from the graph $\mathcal{G}(t)$ by adhering to the subsequent set of rules:

1. With probability θ, a new vertex v is added along with an edge from v to an existing

vertex w, where w is chosen with respect to the distribution,

$$\mathbb{P}(w = w_i) = \frac{d_{in}(w_i) + \delta_{in}}{t + \delta_{in} n(t)},\ w_i \in \mathcal{G}(t).$$

2. With probability η, an edge is added from an existing vertex v to an existing vertex w. The selection of v and w is independent and follows the distribution,

$$\mathbb{P}(v = v_i) = \frac{d_{out}(v_i) + \delta_{out}}{t + \delta_{out} n(t)},\ v_i \in \mathcal{G}(t).$$

$$\mathbb{P}(w = w_i) = \frac{d_{in}(w_i) + \delta_{in}}{t + \delta_{in} n(t)},\ w_i \in \mathcal{G}(t).$$

3. With probability ζ, a new vertex w is added along with an edge from an existing vertex v to w, where v is chosen with respect to the distribution,

$$\mathbb{P}(v = v_i) = \frac{d_{out}(v_i) + \delta_{out}}{t + \delta_{out} n(t)},\ v_i \in \mathcal{G}(t).$$

It is worth noting that the model allows for loops and multiple edges, although their presence does not significantly affect the conclusions drawn. The paper showed that the in-degree and out-degree distribution follow a power law distribution [31, Theorem 3.1].

By constructing the network using the preferential attachment model, we can carry on the estimation of the set-valued systemic risk measure using the grid algorithm as outlined in Chapter 4.

The matrix $\boldsymbol{\pi}$ and vector $\bar{\boldsymbol{p}}$ were generated based on the aforementioned model. This involved generating the adjacency matrix $\boldsymbol{A} \in \{0,1\}^{n \times n}$ of the network using the preferential attachment algorithm as discussed in [31]. In this algorithm, a value of 1 in A_{ij} indicates that node i is connected to node j, while a value of 0 indicates no connection between the two nodes. The core banks set $\mathcal{C}$ is determined from matrix $\boldsymbol{A}$, comprising the four banks with the highest degree nodes. Thus, the cardinality of $\mathcal{C}$, denoted as $n_{\mathcal{C}}$, is equal to 4. The set $\mathcal{P}$ consists of the remaining 16 banks, thus indicating that $n_{\mathcal{P}} = 16$.

Next, we define the intergroup liability matrix $\boldsymbol{M} \in \mathbb{R}^{2\times 2}_{++}$ as follows:

$$\boldsymbol{M} = \begin{pmatrix} CC & CP \\ PC & PP \end{pmatrix}.$$

Here, the block labeled as CC, which stands for "core to core," represents the mean liability observed among the core banks. Conversely, the block labeled as PP, which stands for "periphery to periphery," denotes the average liability observed among the periphery banks. The terms CP ("core to periphery") and PC ("periphery to core") denote the mean exposure between banks in the core and periphery, and periphery and core, respectively.

The interbank nominal liability matrix $\boldsymbol{l} \in \mathbb{R}^{n\times n}$ is constructed based on the generated adjacency matrix $\boldsymbol{A}$ and the intergroup liability matrix $\boldsymbol{M}$. In the event that banks i and j are classified as core banks and the adjacency matrix element A_{ij} is equal to 1, it follows that the link strength l_{ij} is equivalent to the core-core link strength denoted as CC. In contrast, when i and j represent core banks but the value of A_{ij} is zero, it follows that l_{ij} is also zero. In a similar manner, the entries of the matrix $\boldsymbol{l}$ are populated based on the classification of banks i and j, as well as the presence of a connection between them in the adjacency matrix $\boldsymbol{A}$.

After the computation of the matrix $\boldsymbol{l}$, the total liability vector $\bar{\boldsymbol{p}} \in \mathbb{R}^n_{++}$ is obtained by summing the rows of matrix $\boldsymbol{l}$. The relative liability matrix $\boldsymbol{\pi}$ is derived by normalizing the matrix $\boldsymbol{l}$ in such a way that the sum of each row equals one.

Subsequently, the operating cash flow vector $\boldsymbol{X}$ belongs to the set $L(\mathbb{R}^n_+)$ and represents a multivariate random vector. Additionally, Ω is a finite set consisting of S scenarios, where S is a natural number. It is assumed that all scenarios within the sample space Ω have equal probabilities, and there exists a shared correlation coefficient, denoted as ρ, among the banks. This coefficient represents the degree of interdependence and interconnectedness within the financial system. The generation of random operating cash flow $\boldsymbol{X}$ occurs through the assignment of a Pareto-distributed shock to each bank.

In order to generate $\boldsymbol{X}$, a shared shape parameter denoted as ν is employed for all banks. Nonetheless, it is important to note that the scale parameter, represented by the symbol β, is shared only within each group. However, it does vary between the banks in the core group, denoted as $\beta_{\mathcal{C}}$, and the banks in the periphery group, denoted as $\beta_{\mathcal{P}}$. In other words, $\boldsymbol{X} = [\boldsymbol{X}_{\mathcal{C}}\ \boldsymbol{X}_{\mathcal{P}}]$. By Chapter 5 of [44], for $\nu \geq 3$, the expected value and the variance of the operating cash income of a core and a periphery bank are defined as follows:

$$\mathbb{E}[X_{\mathcal{C}}] = \frac{\nu \cdot \beta_{\mathcal{C}}}{\nu - 1}, \quad \mathbb{E}[X_{\mathcal{P}}] = \frac{\nu \cdot \beta_{\mathcal{P}}}{\nu - 1}.$$

$$\text{Var}[X_{\mathcal{C}}] = \frac{\nu \cdot \beta_{\mathcal{C}}^2}{(\nu-1)^2 \cdot (\nu-2)}, \quad \text{Var}[X_{\mathcal{P}}] = \frac{\nu \cdot \beta_{\mathcal{P}}^2}{(\nu-1)^2 \cdot (\nu-2)}.$$

This distinction in the scale parameter takes into consideration the varying sizes of cash flows observed between the core and peripheral banks.

As a result, the random vector $\boldsymbol{X}$ is formed by integrating S occurrences of Pareto shock random vectors, denoted as $\boldsymbol{x}_s = (x_{1s}, \ldots, x_{ns})$, where each $\boldsymbol{x}_s$ signifies the influence of a particular scenario $\omega^s \in \Omega,\ s \in \mathcal{S}$ on the operating cash flow. The Pareto shocks are derived by randomly selecting values from a Pareto distribution characterized by parameters ν and β, while considering the distinct grouping and correlation structure of the banks.

6.2 Grid Algorithm Performance Analysis with Different Approaches

In this section, we assess the efficacy of the grid algorithm by employing two scalarization functions, specifically Pascoletti Serafini as in Algorithm 2 and norm-minimizing functions as in Algorithm 3, on the grid region derived from solving the weighted sum scalarization problem outlined in Chapter 4. We compare these two algorithms with Algorithm 1, where the acceptability check of the grid points is done by solving the optimization formulation outlined in Chapter 3. The grid region denotes the specific location of the efficient frontier within the set-valued risk measure. In order to construct the network for this analysis, we utilize the Bollobás algorithm as described in Section 6.1. The algorithm is implemented with the parameter values specified as follows: $\theta = 0.2$, $\eta = 0.6$, $\zeta = 0.2$, $\delta_{in} = 0.5$, and $\delta_{out} = 0.5$.

To provide a brief recap, we examine a network proposed by Eisenberg and Noe consisting of two groups. This network comprises a total of 20 banks, with 4 core banks denoted as $n_{\mathcal{C}}$ possessing the highest degree nodes, and 16 periphery banks denoted as $n_{\mathcal{P}}$ having nodes with relatively lower degrees. In order to generate operating cash flow, we assign the values of $S = 50$, $\rho = 0.3$, and $\beta = [100, 50]$. Here, the scale parameter of 100 corresponds to core banks, while the scale parameter of 50 corresponds to periphery banks. The value of the shape parameter is specified as $\nu = 3$.

Furthermore, we utilize the interbank matrix $\boldsymbol{M}$ with the following values:

$$\boldsymbol{M} = \begin{pmatrix} 400 & 200 \\ 300 & 150 \end{pmatrix}.$$

Lastly, the parameters for the set-valued risk measure are defined as $\alpha = (0.8) \times \mathbf{1}^\top \bar{\boldsymbol{p}}$ and $\lambda = 0.2$.

The grid algorithm is implemented using six distinct values of the approximation error ϵ in order to showcase different degrees of approximation. The performance of the algorithm, as measured by Algorithms 1, 2 and 3, is presented in Table 6.1 for various values of ϵ ranging from 200 to 1. The number of grid points in the grid region for each respective ϵ is presented in Table 6.2.

Table 6.1: Time Performance of Grid Algorithm in Seconds: A Comparative Analysis of Different Algorithms for Varying Approximation Error Levels (ϵ).

ϵ	**Algorithms**		
	1	**2**	**3**
200	7.77	11.34	13.86
100	13.1	20.46	25.25
50	24.72	38.7	50.04
25	45.68	74.7	99.96
10	114.19	187.77	505.83
1	13846.72	29259.59	163242.83

Table 6.2: Number of Grid Points for Varying Approximation Error Levels (ϵ).

ϵ	**Number of Grid Points**
200	40
100	152
50	570
25	2175
10	13464
1	1328148

The visualization of the corresponding approximation sets can be observed in Figure 6.1. Based on the information depicted in Figure 6.1, it is apparent that a decrease in the value of ϵ corresponds to an improvement in the algorithm's ability to provide a precise estimation of the set-valued systemic risk measure. Moreover, the findings from Table 6.1 indicate that the algorithm demonstrates the best performance when employing Algorithm 1. This algorithm

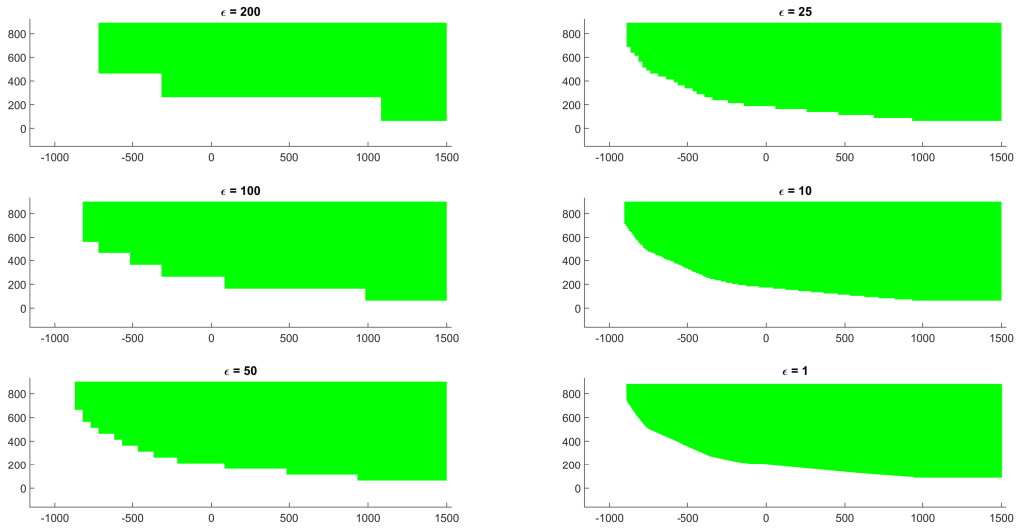

Figure 6.1: Set-Valued Risk Measure Approximation Using Different ϵ.

evaluates the acceptability of each grid point based on the optimization formulation outlined in Chapter 3. The anticipated outcome of this result can be attributed to the fact that the scalarization problems in Algorithms 2 and 3, namely Pascoletti Serafini and norm-minimizing, necessitate the inclusion of a binary variable for each scenario.

Note that in Figure 6.1 the x-axis and y-axis of each subplot represent the capital injection to core and peripheral banks, respectively.

6.3 Sensitivity of the Risk Measure

The main objective of this section is to investigate the sensitivity of the set-valued systemic risk measure to the Bollobás network when the parameters are kept constant. Although the network is operated with identical parameter values, it produces a range of network configurations due to its inherent stochastic nature. Consequently, this leads to disparities in network architectures across multiple iterations. It is important to highlight that the network, operating cash flow, and set-valued risk measure parameters remain consistent with those used in Section 6.2. By ensuring consistency in these factors, we can successfully isolate and assess the influence of network structure on the set-valued systemic risk measure. This allows us to obtain more profound insights into the measure's sensitivity to changes in

the network.

In order to account for the observed variability, a comprehensive analysis is conducted by quantifying the set-valued systemic risk through 10 independently simulated networks. Every iteration generates a unique network, enabling us to encompass the various network configurations that can arise using the identical Bollobás parameters.

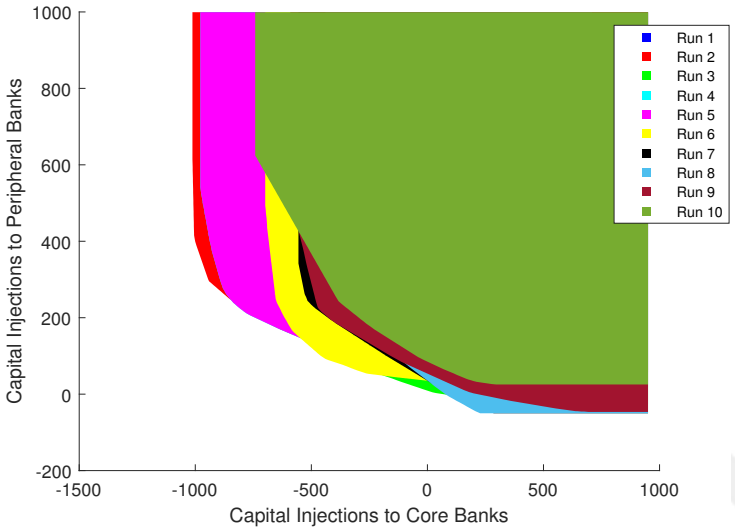

Figure 6.2: Overlapping Regions of 10 Runs with Identical Bollobás Parameters.

The sensitivity of our set-valued risk measure to the network shape resulting from identical Bollobás parameters is clearly illustrated in Figure 6.2 when the approximation error is set to $\epsilon = 1$. The observed sensitivity suggests that even minor alterations in the network's structure can have a substantial impact on the computed measure of systemic risk.

Following this, a comprehensive examination is conducted to evaluate the systemic risk with set-valued characteristics across 100 independently simulated networks with the similar Bollobás parameters. The methodology employed consisted of computing the mean value of 10 unique sets located within the designated grid area. The vertex set of each distinct run was identified, and the average of these vertices was calculated, subsequently including the positive orthant. In the end, this procedure resulted in the generation of 10 distinct sets, each of which represents the mean value derived from 10 separate and independent runs.

The results obtained, as shown in Figure 6.3, demonstrate the convergence of set-valued sensitive risk measures when the average of 10 independent runs is used. The 10 sets, which are derived from the average of 10 iterations, demonstrate a notable degree of overlap,

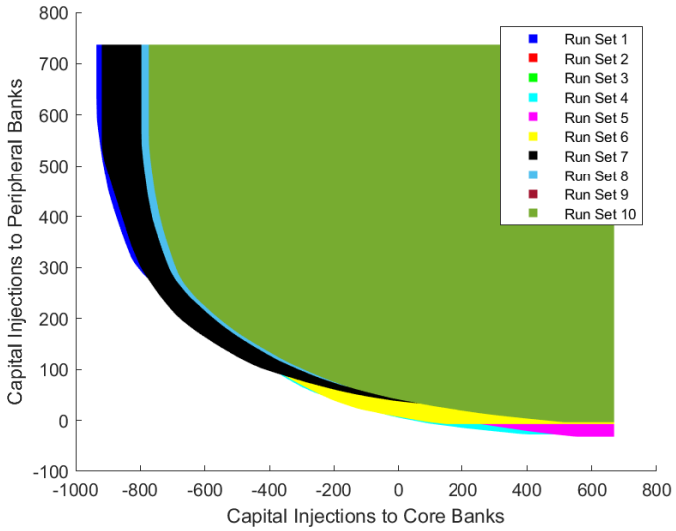

Figure 6.3: Overlapping Regions of 10 Runs with Identical Bollobás Parameters.

indicating a substantial level of consistency.

In the remaining part of this chapter, we perform sensitivity analysis on this network by exploring different numbers of scenarios, correlation coefficients, and Bollobás network parameters.

6.4 Impact of the Number of Scenarios

In this section, we examine the impact of varying the number of scenarios, denoted as S, on both computational performance and systemic risk measures. All parameters mentioned in Section 6.2 are held constant, with the exception of the scenarios count S, enabling us to conduct a sensitivity analysis using this particular parameter. This analysis offers valuable insights into the convergence behavior observed with an increasing number of scenarios.

We examine a set of values for the variable S, which are defined as follows: S takes on the values of 5, 10, 20, 50, 100, 120, 140, 160, 180, and 200. Although the network structure remains consistent, it is anticipated that the systemic risk measures will display slight fluctuations. Nevertheless, it is expected that the computation time will increase as the number of scenarios increases, primarily because each scenario involves n continuous variables.

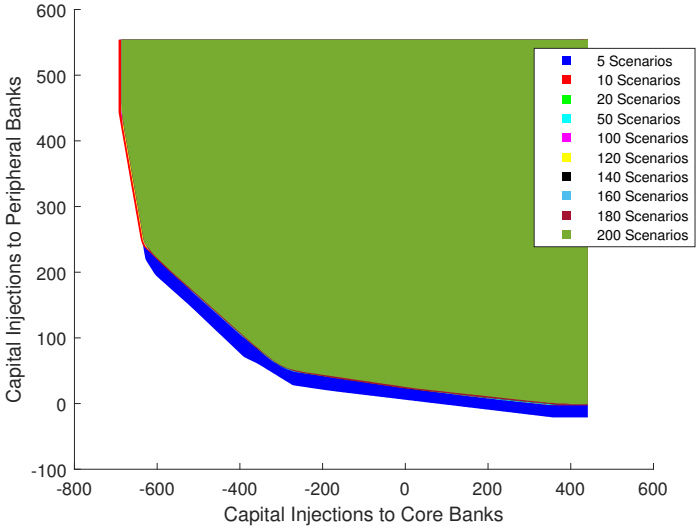

Figure 6.4: Overlapping Regions for Different Scenario Counts.

Table 6.3: Time Performance in Seconds for Algorithm 1 with Different Scenario Counts.

Scenario Count	**Number of Grid Points** ($\times 10^5$)	**Time Performance**
5	6.21	2908.67
10	5.13	2020.09
20	5.68	2515.88
50	5.08	2244.23
100	5.12	2677.92
120	5.63	3403.30
140	5.84	3553.30
160	6.30	4314.21
180	5.13	3361.87
200	5.40	3821.29

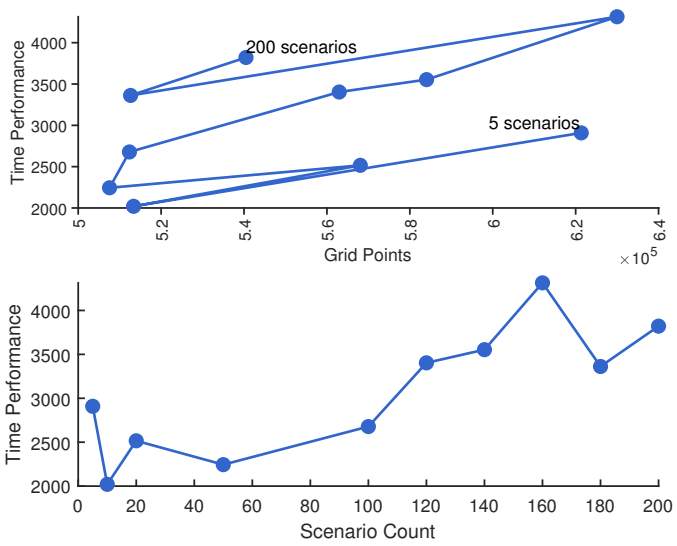

Figure 6.5: Time Performance in Seconds for Algorithm 1 with Different Scenario Counts.

The resulting approximations of the set-valued systemic risk measures for the specific case of approximation error $\epsilon = 1$ are depicted in Figure 6.4. This figure illustrates the relative stability of these approximations across different values of S. The results of this study are consistent with our initial hypotheses and provide evidence supporting the expected association between the set-valued risk measure and the number of scenarios. In contrast, Table 6.3 displays the computational performance and the number of grid points for the algorithm, while maintaining consistent scenario counts and approximation error. The grid algorithm using Algorithm 1 is implemented. This algorithm has been recognized as the most efficient function in Section 6.2. Table 6.3 and Figure 6.5 illustrate that the overall algorithm performance time exhibits inconsistent variations as the number of scenarios increases. This can be ascribed to the irregular fluctuation in the quantity of grid points as the number of scenarios increases (see Table 6.3).

6.5 Impact of the Correlation Coefficient

This section focuses on analyzing the influence of the correlation coefficient ρ on the measures of systemic risk. All parameters mentioned in Section 6.2 are held constant, with the exception of ρ, in order to perform a sensitivity analysis that specifically examines the impact of this parameter.

We examine a set of values for the parameter ρ, specifically $\rho \in \{0.05, 0.1, 0.3, 0.5, 0.8\}$. While the fundamental network structure remains unaltered, it is expected that there will be slight fluctuations in the risk measures.

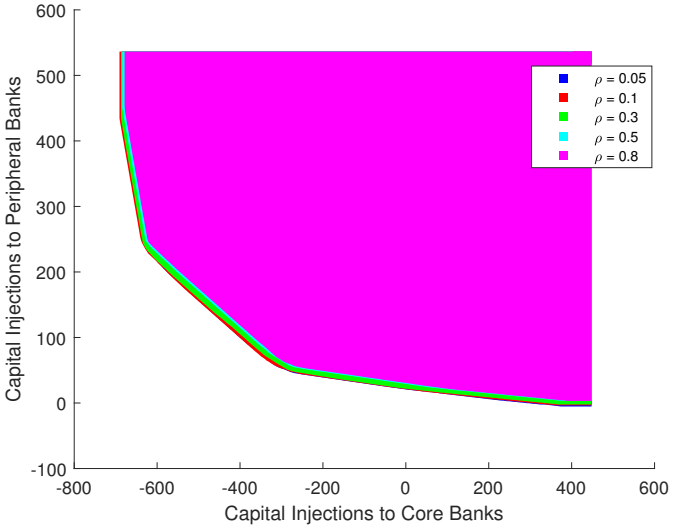

Figure 6.6: Overlapping Regions for Different Correlation coefficients ρ.

The visual representation in Figure 6.6 depicts the approximations of the systemic risk measures with an approximation error of $\epsilon = 1$. It demonstrates the relative stability of these measures across various values of ρ. The results of this study are consistent with our initial hypotheses, suggesting that the correlation coefficient has a minimal effect on the measures of systemic risk.

6.6 Network Parameters

In this section, our objective is to conduct a sensitivity analysis by examining variations in the probabilities of the Bollobás network parameter. These variations have a substantial influence on the network's topology as they determine the presence of liabilities between banks. In order to perform a sensitivity analysis, our attention is directed towards the parameters θ, η, and ζ, while maintaining the remaining parameters discussed in Section 6.2 at constant values.

It should be noted that the visual representations of the resulting approximations of the

systemic risk measures can be observed in Figures 6.7 and 6.8 when the approximation error ϵ is set to 1. The x-axis and y-axis of each subplot correspond to the capital injection directed towards core banks and peripheral banks, respectively. In addition, the subplot adjacent to each set-valued risk measure depicts the corresponding network graph.

We examine the following network statistics for each combination of Bollobás network parameter probabilities:

- Average Degree (AD): The mean value of the number of connections per node within the network, given by the following formula:

$$\text{AD} = \frac{\sum_{i=1}^{n} \sum_{j=1}^{n} A_{ij}}{n},$$

  where n is the total number of nodes in the graph, and $\boldsymbol{A}$ represents the adjacency matrix of the network.

- Network Density (ND): The ratio between the total number of connections and the total number of possible connections within the network, given by the following formula:

$$\text{ND} = \frac{\sum_{i=1}^{n} \sum_{j=1}^{n} A_{ij}}{n(n-1)}.$$

- Total Clustering Coefficient (TCC): The Total Clustering Coefficient is a metric that quantifies the degree to which nodes within a network exhibit a tendency to form clusters [45] [46]. The clustering coefficient (CC) of node i is defined as:

$$\text{CC}_i = \frac{\sum_{j=1}^{n} \sum_{k=1}^{n} A_{ij} A_{ik} A_{kj}}{\sum_{j=1}^{n} \binom{k_j}{2}}.$$

  Here, k_j represents the degree of node j. Therefore, the Total Clustering Coefficient can be computed by summing up the clustering coefficients of all nodes in the network:

$$\text{TCC} = \sum_{i=1}^{n} \text{CC}_i.$$

- Core-Periphery Error (CPE): The Core-Periphery Error (CPE) is a quantitative measure utilized to assess the disparity between the observed and anticipated core-periphery configuration within a network. This concept is explored in the work of Craig et al. in [47], wherein core banks are anticipated to exhibit interconnections

amongst themselves. Consequently, the absence of a link within the core-core block signifies a deviation from the core-periphery model. In a similar vein, it is deemed erroneous for peripheral banks to establish direct connections with one another, as such transactions are not considered appropriate. The presence of errors in the core-periphery (and periphery-core) blocks results in the imposition of penalties on zero rows (columns, respectively), which signifies that a core bank is unable to provide loans to (or borrow from) any periphery bank. The cumulative error score combines the errors observed in all four blocks. The Core-Periphery Index (CPE) is a metric that falls within the range of zero to one, where values closer to zero signify a more pronounced core-periphery structure.

- Core-Periphery Index (CPI): The Core-Periphery Index (CPI) is a robust measure used to evaluate the level of strength exhibited by the core-periphery structure within a network. This offers significant observations regarding the density and cohesiveness of the core, alongside the sparsity and absence of connections in the periphery [48]. CPI values range from zero to one, with higher values indicating a more pronounced and well-defined core-periphery structure. The CPI formula is as follows:
$$\text{CPI} = \frac{\sum_{i=1}^{n}\sum_{j=1}^{n} A_{ij} - \sum_{i\in\mathcal{P}}\sum_{j\in\mathcal{P}} A_{ij}}{\sum_{i=1}^{n}\sum_{j=1}^{n} A_{ij}},$$
where $\mathcal{C}$ and $\mathcal{P}$ represent the core and periphery sets of banks, respectively.

The network statistics presented offer significant insights into the structural characteristics of Bollobás networks across various parameter combinations. The Core-Periphery Error (CPE) and Core-Periphery Index (CPI) are valuable tools for evaluating the degree of core-periphery structure within a network. A lower CPE value and a higher CPI value signify a more prominent core-periphery arrangement.

First, we aim to examine the impact of variations in the parameter η on the sensitivity of the systemic risk measure. Specifically, we keep the parameter θ constant at a value of 0.1, and manipulate the parameter ζ to be equal to 1 minus the sum of 0.1 and η. The computational statistics for various values of the η parameter, specifically $\eta \in \{0.1, 0.3, 0.4, 0.5, 0.6, 0.8\}$, are presented in Table 6.4. The corresponding approximations are displayed in Figure 6.7.

Based on the data presented in Table 6.4, it can be observed that there is a positive correlation between the variable η and the average degree of each node, network density,

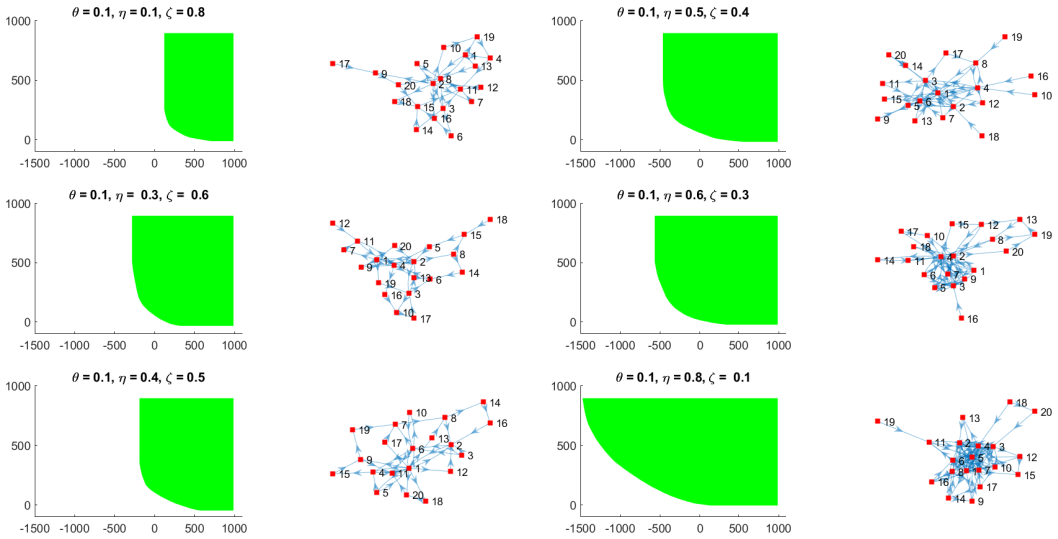

Figure 6.7: Set-Valued Risk Measure along with its Corresponding Network Graph by Changing the Parameter η.

Table 6.4: Network Statistics for Different Bollobás Parameter Probabilities by Changing the Parameter η.

θ, η, ζ	**Network Statistics**				
	AD	**ND**	**TCC**	**CPE**	**CPI**
0.1, 0.1, 0.8	1.7	0.0895	0.3333	0.67	0.6471
0.1, 0.3, 0.6	1.95	0.1026	1.6333	0.4103	0.7179
0.1, 0.4, 0.5	2	0.1053	4.4111	0.375	0.7251
0.1, 0.5, 0.4	2.45	0.1289	7.1659	0.1837	0.8367
0.1, 0.6, 0.3	2.8	0.1474	11.293	0.1786	0.8393
0.1, 0.8, 0.1	3.55	0.1868	14.5913	0.1672	0.8528

and total clustering coefficient. As the value of η increases, these network characteristics consistently increase. Furthermore, the observed rise in the η value signifies a heightened presence of a core-periphery structure within the network. This finding is substantiated by the core-periphery index and core-periphery error measures discussed in [47].

The impact of different values of η on the systemic set-valued risk measure is further illustrated in Figure 6.7. As the parameter η increases, there is a noticeable downward trend in the measure, indicating that higher values of η are associated with a reduction in systemic risk. The correlation between the statistical variations presented in Table 6.4 highlights the significant impact of η on both network dynamics and systemic risk.

In the subsequent analysis, we investigate the impact on the systemic risk measure when the parameters θ and ζ are reversed, while maintaining the η parameter fixed. The following parameter pairs are taken into consideration:

- $(\theta = 0.1, \eta = 0.1, \zeta = 0.8)$ and $(\theta = 0.8, \eta = 0.1, \zeta = 0.1)$.
- $(\theta = 0.1, \eta = 0.3, \zeta = 0.6)$ and $(\theta = 0.6, \eta = 0.3, \zeta = 0.1)$.
- $(\theta = 0.1, \eta = 0.6, \zeta = 0.3)$ and $(\theta = 0.3, \eta = 0.6, \zeta = 0.1)$.

Table 6.5 presents the computational statistics for these different network parameter combinations, and Figure 6.8 provides the corresponding approximations.

Table 6.5: Network Statistics for Different Bollobás Parameter Probabilities by Reversing the Values of the Parameters θ and ζ.

θ, η, ζ	**Network Statistics**				
	AD	**ND**	**TCC**	**CPE**	**CPI**
0.1, 0.1, 0.8	1.7	0.0895	0.3333	0.6765	0.6471
0.8, 0.1, 0.1	1.3	0.0684	2	0.5385	0.8462
0.1, 0.3, 0.6	1.95	0.1026	1.633	0.4103	0.7179
0.6, 0.3, 0.1	1.65	0.0868	6.3	0.4042	0.8485
0.1, 0.6, 0.3	2.8	0.1474	11.293	0.1786	0.8493
0.3, 0.6, 0.1	3.2	0.1684	15.419	0.1744	0.8656

Upon examination of Table 6.5, it is observed that the reversing of parameters θ and ζ does not yield a consistent increase or decrease in both the average degree of each node

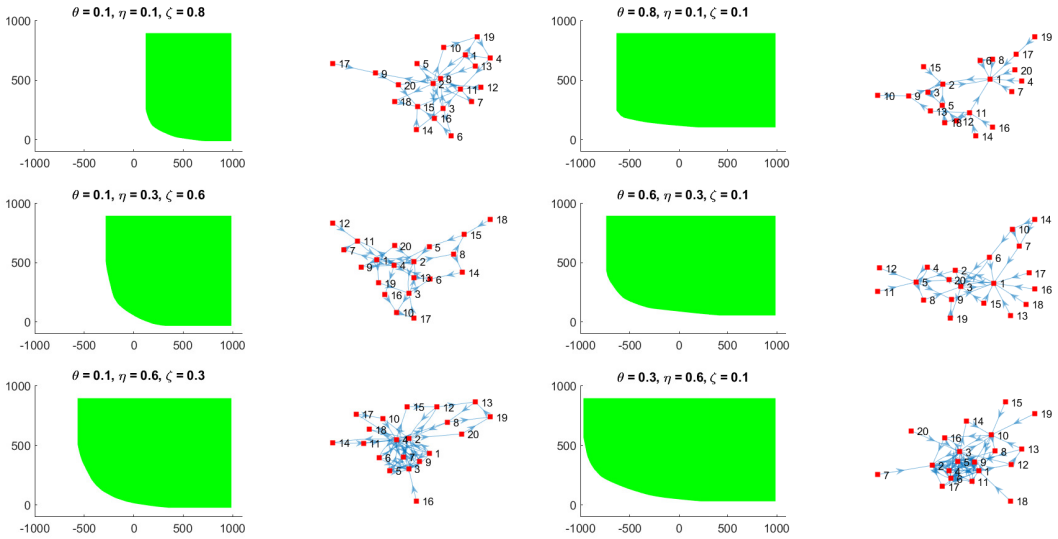

Figure 6.8: Set-Valued Risk Measure Along with its Corresponding Network Graph by Reversing the Values of the Parameters θ and ζ.

and the network density. Nevertheless, the overall clustering coefficient, as well as the core-periphery index and core-periphery error measures, suggest a more evident core-periphery structure in the network when the value of θ exceeds ζ.

The results presented in Figure 6.8 support the conclusions drawn from Table 6.5, indicating that the systemic set-valued risk measure exhibits a decrease in risk as θ is greater than ζ. The observed behavior can be ascribed to the emergence of a core-periphery configuration within the network, which has implications for the interconnectivity and dissemination of risks.

Through the implementation of this sensitivity analysis, we are able to acquire significant insights regarding the impact of various network parameters on the measure of systemic risk. It is worth noting that the presence of a core-periphery structure within the network has a significant impact on decreasing the systemic set-valued risk measure. This suggests that there may be opportunities to develop risk mitigation strategies based on this observation.

Chapter 7

Conclusion

In this thesis, we study a set-valued systemic risk based on Eisenberg-Noe network, which defines the aggregation function and value-at-risk, which served as the underlying risk measure. We have demonstrated that this risk measure can be approximated using the grid algorithm outlined in [5] by three different approaches, all of which employ the weighted sum scalarization in order to find the grid region. After specifying the grid region, we constructed a grid, where the distance between grid points is less that or equal to a prespecified approximation error $\epsilon > 0$. Each grid point was checked in three different approaches; the first approach implemented in Algorithm 1, where no scalarization is used and the rest of the approaches, namely Algorithms 2 and 3, where Pascoletti Serafini and norm-minimizing scalarizations are employed respectively.

In addition to showing the convergence of the optimal solution of the SAA scalarization problems to its true counterpart, we have proved that, under specific conditions, the SAA set-valued risk measure also converges to its true risk measure in the Wijsman and Hausorff senses.

We performed a thorough analysis of algorithm performance and the sensitivity of systemic risk measures in interbank networks. In approximating systemic set-valued risk measures, our evaluation of the grid algorithm with multiple scalarization functions has demonstrated its efficacy. By analyzing various approximation errors, we have determined that approximation error reduction results in a more accurate estimation of systemic risk. Notably, Algorithm 1 without any scalarizations has demonstrated superior performance, primarily

due to its optimization formulation.

Moreover, our sensitivity analysis has provided valuable insight into the effect of important parameters on measures of systemic risk. The effects of the number of scenarios, correlation coefficients, and Bollobás network parameters on the computational performance and stability of risk measures have been extensively investigated. Changes in Bollobás network parameters, particularly η and the reversal of θ and ζ, resulted in significant shifts in systemic risk, whereas the number of scenarios and correlation coefficients demonstrated only minor variations in risk measures. Notably, the network's core-periphery structure led to a reduction in systemic risk.

This study contributes to the comprehension of systemic risk assessment and the sensitivity of risk measures to important parameters in interbank networks. This study's findings have important implications for policymakers and practitioners in the financial industry's development of effective risk mitigation strategies. By advancing our understanding of systemic risk in interbank networks and providing convergence guarantees for the SAA set-valued risk measure, this study hopes to contribute to the development of more robust risk management strategies and policies in the banking industry.

Bibliography

[1] D. M. Kotz, "The financial and economic crisis of 2008: A systemic crisis of neoliberal capitalism," *Review of radical political economics*, vol. 41, no. 3, pp. 305–317, 2009.

[2] T. C. Silva, M. A. da Silva, and B. M. Tabak, "Systemic risk in financial systems: a feedback approach," *Journal of Economic Behavior & Organization*, vol. 144, pp. 97–120, 2017.

[3] C. Chen, G. Iyengar, and C. Moallemi, "An axiomatic approach to systemic risk," *Management Science*, vol. 59, 10 2011.

[4] E. Kromer, L. Overbeck, and K. Zilch, "Systemic risk measures on general measurable spaces," *Mathematical Methods of Operations Research*, vol. 84, pp. 323–357, 2016.

[5] Z. Feinstein, B. Rudloff, and S. Weber, "Measures of systemic risk," *SIAM Journal on Financial Mathematics*, vol. 8, no. 1, pp. 672–708, 2017.

[6] F. Biagini, J.-P. Fouque, M. Frittelli, and T. Meyer-Brandis, "A unified approach to systemic risk measures via acceptance sets," *Mathematical Finance*, vol. 29, no. 1, pp. 329–367, 2019.

[7] Y. Armenti, S. Crépey, S. Drapeau, and A. Papapantoleon, "Multivariate shortfall risk allocation and systemic risk," *SIAM Journal on Financial Mathematics*, vol. 9, no. 1, pp. 90–126, 2018.

[8] V. Acharya, R. Engle, and M. Richardson, "Capital shortfall: A new approach to ranking and regulating systemic risks," *American Economic Review*, vol. 102, no. 3, pp. 59–64, 2012.

[9] N. A. Tarashev, C. E. Borio, and K. Tsatsaronis, "Attributing systemic risk to individual institutions," tech. rep., BIS Working paper, 2010.

[10] A. Tobias and M. K. Brunnermeier, "Covar," *The American Economic Review*, vol. 106, no. 7, p. 1705, 2016.

[11] P. Artzner, F. Delbaen, J.-M. Eber, and D. Heath, "Coherent measures of risk," *Mathematical finance*, vol. 9, no. 3, pp. 203–228, 1999.

[12] H. Amini, D. Filipović, and A. Minca, "Systemic risk and central clearing counterparty design," *Swiss Finance Institute Research Paper*, no. 13-34, 2015.

[13] M. K. Brunnermeier and P. Cheridito, "Measuring and allocating systemic risk," *Risks*, vol. 7, no. 2, p. 46, 2019.

[14] L. Eisenberg and T. H. Noe, "Systemic risk in financial systems," *Management Science*, vol. 47, no. 2, pp. 236–249, 2001.

[15] T. Suzuki, "Valuing corporate debt: the effect of cross-holdings of stock and debt," *Journal of the Operations Research Society of Japan*, vol. 45, no. 2, pp. 123–144, 2002.

[16] R. Cifuentes, G. Ferrucci, and H. S. Shin, "Liquidity risk and contagion," *Journal of the European Economic association*, vol. 3, no. 2-3, pp. 556–566, 2005.

[17] H. Elsinger, "Financial networks, cross holdings, and limited liability," tech. rep., working paper, 2009.

[18] L. C. Rogers and L. A. Veraart, "Failure and rescue in an interbank network," *Management Science*, vol. 59, no. 4, pp. 882–898, 2013.

[19] S. Weber and K. Weske, "The joint impact of bankruptcy costs, fire sales and cross-holdings on systemic risk in financial networks," *Probability, Uncertainty and Quantitative Risk*, vol. 2, pp. 1–38, 2017.

[20] Y. M. Kabanov, R. Mokbel, and K. El Bitar, "Clearing in financial networks," *Theory of Probability & Its Applications*, vol. 62, no. 2, pp. 252–277, 2018.

[21] Ç. Ararat and B. Rudloff, "Dual representations for systemic risk measures," *Mathematics and Financial Economics*, vol. 14, no. 1, pp. 139–174, 2020.

[22] A. H. Hamel, F. Heyde, and B. Rudloff, "Set-valued risk measures for conical market models," *Mathematics and financial economics*, vol. 5, no. 1, pp. 1–28, 2011.

[23] Ç. Ararat and N. Meimanjan, "Computation of systemic risk measures: a mixed-integer programming approach," to appear in *Operations Research*, 2023.

[24] S. Nobakhtian and N. Shafiei, "A benson type algorithm for nonconvex multiobjective programming problems," *Top*, vol. 25, no. 2, pp. 271–287, 2017.

[25] B. Pagnoncelli, S. Ahmed, and A. Shapiro, "Sample average approximation method for chance constrained programming: Theory and applications," *Journal of Optimization Theory and Applications*, vol. 142, pp. 399–416, 08 2009.

[26] S. Ahmed and A. Shapiro, "Solving chance-constrained stochastic programs via sampling and integer programming," in *State-of-the-art decision-making tools in the information-intensive age*, pp. 261–269, Informs, 2008.

[27] X. Chen, A. Shapiro, and H. Sun, "Convergence analysis of sample average approximation of two-stage stochastic generalized equations," *SIAM Journal on Optimization*, vol. 29, no. 1, pp. 135–161, 2019.

[28] C. D. Aliprantis and K. C. Border, *Infinite Dimensional Analysis: a Hitchhiker's Guide*. Berlin; London: Springer, 2006.

[29] G. Beer, "Metric spaces with nice closed balls and distance functions for closed sets," *Bulletin of the Australian Mathematical Society*, vol. 35, no. 1, pp. 81–96, 1987.

[30] R. Van Der Hofstad, "Random graphs and complex networks," *Available on http://www. win. tue. nl/rhofstad/NotesRGCN. pdf*, vol. 11, p. 60, 2009.

[31] B. Bollobás, C. Borgs, J. T. Chayes, and O. Riordan, "Directed scale-free graphs," in *SODA*, vol. 3, pp. 132–139, 2003.

[32] R. Cont, A. Moussa, *et al.*, "Network structure and systemic risk in banking systems," *Edson Bastos e, Network Structure and Systemic Risk in Banking Systems (December 1, 2010)*, 2010.

[33] M. Ó. Searcóid, *Metric spaces*. Springer-Verlag Berlin Heidelberg, 2007.

[34] H. Föllmer and A. Schied, "Stochastic finance," in *Stochastic Finance*, de Gruyter, 2016.

[35] M. Ehrgott, "Weighted sum scalarization," in *Multicriteria Optimization*, pp. 55–75, Springer, 2000.

[36] A. Pascoletti and P. Serafini, "Scalarizing vector optimization problems," *Journal of Optimization Theory and Applications*, vol. 42, pp. 499–524, 1984.

[37] Ç. Ararat, F. Ulus, and M. Umer, "A norm minimization-based convex vector optimization algorithm," *Journal of Optimization Theory and Applications*, vol. 194, no. 2, pp. 681–712, 2022.

[38] R. T. Rockafellar and R. J.-B. Wets, *Variational analysis*, vol. 317. Springer Science & Business Media, 2009.

[39] R. v. d. Hofstad, *Preferential Attachment Models*, pp. 256–300. Cambridge Series in Statistical and Probabilistic Mathematics, Cambridge University Press, 2016.

[40] M. Deijfen, H. Van Den Esker, R. Van Der Hofstad, and G. Hooghiemstra, "A preferential attachment model with random initial degrees," *Arkiv för matematik*, vol. 47, pp. 41–72, 2009.

[41] A.-L. Barabási and R. Albert, "Emergence of scaling in random networks," *science*, vol. 286, no. 5439, pp. 509–512, 1999.

[42] B. Bollobás and O. M. Riordan, "Mathematical results on scale-free random graphs," *Handbook of graphs and networks: from the genome to the internet*, pp. 1–34, 2003.

[43] C. Cooper and A. Frieze, "A general model of web graphs," *Random Structures & Algorithms*, vol. 22, no. 3, pp. 311–335, 2003.

[44] M. H. DeGroot and M. J. Schervish, *Probability and statistics*. Pearson Education, 2012.

[45] D. J. Watts and S. H. Strogatz, "Collective dynamics of 'small-world'networks," *nature*, vol. 393, no. 6684, pp. 440–442, 1998.

[46] P. W. Holland and S. Leinhardt, "Transitivity in structural models of small groups," *Comparative group studies*, vol. 2, no. 2, pp. 107–124, 1971.

[47] B. Craig and G. Von Peter, "Interbank tiering and money center banks," *Journal of Financial Intermediation*, vol. 23, no. 3, pp. 322–347, 2014.

[48] S. P. Borgatti and M. G. Everett, "Models of core/periphery structures," *Social networks*, vol. 21, no. 4, pp. 375–395, 2000.